



# A Nonlinear Finite Element Model for Steel-concrete Composite Beam using a Higher-order Beam Theory

**Md. Alhaz Uddin**

Master of Engineering Science (Structural Engineering & Materials)

Thesis submitted to the Faculty of Engineering, Computer and Mathematical Sciences in total to fulfilment of the requirements for the degree of

**Doctor of Philosophy**

School of Civil, Environmental and Mining Engineering  
The University of Adelaide  
Australia

-November 2016-



## **Abstract**

Steel-concrete composite beams are commonly used in bridges, buildings and other civil engineering infrastructure for their superior structural performances. This is achieved by exploiting the typical configuration of this structural system where the concrete slab is primarily utilised to resist compressive stresses whereas the steel girder is used to sustain tensile stresses. The composite action is realised by connecting the concrete slab with the steel girder by steel shear studs. The interfacial shear slip is always observed due to the deformation of shear studs having a finite stiffness in reality which is commonly known as partial shear interaction. This is an important feature which should be considered in the analysis of these composite beams to get satisfactory results.

It is observed that most of the existing models for simulating composite beams are based on Euler-Bernoulli's beam theory (EBT) which does not consider the effect of shear deformation of the beam layers. In recent past, the incorporation of this effect is becoming popular and some attempts have already been made where Timoshenko's beam theory (TBT) is typically used. In this beam theory (TBT), the true parabolic variation of shear stress over the beam depth is replaced by a uniform shear stress distribution over the beam depth to simplify the problem. In order to address this issue, a higher-order beam theory (HBT) has recently been developed at the University of Adelaide. However, the model is so far applied to the linear analysis of these beams.

In the present study, a comprehensive nonlinear finite element model is developed based on HBT for an accurate prediction of the bending response of steel-concrete composite beams with partial shear interaction. This is achieved by taking a third order variation of longitudinal displacement over the beam depth for the steel and the concrete layers separately. The deformable shear studs used for connecting the concrete slab with the steel girder are modelled as distributed shear springs along the interface between these material layers. The effects of nonlinearities produced by large deformations and inelastic material behaviours are incorporated in the formulation of the proposed one-dimensional finite element model. The Green-Lagrange strain vector is used to capture the effect of geometric nonlinearity due to large deformations. The von Mises yield criterion with an isotropic-hardening rule is used for modelling the inelastic behaviour of steel girders, reinforcements and steel shear studs. This modelling approach is also applied to the region of concrete slab subjected to compressive stress for simplicity. A damage mechanics model is adopted to simulate the cracking behaviour of the concrete under tensile stress. The nonlinear governing

equations are solved by an incremental-iterative technique following the Newton-Raphson method. A robust arc-length method is employed to capture the post peak response successfully where the energy dissipation played an important role. To assess the performance of the proposed model, the results predicted by the model are compared with existing experimental results as well as numerical results produced by using a detailed two dimensional finite element modelling of the composite beams.

## Table of Contents

Abstract.....	iii
Table of Contents.....	v
Statement of Originality.....	vii
List of Manuscripts .....	viii
Acknowledgements.....	ix
Chapter 1: Introductory Background .....	1
1.1 Introduction.....	1
1.2 Nonlinear Analysis .....	3
1.3 Solution Strategy.....	4
1.4 Research gaps and objectives .....	5
1.5 Details of Manuscripts included in the Thesis.....	6
Reference .....	8
Chapter 2: Geometrically Nonlinear Model .....	13
2.1 Introduction.....	13
2.2 List of Manuscripts .....	13
2.3 Statement of Authorship .....	14
2.4 Large deformation analysis of two layered composite beams with partial shear interaction using a higher-order beam theory .....	16
Chapter 3: Material Nonlinear Model.....	45
3.1 Introduction.....	45
3.2 List of Manuscripts .....	45
3.3 Statement of Authorship .....	46
3.4 A higher order model for inelastic response of composite beams with interfacial slip using a dissipation based arc-length method .....	48
Chapter 4: Geometric and Material Nonlinear Model .....	91
4.1 Introduction.....	91

4.2 List of Manuscripts .....	91
4.3 Statement of Authorship .....	92
4.4 Geometrically nonlinear inelastic analysis of steel-concrete composite beams with partial interaction using a higher-order beam theory .....	94
<b>Chapter 5: Summary, Conclusions and Recommendations for Future Study .....</b>	<b>133</b>
5.1 Summary and Conclusions .....	133
5.2 Recommendations for Future Study .....	135

## **Statement of Originality**

I certify that this work contains no material which has been accepted for the award of any other degree or diploma in my name in any university or other tertiary institution and, to the best of my knowledge and belief, contains no material previously published or written by another person, except where due reference has been made in the text. In addition, I certify that no part of this work will, in the future, be used in a submission in my name for any other degree or diploma in any university or other tertiary institution without the prior approval of the University of Adelaide and where applicable, any partner institution responsible for the joint award of this degree.

I give consent to this copy of my thesis when deposited in the University Library, being made available for loan and photocopying, subject to the provisions of the Copyright Act 1968.

The author acknowledges that copyright of published works contained within this thesis resides with the copyright holder(s) of those works.

I also give permission for the digital version of my thesis to be made available on the web, via the University's digital research repository, the Library Search and also through web search engines, unless permission has been granted by the University to restrict access for a period of time.

.....  
Md. Alhaz Uddin

.....  
Date

## List of Manuscripts

Uddin, M. A., Sheikh, A. H., Bennett, T. and Uy, B. (2017). “Large deformation analysis of two layered composite beams with partial shear interaction using a higher-order beam theory.” *International Journal of Mechanical Sciences*, (Elsevier), vol. 122, no. 1, pp. 331-340.

Uddin, M. A., Sheikh, A. H., Brown, D., Bennett, T. and Uy, B. (2017). “A higher-order model for inelastic response of composite beams with interfacial slip using a dissipation based arc-length method.” *Engineering structures*, (Elsevier). (Article in Press).

Uddin, M. A., Sheikh, A. H., Brown, D., Bennett, T. and Uy, B. (2017). “Geometrically nonlinear inelastic analysis of steel-concrete composite beams with partial interaction using a higher-order beam theory.” *International Journal of Non-linear Mechanics*, (Elsevier). (Submitted).

## **Acknowledgements**

*I wish to express my sincere thanks and profound appreciation to my honourable supervisor, Associate Professor Abdul Hamid Sheikh for his guidance, encouragement and valuable time spent on the fruitful discussions throughout the work, which was extremely valuable in conducting this research work.*

*I would also like to express my gratefulness to my supervisor Dr. Terry Bennett for his treasured and relevant advice throughout the study.*

*The financial support provided by the University of Adelaide in the form of an Adelaide Scholarship International (ASI) to fulfill the study is gratefully acknowledged.*

*Finally, I would like to thank the most important people in my life, my parents, wife, brother, and sisters who have provided their endless support and patience throughout the years.*



## Chapter 1: Introductory Background

### 1.1 Introduction

Steel-concrete composite beams (Fig. 1) consist of a concrete slab and a steel girder connected by steel shear studs to have a composite action. These composite structures have widespread applications, especially in bridges, modern buildings and other structures. In this typical structural form, the two material layers are properly utilised to enhance the performance of the overall structural system, whereby the concrete slab is mainly used to carry the compressive stress and the steel girder carries the tensile stress. The shear studs transfer the shear force at the interface between concrete and steel layers. As the shear connectors are not infinitely stiff in reality, interfacial shear slip as well as vertical separation may occur between the two layers. The vertical separation between the layers is not common (Battini et al. 2009) under static loading for a straight beam. However, the interfacial slip has always been found (Oehlers & Bradford 1995) in reality at the interface between the steel and concrete layers, which is commonly defined as partial interaction. The effect of partial shear interaction on the structural performance has been found to be significant e.g. (Loh et al. 2004; Uy & Nethercot 2005), it should therefore be considered in the analysis of these composite beams.

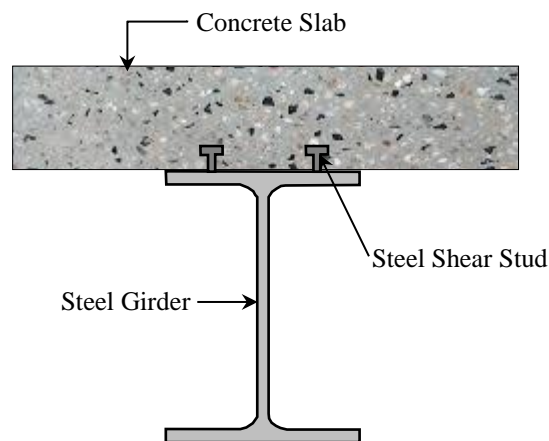


Fig. 1. Cross-section of steel-concrete composite beam

A number of researchers e.g. (Adekola 1968; Faella et al. 2002; Girhammar & Pan 1993; Huang & Su 2008; Jasim 1997; Ko 1972; Newmark et al. 1951; Ranzi, G et al. 2004; Ranzi, Gianluca et al. 2006; Salari et al. 1998; Schnabl et al. 2006; Wu et al. 2002; Yasunori et al. 1981) have developed models for composite beams considering the effect of partial interaction based on Euler Bernoulli beam theory (EBT). It has been recognised that a model

based on EBT underestimates the deflection of the beam as it ignores the effect of transverse shear deformation.

In the recent past, there is a growing trend to incorporate the effect of shear deformation in the modelling of composite beams using Timoshenko's beam theory (TBT). Zona and Reddy (2011), and Ranzi and Zona (2007) have investigated the effect of shear deformation on the behaviour of steel-concrete composite beams with partial interaction but they have been applied TBT to the steel girder only, while EBT has been used to model the concrete slab. They have shown that the concrete slab gives a more conservative result, and emphasised the need to consider the effect of shear deformation in the modelling of composite beam. This is especially true for beams with a low span-to-depth ratio, steel I-girders having wide flanges and thin web. Berczyński & Wróblewski (2005); Schnabl et al. (2007); Xu & Wu (2007) have applied TBT to model both material layers. It is shown that a model based on TBT is capable of predicting the global response (e.g., deflection) of a beam satisfactorily. However, the model based on TBT is not adequate for predicting the actual distribution of stresses (local response). In this beam theory (TBT), the actual parabolic variation of shear stress over the beam depth is replaced by a uniform shear stress distribution over the beam depth to simplify the problem. In order to address this problem, an arbitrary factor known as a shear correction factor is artificially introduced which helps to get a satisfactory global response. Moreover, the calculation of the exact value of this shear correction factor for a composite beam with partial shear interaction is cumbersome.

In order to address these problems, a higher-order beam theory (HBT) has recently been developed at the University of Adelaide (Chakrabarti et al. 2012a, 2012b, 2012c) for accurately predicting the global as well as local response of these beam. This beam theory (HBT) utilised the concept of Reddy's higher order shear deformation theory (Reddy 1984) developed for multi-layered laminated composite plates modelled as a single layered plate without any interfacial slip. The cross-sectional warping of the beam layers produced by the parabolic (nonlinear) variation of shear stress is modelled by taking a higher order (3<sup>rd</sup> order) variation of longitudinal displacement of the fibres across the beam depth. However, the development of these models (Chakrabarti et al. 2012a, 2012b, 2012c) is based on small deformation and elastic material behaviour. In reality these composite beams often undergo large deformations, where the assumption of geometric linearity is no longer appropriate. Moreover, the beam materials can found to exhibit an inelastic response even with a moderate range of loading.

## 1.2 Nonlinear Analysis

The effect of geometric nonlinearity due to large deformations is incorporated in the finite element models by Erkmen and Bradford (2009) for the analysis of steel-concrete composite beams being curved in plane, and Battini et al. (2009) and Ranzi et al. (2010) for the two-layered straight composite beams. These models are all based on EBT with the inherent drawback of this theory as outlined previously. Hijaj et al. (2012) developed a model based on TBT considering the effect of large deformation. Whilst this represents an improvement over the models using EBT, the model is not capable of predicting the actual distribution of stresses (local response) and in addition ignored the effects of inelastic material behaviour which is encountered even within a low to moderate range of loading.

The material nonlinearity due to inelastic material behaviours has incorporated by Yasunori et al. (1981) in their finite element model for composite beams using the von Mises yield criterion. However, they have used a very simple material model based on an elastic perfectly-plastic idealisation for all materials including concrete, which is not realistic especially for the tensile response of concrete. Similar studies have been carried out by Salari et al. (1998) using a bi-linear elasto-plastic material model with a strain hardening parameter. A further development in this direction is due to Dall'Asta and Zona (2002) and Erkmen and Attard (2011) who have used realistic stress-strain curves for the beam materials. In their model, Dall'Asta and Zona (2002) have ignored the contribution of concrete in tension whereas Erkmen and Attard (2011) have used the concept of tension stiffening for its modelling. However, these investigators (Dall'Asta & Zona 2002; Erkmen & Attard 2011; Salari et al. 1998; Yasunori et al. 1981) have developed models based on EBT and did not consider the effects of large deformation in the modelling of composite beams.

A nonlinear model considering the effect of inelastic material behaviour along with the large deformation can ideally be the best model for predicting the response of these composite structures accurately. For this purpose, Hozjan et al. (2013) developed a nonlinear finite element model for composite beams with interfacial slip based on the shear-stiff Reissner beam theory. However, this beam theory suffers from similar drawbacks to EBT and neglected the tensile behaviour of concrete. A comprehensive finite element model is proposed by Liu et al. (2013) where the tensile behaviour of concrete is simulated using a damage mechanics model which can precisely model the tensile response of plain concrete without reinforcement. They also employed EBT for simulating composite beams that neglected the effect of transverse shear deformation. Nguyen et al. (2014) considered the

effect of shear deformations using TBT in the modelling of composite beams. Both geometric and material nonlinearities are included in their models, however they (Nguyen et al. 2014) have used very simple constitutive models for the beam material. Moreover, they treated the behaviour of concrete in tension and compression identically.

The review of existing studies as presented above leads to the conclusion that there is a need for a development of an efficient numerical model based on HBT considering all the aforementioned aspects for accurately predicting the response of steel-concrete composite beams.

### **1.3 Solution Strategy**

The nonlinear response of these structures is typically manifested in the form of nonlinear load-deflection curves which are found to have a descending branch after attaining the peak load due to the strain-softening behaviour of concrete. It is observed that most of the investigations carried out on the inelastic response of composite beams could not capture the descending branch of the nonlinear load-deflection curve successfully. The solution of this typical nonlinear problem is quite challenging and a load control based technique cannot trace the descending branch of the load-deflection curve. In order to overcome this problem, a displacement control based technique may be used, however this will also fail if the load-deflection curve has a snap-back response. In this situation, an arc-length based solution technique seems to be the only possible option.

The arc-length method was initially proposed by Riks (1979) and subsequently enhanced by various investigators (Crisfield 1981, 1983) for solving different nonlinear problems. Although these developments helped to solve complex geometric nonlinear problems successfully, they encountered severe convergence problems in solving material nonlinear problems. This has proved to be especially the case in the modelling of quasi-brittle materials which exhibit localised failure. In order to address this specific issue, the localised nature of damage has been utilised by May and Duan (1997) to develop an arc-length method known as a damage localization approach. This method can provide a satisfactory solution but it requires the position of damaged elements to be known, which may be difficult to locate in a complex structural system. A further advancement in this direction is due to Gutiérrez (2004) who initially proposed an energy dissipation based arc-length method (Fig. 2) for continuum damage model. Subsequently, this method has been extended by Verhoosel et al.

(2009) to include plasticity as an additional mechanism which is utilised to solve the nonlinear equations in terms of incremental iterative process.

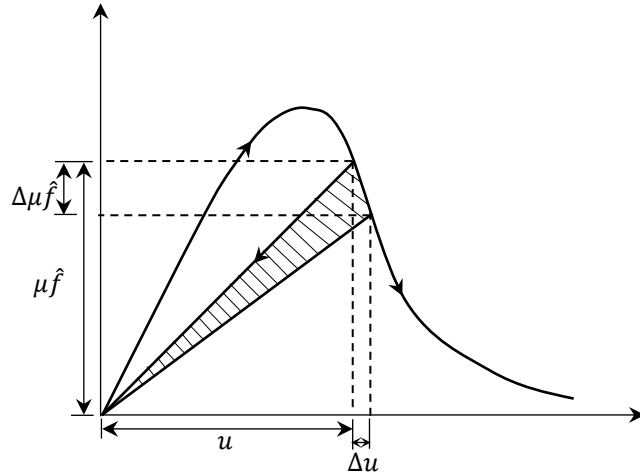


Fig. 2. Energy dissipation based arc-length method

#### 1.4 Research gaps and objectives

The literature review shows a number of research gaps related to modelling of steel-concrete composite beams, which are attempted to address in the present study by developing the following models:

The existing models incorporation the effect of large deformation for simulating composite beams with partial interaction are limited and these are developed using EBT and first order beam theory (TBT). These beam theories are not adequate for predicting the local response and even the global response in some situation such as beams with a small span-to-depth ratio, localised concentrated loads and clamped boundary conditions.

- Objective 1: To develop a one dimensional finite element model based on a higher-order beam theory (HBT) considering the effect geometric nonlinearity using Green-Lagrange strain vector for predicting the response of two-layered composite beam with partial interaction.

The existing models considering material nonlinear behaviours of the beam constituents are also limited in number and these models are based on EBT and TBT. Moreover, most of these investigations are used a simplified material model specifically for the concrete slab. In some studies, a simple stress return technique is used for the plasticity model which may cause a divergence problem in the solution of nonlinear equations. The nonlinear response in the form of load-deflection curve has a descending branch due to the strain-softening

behaviour of the concrete slab and it is really a challenging problem to capture this response. Unfortunately, most of the existing techniques could not capture the descending branch of the nonlinear response successfully.

- Objective 2: To develop an efficient nonlinear model based on HBT considering inelastic material behaviours using von Mises plasticity theory and a damage mechanics model for an accurate prediction of the inelastic response of steel-concrete composite beams with partial interaction. To implement a robust arc-length technique for solving the nonlinear equation so as to capture the post peak response successfully.

In the existing literature, the available finite element models considering the effect of geometric and material nonlinearity are very limited and none of those models are developed using HBT. In addition, most of the existing models are developed by using very simple constitutive models for the beam material and neglected the contribution of concrete in tension. The effect of large deformations and inelastic material behaviours are responsible for inducing nonlinear in the structural response, which also has a descending branch because the material nonlinearity is usually having a dominant contribution for the type of structures investigated in this research. It is also observed that none of the existing studied paid a proper attention on the prediction of the softening branch of the load deflection curve.

- Objective 3: To develop a comprehensive nonlinear finite element model based on HBT incorporating all aspects of geometric and material nonlinearities to be considered in objective 1 and objective 2 for a reliable prediction of the nonlinear response of steel-concrete composite beams with interfacial slip.

### **1.5 Details of Manuscripts included in the Thesis**

This thesis contains a number of manuscripts which are submitted/to be submitted to internationally recognised journals. Each chapter of the thesis is presented in the form of a journal paper which is self-sufficient individually and do not need the accumulation of information from the previous chapters.

Chapter 2 presents a study on large deformation response of two-layered composite beam with inter layer slip by developing a one-dimensional finite element model based on a higher-order beam theory (HBT). The Green-Lagrange strain vector is used to consider the

effect of large deformations. Numerical examples of composite beams are solved by the model taking into account different layer configurations, loading, support conditions, and shear interactions to assess the performance and range of applicability of the model. The model performance is verified and validated using 2D finite element model results and existing published results respectively.

Chapter 3 presents an investigation on the behaviour of steel-concrete composite beams with partial interaction due to inelastic material behaviours through development of a computationally efficient finite element model. A plasticity model based on von Mises yield criterion and a damage mechanics model are used to simulate the inelastic behaviour of beam materials. An energy dissipation based arc-length method is employed to solve the nonlinear equations and capture the post peak response effectively. The proposed one dimensional model based on HBT is validated with existing experimental results and verified with numerical results obtained from a detailed two dimensional finite element model of composite beams.

Chapter 4 presents a study on the response of steel-concrete composite beams with interfacial slip considering large deformations as well as inelastic material behaviours through development of a similar finite element model based on HBT. The effect of large deformation is incorporated using the Green-Lagrange strain vector whereas the von Mises plasticity model is used to simulate the inelastic material behaviour of most of the constituents of these beams. A damage mechanics model is also used for modelling the inelastic behaviour of concrete under tension. A robust arc-length method is adopted to solve the nonlinear equations and capture the post peak response. Numerical results are generated with a detailed 2D finite element model which are used for the verification of the proposed model. The existing experimental data are also used to validate the proposed model.

Chapter 5 of this thesis presents the concluding remarks based on the major findings of this research. Suggestions for possible future research are also listed in this chapter.

## Reference

- Adekola, A 1968, 'Partial interaction between elastically connected elements of a composite beam', *International Journal of Solids and Structures*, vol. 4, no. 11, pp. 1125-1135.
- Battini, J-M, Nguyen, Q-H & Hjiaj, M 2009, 'Non-linear finite element analysis of composite beams with interlayer slips', *Computers & Structures*, vol. 87, no. 13, pp. 904-912.
- Berczyński, S & Wróblewski, T 2005, 'Vibration of steel–concrete composite beams using the Timoshenko beam model', *Journal of Vibration and Control*, vol. 11, no. 6, pp. 829-848.
- Chakrabarti, A, Sheikh, A, Griffith, M & Oehlers, D 2012a, 'Analysis of composite beams with longitudinal and transverse partial interactions using higher order beam theory', *International Journal of Mechanical Sciences*, vol. 59, no. 1, pp. 115-125.
- Chakrabarti, A, Sheikh, A, Griffith, M & Oehlers, D 2012b, 'Analysis of composite beams with partial shear interactions using a higher order beam theory', *Engineering Structures*, vol. 36, pp. 283-291.
- Chakrabarti, A, Sheikh, A, Griffith, M & Oehlers, D 2012c, 'Dynamic response of composite beams with partial shear interaction using a higher-order beam theory', *Journal of Structural Engineering*, vol. 139, no. 1, pp. 47-56.
- Crisfield, MA 1981, 'A fast incremental/iterative solution procedure that handles “snap-through”', *Computers & Structures*, vol. 13, no. 1, pp. 55-62.
- Crisfield, MA 1983, 'An arc-length method including line searches and accelerations', *International Journal for Numerical Methods in Engineering*, vol. 19, no. 9, pp. 1269-1289.
- Dall’Asta, A & Zona, A 2002, 'Non-linear analysis of composite beams by a displacement approach', *Computers & Structures*, vol. 80, no. 27–30, pp. 2217-2228.

- Erkmen, RE & Attard, MM 2011, 'Displacement-based finite element formulations for material-nonlinear analysis of composite beams and treatment of locking behaviour', *Finite Elements in Analysis and Design*, vol. 47, no. 12, pp. 1293-1305.
- Erkmen, RE & Bradford, MA 2009, 'Nonlinear elastic analysis of composite beams curved in-plan', *Engineering Structures*, vol. 31, no. 7, pp. 1613-1624.
- Faella, C, Martinelli, E & Nigro, E 2002, 'Steel and concrete composite beams with flexible shear connection: "exact" analytical expression of the stiffness matrix and applications', *Computers & Structures*, vol. 80, no. 11, pp. 1001-1009.
- Girhammar, UA & Pan, D 1993, 'Dynamic analysis of composite members with interlayer slip', *International Journal of Solids and Structures*, vol. 30, no. 6, pp. 797-823.
- Gutiérrez, MA 2004, 'Energy release control for numerical simulations of failure in quasi-brittle solids', *Communications in Numerical Methods in Engineering*, vol. 20, no. 1, pp. 19-29.
- Hjiiaj, M, Battini, J-M & Nguyen, QH 2012, 'Large displacement analysis of shear deformable composite beams with interlayer slips', *International Journal of Non-Linear Mechanics*, vol. 47, no. 8, pp. 895-904.
- Hozjan, T, Saje, M, Srpčič, S & Planinc, I 2013, 'Geometrically and materially non-linear analysis of planar composite structures with an interlayer slip', *Computers & Structures*, vol. 114-115, pp. 1-17.
- Huang, C & Su, Y 2008, 'Dynamic characteristics of partial composite beams', *International Journal of Structural Stability and Dynamics*, vol. 8, no. 04, pp. 665-685.

- Jasim, N 1997, 'Computation of deflections for continuous composite beams with partial interaction', *Proceedings of the Institution of Civil Engineers. Structures and buildings*, vol. 122, no. 3, pp. 347-354.
- Ko, M-F 1972, *Layered beam systems with interlayer slip*, Civil Engineering Department, Colorado State University.
- Liu, X, Bradford, MA & Erkmen, RE 2013, 'Non-linear inelastic analysis of steel–concrete composite beams curved in-plan', *Engineering Structures*, vol. 57, pp. 484-492.
- Loh, H, Uy, B & Bradford, M 2004, 'The effects of partial shear connection in the hogging moment regions of composite beams: Part I—Experimental study', *Journal of Constructional Steel Research*, vol. 60, no. 6, pp. 897-919.
- May, I & Duan, Y 1997, 'A local arc-length procedure for strain softening', *Computers & Structures*, vol. 64, no. 1, pp. 297-303.
- Newmark, NM, Siess, CP & Viest, I 1951, 'Tests and analysis of composite beams with incomplete interaction', *Proc. Soc. Exp. Stress Anal*, vol. 9, no. 1, pp. 75-92.
- Nguyen, Q-H, Hjiij, M & Lai, V-A 2014, 'Force-based FE for large displacement inelastic analysis of two-layer Timoshenko beams with interlayer slips', *Finite Elements in Analysis and Design*, vol. 85, pp. 1-10.
- Oehlers, D & Bradford, MA 1995, 'Composite Steel and Concrete Structural Members', *Fundamental Behaviour, Australia*.
- Ranzi, G, Bradford, M & Uy, B 2004, 'A direct stiffness analysis of a composite beam with partial interaction', *International Journal for Numerical Methods in Engineering*, vol. 61, no. 5, pp. 657-672.

- Ranzi, G, Dall'Asta, A, Ragni, L & Zona, A 2010, 'A geometric nonlinear model for composite beams with partial interaction', *Engineering Structures*, vol. 32, no. 5, pp. 1384-1396.
- Ranzi, G, Gara, F, Leoni, G & Bradford, MA 2006, 'Analysis of composite beams with partial shear interaction using available modelling techniques: A comparative study', *Computers & Structures*, vol. 84, no. 13, pp. 930-941.
- Ranzi, G & Zona, A 2007, 'A steel–concrete composite beam model with partial interaction including the shear deformability of the steel component', *Engineering Structures*, vol. 29, no. 11, pp. 3026-3041.
- Reddy, JN 1984, 'A simple higher-order theory for laminated composite plates', *Journal of applied mechanics*, vol. 51, no. 4, pp. 745-752.
- Riks, E 1979, 'An incremental approach to the solution of snapping and buckling problems', *International Journal of Solids and Structures*, vol. 15, no. 7, pp. 529-551.
- Salari, MR, Spacone, E, Shing, PB & Frangopol, DM 1998, 'Nonlinear analysis of composite beams with deformable shear connectors', *Journal of Structural Engineering*, vol. 124, no. 10, pp. 1148-1158.
- Schnabl, S, Planinc, I, Saje, M, Oas, B & Turk, G 2006, 'An analytical model of layered continuous beams with partial interaction', *Structural Engineering and Mechanics*, vol. 22, no. 3, pp. 263-278.
- Schnabl, S, Saje, M, Turk, G & Planinc, I 2007, 'Locking-free two-layer Timoshenko beam element with interlayer slip', *Finite Elements in Analysis and Design*, vol. 43, no. 9, pp. 705-714.

Uy, B & Nethercot, D 2005, 'Effects of partial shear connection on the required and available rotations of semi-continuous composite beam systems', *The Structural Engineer*, vol. 83, no. 4.

Verhoosel, CV, Remmers, JJ & Gutiérrez, MA 2009, 'A dissipation-based arc-length method for robust simulation of brittle and ductile failure', *International Journal for Numerical Methods in Engineering*, vol. 77, no. 9, pp. 1290-1321.

Wu, Y, Oehlers, DJ & Griffith, MC 2002, 'Partial-interaction analysis of composite beam/column members', *Mechanics of structures and machines*, vol. 30, no. 3, pp. 309-332.

Xu, R & Wu, Y 2007, 'Static, dynamic, and buckling analysis of partial interaction composite members using Timoshenko's beam theory', *International Journal of Mechanical Sciences*, vol. 49, no. 10, pp. 1139-1155.

Yasunori, A, Sumio, H & Kajita, T 1981, 'Elastic-plastic analysis of composite beams with incomplete interaction by finite element method', *Computers & Structures*, vol. 14, no. 5–6, pp. 453-462.

Zona, A & Ranzi, G 2011, 'Finite element models for nonlinear analysis of steel–concrete composite beams with partial interaction in combined bending and shear', *Finite Elements in Analysis and Design*, vol. 47, no. 2, pp. 98-118.

## **Chapter 2: Geometrically Nonlinear Model**

### **2.1 Introduction**

The manuscript of this chapter “Large deformation analysis of two layered composite beams with partial shear interaction using a higher-order beam theory” presents the development an efficient finite element model based on higher-order beam theory (HBT) for composite beams considering the effect of geometric nonlinearity. The aim of this study to investigate the effect of large deformations on the response of these composite beams with interfacial slip. The Green-Lagrange strain vector is used to capture the effect of geometric nonlinearity in the present formulation. Numerical examples are solved by the proposed model to assess the performance and range of applicability of the model by taking into account different loading, supporting conditions and shear interactions. It is shown that the proposed model has improved capabilities compared with existing techniques in predicting the local response (stress distribution) of composite beams, especially TBT is not capable of predicting the actual variation of shear stress. It is also shown that the proposed model achieved some improvement in the prediction of global response of these beams.

### **2.2 List of Manuscripts**

Uddin, M. A., Sheikh, A. H., Bennett, T. and Uy, B. (2016). “Large deformation analysis of two layered composite beams with partial shear interaction using a higher-order beam theory.” *International Journal of Mechanical Sciences*, (Elsevier), vol. 122, no. 1, pp. 331-340.

## 2.3 Statement of Authorship

Title of Paper	Large deformation analysis of two layered composite beams with partial shear interaction using a higher-order beam theory
Publication Status	Published
Publication Details	Uddin, M. A., Sheikh, A. H., Bennett, T. and Uy, B. (2016). "Large deformation analysis of two layered composite beams with partial shear interaction using a higher-order beam theory." <i>International Journal of Mechanical Sciences</i> , (Elsevier), vol. 122, no. 1, pp. 331-340.

### Principal Author

Name of Principal Author (Candidate)	Md. Alhaz Uddin
Contribution to the Paper	Developed finite element model, performed numerical analysis and prepared manuscript.
Overall percentage (%)	80%
Certification:	This paper reports on original research I conducted during the period of my Higher Degree by Research candidature and is not subject to any obligations or contractual agreements with a third party that would constrain its inclusion in this thesis. I am the primary author of this paper.
Signature	Date

### Co-Author Contributions

By signing the Statement of Authorship, each author certifies that:

- i. the candidate's stated contribution to the publication is accurate (as detailed above);
- ii. permission is granted for the candidate to include the publication in the thesis; and
- iii. the sum of all co-author contributions is equal to 100% less the candidate's stated contribution.

Name of Co-Author	Abdul Hamid Sheikh
Contribution to the Paper	Supervised for development of model, helped in data interpretation, provided critical manuscript evaluation and acted as corresponding author.
Signature	Date 22/11/2016

Name of Co-Author	Terry Bennett
Contribution to the Paper	Helped to evaluate and edit manuscript.
Signature	Date 22/11/16.

Name of Co-Author	Brian Uy		
Contribution to the Paper	Provided for manuscript evaluation. <i>Ensuring paper reflects state of the art and          reviews existing experimental work.</i>		
Signature		Date	14/11/16

## 2.4 Large deformation analysis of two layered composite beams with partial shear interaction using a higher-order beam theory

Md. Alhaz Uddin, Abdul Hamid Sheikh, Terry Bennett and Brian Uy

### ABSTRACT

An efficient nonlinear finite element model based on a higher-order beam theory is developed for accurately predicting the response of two layered composite beams with partial shear interaction. This is achieved by taking a third order variation of the longitudinal displacement over the beam depth for the two layers separately. The deformable shear connectors joining the two different material layers are modelled as distributed shear springs along the beam length at their interface. In order to capture the geometric nonlinear effects of the beam, the Green-Lagrange strain vector is used to develop the one dimensional finite element model. The nonlinear governing equations are solved by an incremental-iterative technique following the Newton-Raphson method. To assess the performance of the proposed model, the results predicted by the model are compared with published results as well as numerical results produced by using a detailed two dimensional finite element modelling of the composite beams.

**Keywords:** Composite beam, Partial shear interaction, Higher-order beam theory, Finite element model, Geometric nonlinearity.

### Nomenclature

$A_a, A_b$  cross-sectional area of upper and lower layers of the beam

$[B_L]_k$  linear strain-displacement matrix for the  $k$ -th layer ( $k=c$  for concrete,  $k=s$  for steel)

$[B_p]$  strain-displacement matrix for the penalty function

$[B]_{sh}$  strain-displacement matrix for shear connectors

$[D]_k$  constitutive matrix for the  $k$ -th layer

$E_k$ , elastic modulus for the  $k$ -th layer

$\{F\}$  nodal load vector

$G_k$	shear modulus for the $k$ -th layer
$[G]_k$	nonlinear strain-displacement matrix for the $k$ -th layer
$[H_L]_k$	linear cross-sectional matrix for the $k$ -th layer
$[H_N]_k$	nonlinear cross-sectional matrix for the $k$ -th layer
$[K_L]$	linear stiffness matrix
$[K_N]$	nonlinear stiffness matrix
$k_p$	penalty parameter
$k_{sh}$	stiffness of distributed springs used for modelling shear connectors
$[K_T]$	tangent stiffness matrix
$[K_\sigma]$	geometric stiffness matrix
$N$	shape function
$q$	distributed external load
$s$	interfacial slip between upper and lower layers
$u_{a0}$	longitudinal displacement of the upper layer at its centroidal or reference axis
$\bar{u}_a$	longitudinal displacement at the bottom fibre of the upper layer
$u_{b0}$	longitudinal displacement of the lower layer at its reference axis
$\bar{u}_b$	longitudinal displacement at the top fibre of the lower layer
$U_p$	strain energy due to penalty function
$w$	transverse displacement
$\alpha, \beta$	higher order terms
$\{\delta R\}$	residual force vector
$\{\Delta\}$	nodal displacement vector
$\{\boldsymbol{\varepsilon}\}_a, \{\boldsymbol{\varepsilon}\}_b$	strain vectors of upper and lower layers
$\{\boldsymbol{\varepsilon}_L\}_k$	linear strain vector for the $k$ -th layer
$\{\bar{\boldsymbol{\varepsilon}}_L\}_k$	linear one dimensional strain vector for the $k$ -th layer
$\{\boldsymbol{\varepsilon}_N\}_k$	nonlinear strain vector for the $k$ -th layer
$\{\boldsymbol{\varepsilon}_{N\theta}\}_k$	nonlinear one dimensional strain vector for the $k$ -th layer

$\theta_a, \theta_b$  bending rotations of upper and lower layers

$\{\sigma\}_a, \{\sigma\}_b$  stress vectors of upper and lower layers

$\tau_{sh}$  distributed shear force (per unit length) at the interface between upper and lower layers

## 1. INTRODUCTION

Composite beams are widely used in many structural engineering applications for their superior structural performance. A two layered composite beam such as timber-timber, timber-steel, timber-concrete and steel-concrete are typically used in the construction industry. In these structures, the two material layers are properly utilised (e.g., in steel-concrete composite beams, the concrete layer is primarily used to carry the compressive stress whereas the steel layer carries the tensile stress) to enhance the performance of the overall structural system. The composite action of these beams is achieved by connecting the two different material layers with shear connectors such as nails or steel shear studs. Theoretically, if the shear connectors have infinite stiffness, full composite action can be achieved. In this case, the benefit of the composite beam can be fully exploited where no shear slip develops at the interface between the two layers and full shear interaction is achieved. However, shear connectors have finite stiffness in reality, which results in the development of interfacial slip between the two layers and partial shear interaction is therefore developed [1]. As the effect of partial shear interaction on the behaviour of structural performance has been found to be significant (e.g. [2, 3]), it should be considered in the analysis of these composite beams. This is an active area of research which is best demonstrated by the large number of studies on different aspects of composite beams carried out by many researchers (e.g. [4-20]). However, the main objective of the present study is to develop a computationally efficient numerical model for these composite beams which can capture the large deformation behaviour of these structures realistically.

One of the initial significant research attempts on the modelling of composite beams was conducted by Newmark et al. [21] who developed an analytical solution based on the Euler-Bernoulli beam theory (EBT) considering the effects of partial shear interaction. The model can only accommodate simple loading and boundary conditions due to its analytical nature. In order to introduce generality in the analysis, a number of numerical models based on the finite element method (FEM) or some similar methods have subsequently been developed by different researchers (e.g., [9-20]). However, most of the studies [12-16] conducted so

far on these composite beams are based on EBT, where the effect of small deformation is considered for a simple linear solution of the problem. In reality, these structures can undergo large deformations under service loads and their effects should be considered in the analysis to predict the actual behaviour of these composite beams. This introduces nonlinearity in the model which is regarded as geometric nonlinearity. It is interesting to note that the number of existing studies on geometric nonlinear analysis of these composite beams is very limited [17, 18].

The effect of geometric nonlinear response is incorporated in the finite element models by Ranzi et al. [17], and Erkmen and Bradford [18] for the analysis of composite beams having curved and straight alignments respectively. The authors however have not considered the effect of transverse shear deformation of the beam material layers, as the models are based on EBT. As the effect of shear deformation is significant in some situations such as beams with a small span-to-depth ratio, localized concentrated loads, clamped boundary conditions and some other cases, there is a growing trend of incorporating shear deformation in recent past [7-11]. Zona and Reddy [10], and Ranzi and Zona [11] have investigated the effect of shear deformation on the behaviour of steel-concrete composite beams where they used Timoshenko's beam theory (TBT) to incorporate the contribution of shear deformation but this has been applied to the steel girder only, while EBT has been used to model the concrete slab. On the other hand, the other investigators [7-9] have applied TBT to model both layers. All these studies [7-11] considering shear deformation are based on small deformation theory leading to a linear analysis. Recently, Hjiiaj et al. [22] presented a finite element model for these composite beams where the effect of geometric nonlinearity as well as shear deformation based on TBT have been considered.

It has been observed that a model based on TBT is capable of predicting the global response (e.g., deflection) of beams satisfactorily, but it is not adequate for the prediction of the actual distribution of stresses (local response) [23-25]. In this beam theory (TBT), the actual parabolic variation of shear stress over the beam depth is simplified by taking a constant average shear stress distribution over the beam depth. This simplification requires the use of a factor known as a shear correction factor to get a satisfactory global response. Unfortunately, the calculation of the exact value of this shear correction factor for a composite beam with partial shear interaction is cumbersome in comparison with that of a single layer homogeneous beam.

In order to address these problems, a higher-order beam theory (HBT) has recently been developed by Sheikh and co-workers [23-25] for an accurate prediction of global as well as local responses of these composite beams. The cross-sectional warping of the beam layers produced by the parabolic (nonlinear) variation of shear stress is modelled by taking a higher order (3rd order) variation of longitudinal displacement of the fibres throughout the beam depth. This beam theory (HBT) utilized the concept of Reddy's higher order shear deformation theory [26] developed for multi-layered laminated composite plates modelled as single layered plates with no interfacial slip. The HBT [23-25] has been implemented by a one dimensional finite element model which has exhibited very good performance but the model is so far restricted to small deformation analysis of these composite beams.

In the present study, a nonlinear finite element model based on HBT is developed considering the effect of large deformations based on the Green-Lagrange strain vector. This leads to nonlinear governing equations which are solved by an incremental iterative technique following the Newton-Raphson method. The results predicted by the proposed models are validated with the published results and the numerical results produced by detailed two-dimensional finite element modelling of composite beams using a commercial finite element program (ABAQUS). It is noted that the stress distributions in composite beams, considering geometrically nonlinear effects, were not found in the existing literature. Therefore, the dataset reported contributes an important resource for future references.

## 2. FORMULATION

### 2.1. Higher-order Beam Theory

Fig.1 shows a typical two layered composite beam with a flexible interface. According to the HBT, the variation of longitudinal displacement of the two layers over their depths can be expressed as

$$u_a = u_{a0} - y_a \theta_a + y_a^2 \alpha_a + y_a^3 \beta_a, \quad (1)$$

$$u_b = u_{b0} - y_b \theta_b + y_b^2 \alpha_b + y_b^3 \beta_b, \quad (2)$$

where  $u_{a0}$  and  $u_{b0}$  are longitudinal displacements of the two layers at their reference axis ( $y_a = 0$  or  $y_b = 0$ ),  $\theta_a$  and  $\theta_b$  are bending rotations of these layers, and  $\alpha$  and  $\beta$  are higher order terms. As the vertical separation between the layers is not common under static loading for

a straight beam, its effect is not considered in this study. Thus the vertical displacement is assumed to be the same for both the layers and it can be expressed as

$$w_a = w_b = w(x). \quad (3)$$

The partial shear interaction between the two layers is modelled by uniformly distributed springs along the entire length of the interface between these layers. The interlayer slip is defined as the relative longitudinal displacement between the upper and lower layer at their interface and it can be expressed as

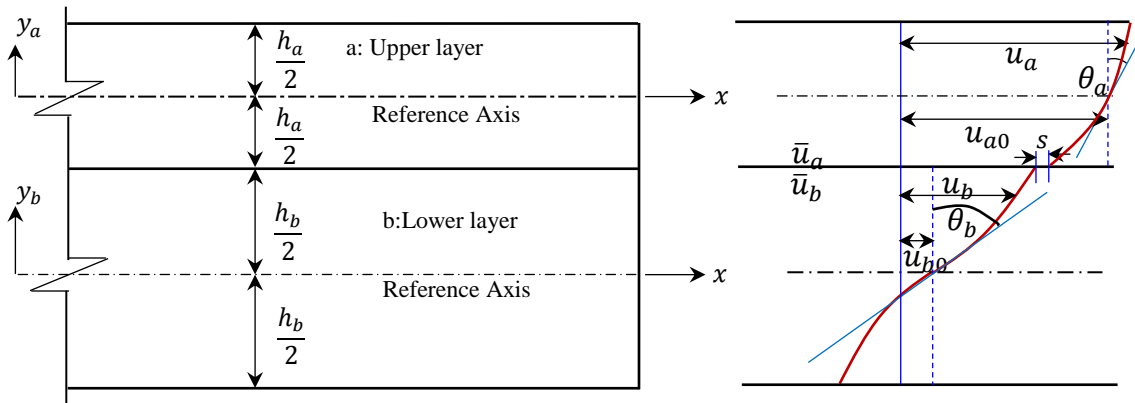


Fig. 1. Typical two layer composite beam with displacement variations throughout the beam depth.

$$s = \bar{u}_b - \bar{u}_a \quad (4)$$

where  $\bar{u}_a$  is the longitudinal displacement at the bottom fibre of the upper layer and  $\bar{u}_b$  is that at the top fibre of the lower layer.

The shear strain for the upper material layer of the beam ( $\gamma_a$ ) at its top surface is zero, as the shear stress ( $\tau_a = G_a \gamma_a$ ) becomes zero at this free surface. Using Eqs. (1) and (3), the shear strain at any point of the upper layer may be expressed as

$$\gamma_a = \frac{\partial u_a}{\partial y_a} + \frac{\partial w}{\partial x} = -\theta_a + 2\alpha_a y_a + 3\beta_a y_a^2 + \frac{dw}{dx} \quad (5)$$

The shear stress free condition at the top surface of the upper material layer can now be employed by substituting  $y_a = h_a/2$  (Fig. 1) in the above equation which is lead to

$$-\theta_a + \alpha_a h_a + \frac{3}{4} \beta_a h_a^2 + \frac{dw}{dx} = 0 \quad (6)$$

Similarly, the shear stress free condition at the bottom surface of the lower material layer ( $\tau_b = G_b \gamma_b = 0$  at  $y_b = -h_b/2$ ) can be employed to get the following equation

$$-\theta_b - \alpha_b h_b + \frac{3}{4} \beta_b h_b^2 + \frac{dw}{dx} = 0 \quad (7)$$

Now, substituting  $y_a = -h_a/2$  in Eq. (1), the longitudinal displacement at the bottom surface of the upper material layer  $\bar{u}_a$  can be expressed as

$$\bar{u}_a = u_{a0} + \frac{h_a}{2} \theta_a + \alpha_a \frac{h_a^2}{4} - \beta_a \frac{h_a^3}{8} \quad (8)$$

Similarly, substituting  $y_b = h_b/2$  in Eq. (2), the longitudinal displacement at the top surface of the lower material layer  $\bar{u}_b$  can be expressed as

$$\bar{u}_b = u_{b0} - \frac{h_b}{2} \theta_b + \alpha_b \frac{h_b^2}{4} + \beta_b \frac{h_b^3}{8} \quad (9)$$

These four equations (6-9) are used to eliminate the four higher order non-physical terms ( $\alpha_a, \beta_a, \alpha_b, \beta_b$ ) appeared in Eqs. (1) and (2) are these two equations (1-2) are rewritten as

$$u_a = A_a u_{a0} + B_a \bar{u}_a + C_a \theta_a + D_a \phi \quad (10)$$

$$u_b = A_b u_{b0} + B_b \bar{u}_b + C_b \theta_b + D_b \phi \quad (11)$$

where the parameters  $A, B, C$  and  $D$  are functions of  $y$ , cross-sectional properties of the two layers and their material properties. The explicit expression of these parameters are as follows:

$$\begin{aligned} A_a &= 1 - \frac{12}{5h_a^2} y_a^2 + \frac{16}{5h_a^3} y_a^3, & B_a &= \frac{12}{5h_a^2} y_a^2 - \frac{16}{5h_a^3} y_a^3, & C_a &= -y_a - \frac{4}{5h_a} y_a^2 + \frac{12}{5h_a^2} y_a^3, \\ D_a &= -\frac{2}{5h_a} y_a^2 - \frac{4}{5h_a^2} y_a^3, & A_b &= 1 - \frac{12}{5h_b^2} y_b^2 - \frac{16}{5h_b^3} y_b^3, & B_b &= \frac{12}{5h_b^2} y_b^2 + \frac{16}{5h_b^3} y_b^3, \\ C_b &= -y_b + \frac{4}{5h_b} y_b^2 + \frac{12}{5h_b^2} y_b^3, & D_b &= \frac{2}{5h_b} y_b^2 - \frac{4}{5h_b^2} y_b^3. \end{aligned}$$

In the above equations,  $\phi$  ( $=dw/dx$ ) is taken as an independent field variable to have a straightforward  $C^0$  continuous formulation for its finite element implementation and avoid  $C^1$  continuous formulation.

## 2.2. Variational Formulations and its Finite Element Implementation

The equilibrium equation can be derived using the principle of virtual work and it can be expressed as

$$\int_x \int_{A_a} \{\delta \boldsymbol{\varepsilon}\}_a^T \{\boldsymbol{\sigma}\}_a dA dx + \int_x \int_{A_b} \{\delta \boldsymbol{\varepsilon}\}_b^T \{\boldsymbol{\sigma}\}_b dA dx + \int_x \delta s \tau_{sh} dx = \int_x \delta w q dx, \quad (12)$$

where  $\delta$  is an operate to show the variation of any parameter,  $\{\boldsymbol{\varepsilon}\}_a$  and  $\{\boldsymbol{\varepsilon}\}_b$  are strain vectors (consisting of longitudinal normal and transverse shear strains) of the upper and lower layers respectively,  $\{\boldsymbol{\sigma}\}_a$  and  $\{\boldsymbol{\sigma}\}_b$  are stress vectors (consisting of longitudinal normal and transverse shear stresses) of these layers,  $\tau_{sh}$  is the distributed shear force (per unit length) at their interface,  $q$  is the distributed external load (per unit length) acting on the beam and  $A$  represents the cross-sectional area.

From Eqs. (10) and (11), the Green-Lagrange strain vector [27] at a point within a material layer may be written as

$$\begin{aligned} \{\boldsymbol{\varepsilon}\}_k &= \begin{Bmatrix} \boldsymbol{\varepsilon}_k \\ \boldsymbol{\gamma}_k \end{Bmatrix} = \begin{Bmatrix} \frac{\partial u}{\partial x} \\ \frac{\partial u}{\partial y} + \frac{\partial w}{\partial x} \end{Bmatrix} + \begin{Bmatrix} \frac{1}{2} \left[ \left( \frac{\partial u}{\partial x} \right)^2 + \left( \frac{\partial w}{\partial x} \right)^2 \right] \\ 0 \end{Bmatrix} \\ &= \{\boldsymbol{\varepsilon}_L\}_k + \{\boldsymbol{\varepsilon}_N\}_k, \end{aligned} \quad (13)$$

where  $\{\boldsymbol{\varepsilon}_L\}_k$  and  $\{\boldsymbol{\varepsilon}_N\}_k$  are the linear and nonlinear strain vectors in which the index  $k = a$  for the upper layer and  $k = b$  for the lower layer. The linear strain vectors may be written in terms of the cross-sectional matrix  $[H_L]_k$  and the one dimensional strain vector  $\{\bar{\boldsymbol{\varepsilon}}_L\}_k$  as

$$\{\boldsymbol{\varepsilon}_L\}_k = [H_L]_k \{\bar{\boldsymbol{\varepsilon}}_L\}_k, \quad (14)$$

$$\text{where, } [H_L]_k = \begin{bmatrix} A_k & B_k & C_k & D_k & 0 & 0 & 0 & 0 & 0 \\ 0 & 0 & 0 & 0 & \frac{dA_k}{dy_k} & \frac{dB_k}{dy_k} & \frac{dC_k}{dy_k} & \frac{dD_k}{dy_k} & 1 \end{bmatrix}, \quad (15)$$

$$\text{and } \{\bar{\boldsymbol{\varepsilon}}_L\}_k^T = \left( \frac{du_{k0}}{dx} \quad \frac{d\bar{u}_k}{dx} \quad \frac{d\theta_k}{dx} \quad \frac{d\phi}{dx} \quad u_{k0} \quad \bar{u}_k \quad \theta_k \quad \phi \quad \frac{dw}{dx} \right). \quad (16)$$

For the finite element implementation of the proposed beam model, a displacement based quadratic isoparametric beam element with three nodes is used to have a simple formulation and no unexpected numerical inconsistencies. A typical element having a length of  $l_e$  is shown in Fig. 2. However, a displacement based formulation can have locking problem, which is eliminated by using the field consistent technique [28]. The field variables of the

element are  $u_{a0}$ ,  $\bar{u}_a$ ,  $\theta_a$ ,  $w$ ,  $\phi$ ,  $u_{b0}$ ,  $\bar{u}_b$  and  $\theta_b$ , and these are expressed in terms of their nodal unknowns using interpolation functions of the element  $N_j$  [27] as follows.

$$\begin{aligned}
 u_{a0} &= \sum_{j=1}^3 N_j u_{a0j}, \quad \bar{u}_a = \sum_{j=1}^3 N_j \bar{u}_{aj}, \quad \theta_a = \sum_{j=1}^3 N_j \theta_{aj}, \quad w = \sum_{j=1}^3 N_j w_j, \\
 u_{b0} &= \sum_{j=1}^3 N_j u_{b0j}, \quad \bar{u}_b = \sum_{j=1}^3 N_j \bar{u}_{bj}, \quad \theta_b = \sum_{j=1}^3 N_j \theta_{bj}, \quad \phi = \sum_{j=1}^3 N_j \phi_j.
 \end{aligned} \tag{17}$$

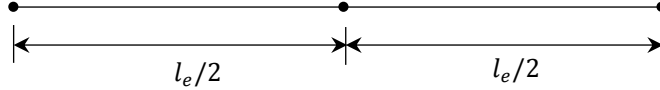


Fig. 2. Three noded beam element

Using Eq. (17), the one dimensional strain vectors (16) can be expressed as

$$\{\bar{\epsilon}_L\}_k = \begin{bmatrix} [B_L^1]_k & [B_L^2]_k & [B_L^3]_k \end{bmatrix} \begin{Bmatrix} \{\Delta_1\} \\ \{\Delta_2\} \\ \{\Delta_3\} \end{Bmatrix} = [B_L]_k \{\Delta\}, \tag{18}$$

where a typical component of the strain-displacement matrix  $[B_L^j]_k$  corresponding to node  $j$  (1, 2 or 3) is:

$$[B_L^j]_a = \begin{bmatrix} \frac{dN_j}{dx} & 0 & 0 & 0 & 0 & 0 & 0 & 0 \\ 0 & \frac{dN_j}{dx} & 0 & 0 & 0 & 0 & 0 & 0 \\ 0 & 0 & \frac{dN_j}{dx} & 0 & 0 & 0 & 0 & 0 \\ 0 & 0 & 0 & 0 & \frac{dN_j}{dx} & 0 & 0 & 0 \\ N_j & 0 & 0 & 0 & 0 & 0 & 0 & 0 \\ 0 & N_j & 0 & 0 & 0 & 0 & 0 & 0 \\ 0 & 0 & N_j & 0 & 0 & 0 & 0 & 0 \\ 0 & 0 & 0 & 0 & N_j & 0 & 0 & 0 \\ 0 & 0 & 0 & \frac{dN_j}{dx} & 0 & 0 & 0 & 0 \end{bmatrix},$$

$$[B_L^j]_b = \begin{bmatrix} 0 & 0 & 0 & 0 & 0 & \frac{dN_j}{dx} & 0 & 0 \\ 0 & 0 & 0 & 0 & 0 & 0 & \frac{dN_j}{dx} & 0 \\ 0 & 0 & 0 & 0 & 0 & 0 & 0 & \frac{dN_j}{dx} \\ 0 & 0 & 0 & 0 & \frac{dN_j}{dx} & 0 & 0 & 0 \\ 0 & 0 & 0 & 0 & 0 & N_j & 0 & 0 \\ 0 & 0 & 0 & 0 & 0 & 0 & N_j & 0 \\ 0 & 0 & 0 & 0 & 0 & 0 & 0 & N_j \\ 0 & 0 & 0 & 0 & N_j & 0 & 0 & 0 \\ 0 & 0 & 0 & \frac{dN_j}{dx} & 0 & 0 & 0 & 0 \end{bmatrix}$$

and the nodal displacement vector is:

$$\{\Delta_j\} = \left\{ u_{c0j} \quad \bar{u}_{cj} \quad \theta_{cj} \quad w_j \quad \phi_j \quad u_{s0j} \quad \bar{u}_{sj} \quad \theta_{sj} \right\}^T, j = 1, 2 \text{ or } 3.$$

Now the nonlinear strain vectors may be expressed as

$$\{\epsilon_N\}_k = \frac{1}{2} \begin{bmatrix} \frac{du}{dx} & \frac{dw}{dx} \\ 0 & 0 \end{bmatrix} \begin{Bmatrix} \frac{du}{dx} \\ \frac{dw}{dx} \end{Bmatrix} = \frac{1}{2} [A]_k \{\theta\}_k. \quad (19)$$

The vectors  $\{\theta\}_k$  of the two layers may be expressed in terms of their cross-sectional matrices  $[H_N]_k$  and one dimensional strain vectors  $\{\epsilon_{N\theta}\}_k$  (dependent on  $x$  only) as

$$\{\theta\}_k = [H_N]_k \{\epsilon_{N\theta}\}_k, \quad (20)$$

$$\text{where, } [H_N]_k = \begin{bmatrix} A_k & B_k & C_k & D_k & 0 \\ 0 & 0 & 0 & 0 & 1 \end{bmatrix}, \quad (21)$$

$$\text{and } \{\epsilon_{N\theta}\}_k^T = \left( \frac{du_{k0}}{dx} \quad \frac{d\bar{u}_k}{dx} \quad \frac{d\theta_k}{dx} \quad \frac{d\phi}{dx} \quad \frac{dw}{dx} \right). \quad (22)$$

The matrix  $[A]_k$  in Eq. (19) is dependent on displacements of the beam and is evaluated for updating in each iteration within the solution scheme of the nonlinear governing equations utilising  $\{\theta\}_k$ .

The one dimensional strain vector shown in Eq. (22) can be expressed in terms of the nodal displacement using Eq. (17) as

$$\{\varepsilon_{N\theta}\}_k = \begin{bmatrix} [G_1]_k & [G_2]_k & [G_3]_k \end{bmatrix} \begin{Bmatrix} \{\Delta_1\} \\ \{\Delta_2\} \\ \{\Delta_3\} \end{Bmatrix} = [G]_k \{\Delta\}, \quad (23)$$

where

$$[G_j]_a = \begin{bmatrix} \frac{dN_j}{dx} & 0 & 0 & 0 & 0 & 0 & 0 & 0 \\ 0 & \frac{dN_j}{dx} & 0 & 0 & 0 & 0 & 0 & 0 \\ 0 & 0 & \frac{dN_j}{dx} & 0 & 0 & 0 & 0 & 0 \\ 0 & 0 & 0 & 0 & \frac{dN_j}{dx} & 0 & 0 & 0 \\ 0 & 0 & 0 & \frac{dN_j}{dx} & 0 & 0 & 0 & 0 \end{bmatrix}, j = 1, 2 \text{ or } 3$$

$$\text{and } [G_j]_b = \begin{bmatrix} 0 & 0 & 0 & 0 & 0 & \frac{dN_j}{dx} & 0 & 0 \\ 0 & 0 & 0 & 0 & 0 & 0 & \frac{dN_j}{dx} & 0 \\ 0 & 0 & 0 & 0 & 0 & 0 & 0 & \frac{dN_j}{dx} \\ 0 & 0 & 0 & 0 & \frac{dN_j}{dx} & 0 & 0 & 0 \\ 0 & 0 & 0 & \frac{dN_j}{dx} & 0 & 0 & 0 & 0 \end{bmatrix}, j = 1, 2 \text{ or } 3.$$

Employing the above Eqs. (14), (18), (19), (20) and (23), the total strain vector of Eq. (13) can be expressed as

$$\{\varepsilon\}_k = \left( [H_L]_k [B_L]_k + \frac{1}{2} [A]_k [H_N]_k [G]_k \right) \{\Delta\} = \left( [\bar{B}_L]_k + \frac{1}{2} [\bar{B}_N]_k \right) \{\Delta\}. \quad (24)$$

Taking the variation of Eq. (24), the incremental strain vector can be obtained [27] and be expressed as

$$\{\delta\varepsilon\}_k = \left( [H_L]_k [B_L]_k + [A]_k [H_N]_k [G]_k \right) \{\delta\Delta\} = \left( [\bar{B}_L]_k + [\bar{B}_N]_k \right) \{\delta\Delta\} = [\bar{B}]_k \{\delta\Delta\}. \quad (25)$$

Similarly, the slip at the interface between the two layers (4) can be expressed in terms of the nodal displacement vector as

$$s = (\bar{u}_b - \bar{u}_a) = \begin{bmatrix} [B_1]_{sh} & [B_2]_{sh} & [B_3]_{sh} \end{bmatrix} \begin{Bmatrix} \{\Delta_1\} \\ \{\Delta_2\} \\ \{\Delta_3\} \end{Bmatrix} = [B]_{sh} \{\Delta\}, \quad (26)$$

where  $[B_j]_{sh} = [0 \ N_j \ 0 \ 0 \ 0 \ 0 \ -N_j \ 0]$ ,  $j = 1, 2 \text{ or } 3$ .

As there is no nonlinear term in the expression of the interfacial slip (26), the incremental slip can simply be written as

$$\delta s = [B]_{sh} \{\delta \Delta\} \quad (27)$$

The virtual work done by an externally applied distributed load  $q$  can be expressed in terms of the nodal load vector  $\{F\}$  as

$$\int \delta w q dx = \{\delta \Delta\}^T \{F\}, \quad (28)$$

$$\text{where, } \{F\} = \int \left[ [N_1] \quad [N_2] \quad [N_3] \right]^T q dx = \int [N]^T q dx \quad (29)$$

in which  $[N_j] = [0 \ 0 \ 0 \ N_j \ 0 \ 0 \ 0 \ 0]$ ,  $j = 1, 2$  or  $3$ .

Substituting Eqs. (25), (27) and (28) into Eq. (12), the equilibrium equation can be obtained and expressed as

$$\int_x \int_{A_a} [\bar{B}]_a^T \{\sigma\}_a dA dx + \int_x \int_{A_b} [\bar{B}]_b^T \{\sigma\}_b dA dx + \int_x [B]_{sh}^T \tau_{sh} dx = \int_x [N]^T q dx. \quad (30)$$

### 2.3. Incremental Equilibrium Equation

The stresses in the above equation (30) can be expressed in terms of strains using appropriate constitutive relationships and these strains can subsequently be expressed in terms of nodal displacements. However, this resulting equation cannot be solved for displacements or nodal displacements directly due to the occurrence of the displacement dependent nonlinear components of the strain displacement matrices. Thus the equation (30) is solved iteratively which will help to update and improve the displacement values successively and this iterative process will be continued until an acceptable level of accuracy is achieved. This can be quantified with the norm of residual force vector which should be less than a user defined tolerance to stop the iteration. The residual force vector  $\{\delta R\}$  will be obtained from Eq. (30) and it can be expressed as

$$\{\delta R\} = \int_x [N]^T q dx - \left( \int_x \int_{A_a} [\bar{B}]_a^T \{\sigma\}_a dA dx + \int_x \int_{A_b} [\bar{B}]_b^T \{\sigma\}_b dA dx + \int_x [B]_{sh}^T \tau_{sh} dx \right). \quad (31)$$

The Newton-Raphson technique will be used for the iterative solution of the nonlinear equilibrium equation (30) which needs an incremental form of this equation. This can be obtained by taking a variation of the equilibrium equation with respect to displacements as

$$\begin{aligned} & \int_x \int_{A_a} [\delta \bar{B}]_a^T \{\delta \sigma\}_a dA dx + \int_x \int_{A_a} [\bar{B}]_a^T \{\delta \sigma\}_a dA dx + \int_x \int_{A_b} [\delta \bar{B}]_b^T \{\sigma\}_b dA dx \\ & + \int_x \int_{A_b} [\bar{B}]_b^T \{\delta \sigma\}_b dA dx + \int_x [\bar{B}]_{sh}^T \delta \tau_{sh} dx = \{\delta R\}. \end{aligned} \quad (32)$$

The incremental strain displacement matrix of a material layer used in the above equation can be expressed by invoking Eq. (25) as

$$[\delta \bar{B}]_k = [\delta \bar{B}_N]_k = [\delta A]_k [H_N]_k [G]_k. \quad (33)$$

Again, the incremental stress vector of a layer can be expressed by invoking Eq. (25) as

$$\{\delta \sigma\}_k = [D]_k \{\delta \epsilon\}_k = [D]_k ([\bar{B}_L]_k + [\bar{B}_N]_k) \{\delta \Delta\}. \quad (34)$$

The constitutive matrix  $[D]_k$  used in the above equation can be expressed as

$$[D]_k = \begin{bmatrix} E_k & 0 \\ 0 & G_k \end{bmatrix}, \quad (35)$$

where  $E_k$  and  $G_k$  are the elastic modulus and shear modulus of the  $k^{\text{th}}$  material layer.

The incremental interfacial shear force can be expressed in terms of the incremental slip as

$$\delta \tau_{sh} = k_{sh} \delta s, \quad (36)$$

where  $k_{sh}$  is the spring stiffness for the shear connectors.

In the proposed finite element formulation,  $dw/dx$  is taken as an independent field variable  $\phi$  (see Eqs. (10) and (11)), which has introduced a mathematical inconsistency, since  $\phi$  can be obtained from  $w$  by taking its derivative, i.e.,  $\phi$  is dependent on  $w$ . In order to avoid this inconsistency, a penalty function approach [29] is used to satisfy a constraint condition  $(dw/dx) - \phi = 0$  variationally which leads to an additional strain energy as follows

$$U_p = \frac{1}{2} \int_x k_p \left( \frac{dw}{dx} - \phi \right)^2 dx \quad (37)$$

where  $k_p$  is the penalty stiffness parameter which is usually having a large value.

Using Eq. (17), the constraint condition can be expressed in terms of the nodal displacement vector as

$$\frac{dw}{dx} - \phi = \begin{bmatrix} [B_p^1] \\ [B_p^2] \\ [B_p^3] \end{bmatrix} \begin{Bmatrix} \{\Delta_1\} \\ \{\Delta_2\} \\ \{\Delta_3\} \end{Bmatrix} = [B_p] \{\Delta\} \quad (38)$$

where  $[B_p] = [0 \ 0 \ 0 \ \frac{dN_j}{dx} \ -N_j \ 0 \ 0 \ 0]$ ,  $j = 1, 2$  or  $3$ .

After substitution of Eqs. (33) to (38) into Eq. (32), the incremental equilibrium equation can finally be written as

$$[K_T] \{\delta\Delta\} = \{\delta\mathcal{R}\}. \quad (39)$$

The tangent stiffness matrix  $[K_T]$  used in the above equation can conveniently be expressed in terms of linear, nonlinear and geometric stiffness matrices ( $[K_L]$ ,  $[K_N]$ ,  $[K_\sigma]$ ) as

$$[K_T] = [K_L] + [K_N] + [K_\sigma], \quad (40)$$

where these matrices can be expressed with the help of the above equations as follow:

$$\begin{aligned} [K_L] = & \int_x [B_L]_a^T \left( \int_{A_a} [H_L]_a^T [D]_a [H_L]_a dA \right) [B_L]_a dx + \int_x [B_L]_b^T \left( \int_{A_b} [H_L]_b^T [D]_b [H_L]_b dA \right) [B_L]_b dx \\ & + \int_x [B]_{sh}^T k_{sh} [B]_{sh} dx + \int_x [B_p]^T k_p [B_p] dx, \end{aligned} \quad (41)$$

$$\begin{aligned} [K_N] = & \int_x [B_L]_a^T \left( \int_{A_a} [H_L]_a^T [D]_a [A]_a [H_N]_a dA \right) [G]_a dx + \int_x [B_L]_b^T \left( \int_{A_b} [H_L]_b^T [D]_b [A]_b [H_N]_b dA \right) [G]_b dx \\ & + \int_x [G]_a^T \left( \int_{A_a} [H_N]_a^T [A]_a^T [D]_a [H_L]_a dA \right) [B_L]_a dx + \int_x [G]_b^T \left( \int_{A_b} [H_N]_b^T [A]_b^T [D]_b [H_L]_b dA \right) [B_L]_b dx \\ & + \int_x [G]_a^T \left( \int_{A_a} [H_N]_a^T [A]_a^T [D]_a [A]_a [H_N]_a dA \right) [G]_a dx + \int_x [G]_b^T \left( \int_{A_b} [H_N]_b^T [A]_b^T [D]_b [A]_b [H_N]_b dA \right) [G]_b dx, \end{aligned} \quad (42)$$

$$[K_\sigma] = \int_x [G]_a^T \left( \int_{A_a} [H_N]_a^T \sigma_a [H_N]_a dA \right) [G]_a dx + \int_x [G]_b^T \left( \int_{A_b} [H_N]_b^T \sigma_b [H_N]_b dA \right) [G]_b dx. \quad (43)$$

The system of nonlinear equations is solved using the incremental equilibrium equation (39) and other equations such as Eq. (32) where an incremental integrative approach of solution is adopted so as to avoid any possible divergence. The entire load is divided into a number of load steps and they are applied gradually in increments where the iterative solution

technique is activated within each load step. The iteration within a load step is stopped once the following condition is satisfied.

$$\frac{\sqrt{\{\delta R\}^T \{\delta R\}}}{\sqrt{\{F\}^T \{F\}}} \times 100 \leq Tol \quad (44)$$

where *Tol* is the tolerance for convergence and it is taken as 0.1% in the present study.

### 3. NUMERICAL RESULTS

#### 3.1. Simply Supported Composite Beam with Rectangular Section

An example of a 1000 mm long two layered composite beam, subjected to a uniformly distributed load, studied by Hjjaj et al. [22] is considered in this section for the validation of the proposed one dimensional nonlinear finite element model. The cross-section of the beam is 200 mm wide and 50 mm deep and it consists of two identical layers (each 200 mm wide and 25 mm deep) where the shear stiffness at their interface is 1000 MPa/mm. The modulus of elasticity is 10 GPa for the upper layer and 1 GPa for the lower layer whereas the Poisson's ratio is 0.3 for both material layers. The ends of the beam are pinned at mid-depth.

The finite element model of Hjjaj et al. [22] is based on TBT but they have also shown results based on EBT. The proposed model is derived using HBT but the formulation can easily be modified to accommodate a lower order beam theory (e.g., TBT, EBT) by elimination of a few terms of Eqs. (1) and (2). The composite beam is analysed with the proposed approach using different number of beam elements (Fig. 2) and the results confirmed that 30 beam elements, which generates a total degrees of freedom of 488, are adequate to achieve a convergent solution. The number of load increments used for solving the problem was 50 where the maximum number of iterations required to get a converged solution within a load increment was 4. The whole analysis required 120 iterations and a computing time of 4.9 sec where an ordinary desktop computer (i5-3470T CPU @ 2.90 GHz and RAM 8.0 GB, 64 bit operating system) is used.

The variation of the mid-span deflection with respect to the distributed load acting vertically downward, found in the present analysis using HBT as well as TBT, is presented in Fig. 3 along with that found by Hjjaj et al. [22] using TBT and EBT. The figure also includes results obtained from a detailed two dimensional (2D) finite element analysis of the composite beam

utilising a commercially available finite element code (ABAQUS). The entire beam is modelled with ABAQUS using four node plane stress (CPS4R) rectangular elements laying in the vertical plane where 50 elements are used along the beam length and 20 elements are used along the entire depth. This specific mesh size produced a total DOF of 2142. The analysis is carried in a similar manner using 50 load increments but the maximum number of iterations required within a load increment was 10 for this 2D analysis. The same computer is used for running this 2D analysis where the computing time consumed was 1 minute 40 sec for solving the whole problem. It should be noted that the solver used by ABAQUS is expected to be more efficient than a relatively simple solver used in the computer program (FORTRAN) developed for implementing the proposed model. Moreover, it needs a significant amount of time for model generation in ABAQUS. The interface of the two material layers is simulated with the cohesive contact model. Fig. 3 shows reasonable agreement between the results produced by the different models. However, the performance of the proposed one dimensional (1D) model based on HBT is found to be most superior amongst 1D models when compared with the results based on the 2D finite element model.

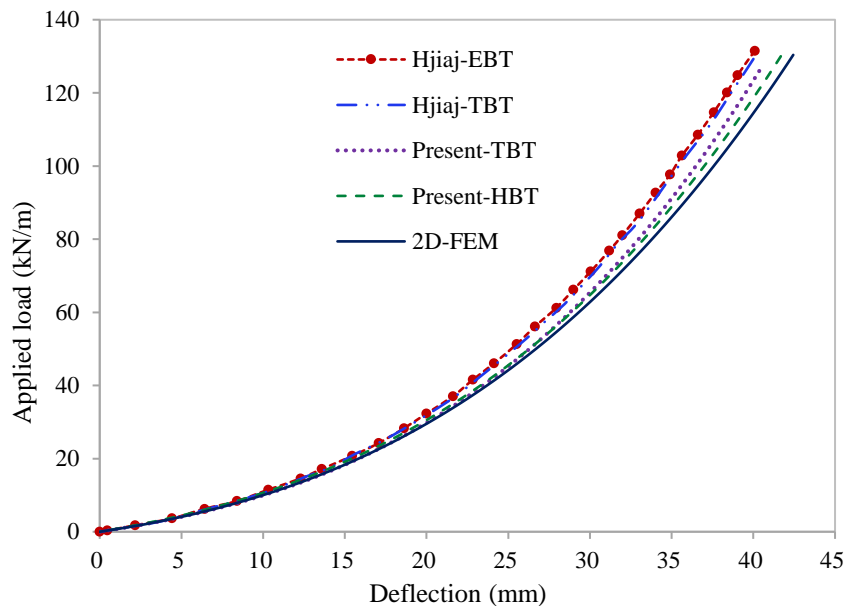


Fig. 3. Mid-span deflection of the composite beam with rectangular section (50 mm deep).

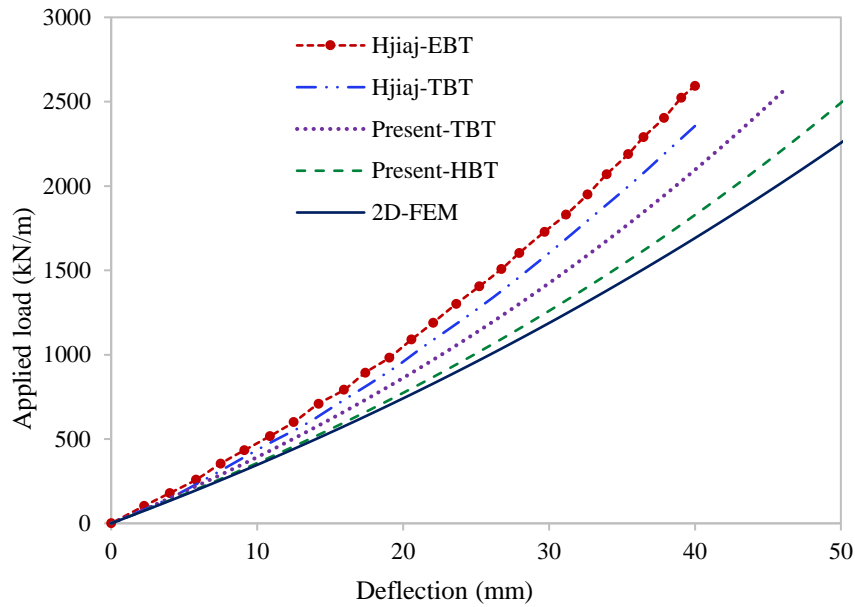


Fig. 4. Mid-span deflection of the composite beam with rectangular section (200 mm deep).

Hjiiaj et al. [22] have investigated the problem by changing the depth of the beam as 200 mm (each layer 100 mm thick) in order to have a beam having lower span to depth ratio, which should help to highlight the improvement of their TBT model over the EBT model. This 200 mm thick beam is also analysed with the proposed model (HBT) and compared with TBT as well as the 2D finite element model, the results obtained for the mid-span deflection are plotted in Fig. 4. It has followed a similar trend but the deviation of the results obtained by the different models are magnified as expected.

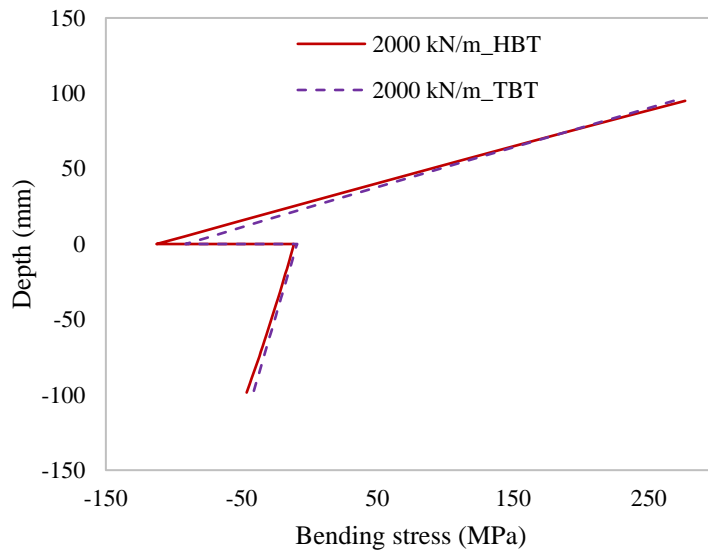


Fig. 5. Bending stress at mid-span of the composite beam with rectangular section (200 mm deep).

The variation of bending stress over the depth of this beam (200 mm deep) at mid-span as predicted by the proposed models is plotted in Fig. 5. It shows that HBT predicts a higher value of the bending stress at critical points. In a similar manner, the variation of shear stress over the beam depth found in the present analysis at the quarter span and support of the beam is presented in Fig. 6 and Fig. 7 respectively. The figures clearly indicate that TBT is not capable of predicting the actual variation of shear stress.

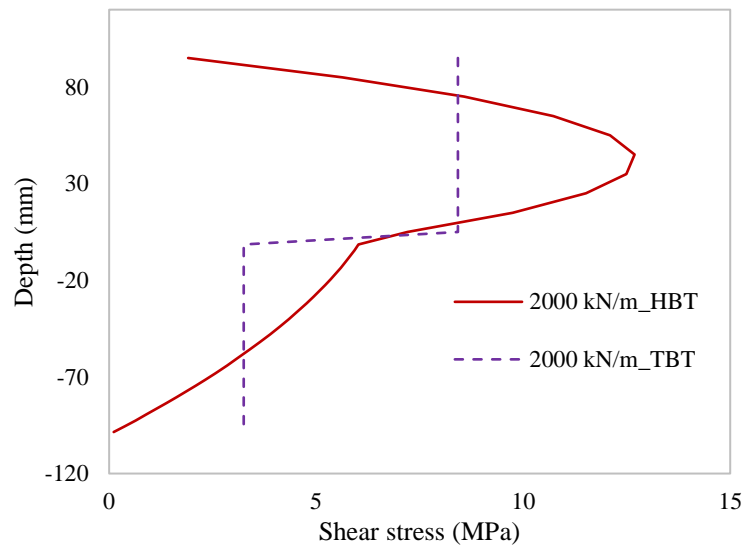


Fig. 6. Shear stress at quarter-span of the composite beam with rectangular section (200 mm deep).

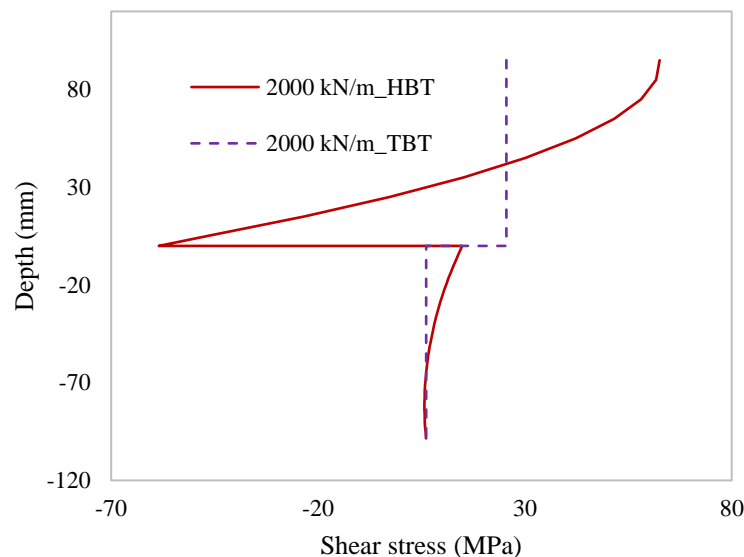


Fig. 7. Shear stress at a support of the composite beam with rectangular section (200 mm deep).

### 3.2. Simply Supported Composite Beam with T-section

An 8.0 m long two layered composite beam having a T-section as shown in Fig. 8 is considered in this example. The material properties of the two layers are taken as:  $E_I = 26$  GPa (modulus of elasticity of layer-I),  $\nu_I = 0.15$  (Poisson's ratio of layer-I),  $E_{II} = 200$  GPa and  $\nu_{II} = 0.3$ . The interfacial stiffness of the shear connectors is taken as 11.70 MPa. The beam is simply supported at its two ends and subjected to a uniformly distributed load, with a maximum magnitude of 4500 kN/m. The composite beam is analysed with the proposed 1D finite element model based on HBT as well as ABAQUS model where the beam is modelled in 2D laying in the vertical plane, where the thickness of the layers are explicitly modelled as 500 mm and 150 mm for modelling Layer-I and Layer-II respectively as shown in Fig. 8. The solution of this composite beam problem also required 30 beam elements (total DOF: 488) and the analysis is also carried with 50 load increments where the maximum number iteration required in a load increment was 3. The total number of iterations required for these 50 load increments was 100 which required a computing time of 4.6 sec. On the other hands, the 2D finite element model (ABAQUS) required a total DOF of 1134 which required a computing time of 1 min and 30sec for the whole solution consisting of 50 load increments.

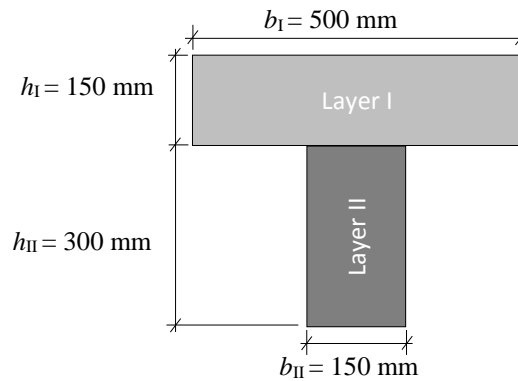


Fig. 8. Cross-section of the 8 m long simply supported composite beam

The load-deflection curve obtained from both modelling techniques at mid-span and quarter-span sections of the beam is plotted in Fig. 9 which shows very good agreement between the results. The variation of deflection along the length of the beam obtained from both models for load intensity of 2000 kN/m, 3000 kN/m and 4500 kN/m is presented in Fig. 10. All these results show a good and consistent performance of the proposed model.

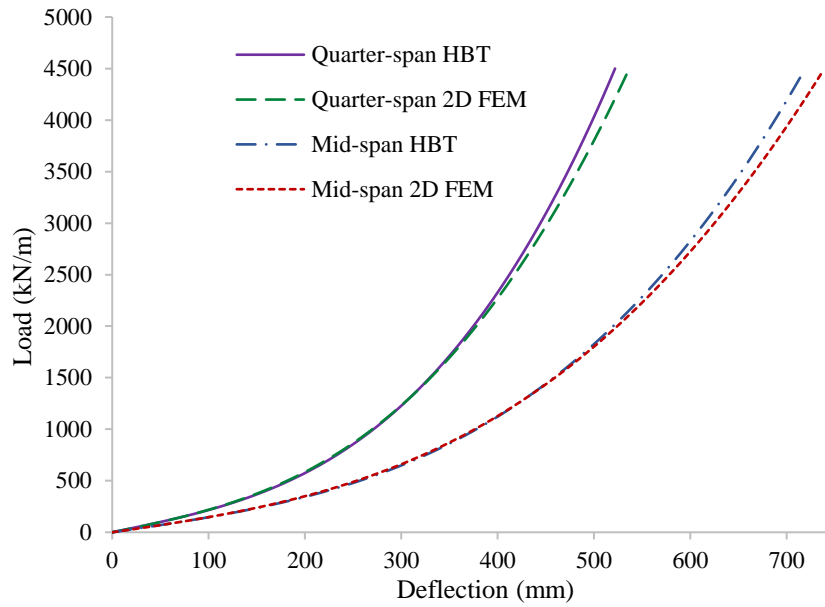


Fig. 9. Deflection at mid-span and quarter-span of the simply supported composite beam with T section (Fig. 8).

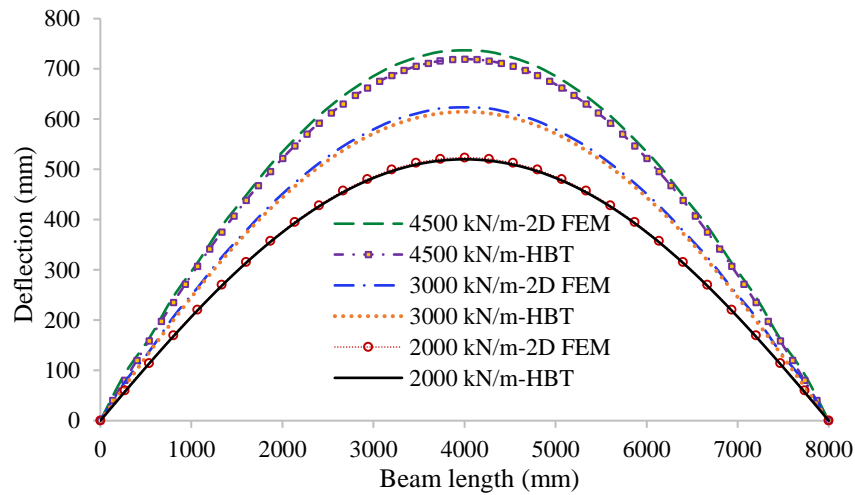


Fig. 10. Deflection along the length of the simply supported composite beam with T section (Fig. 8).

### 3.3. Composite Beam with Fixed Supports at Two Ends

The behaviour of a 2 m long two layered composite beam having a rectangular section and fixed supports at its ends (Fig. 11) is studied in this section. It includes the response of the beam in geometric nonlinear (GNL) and linear (GL) ranges considering flexible (PI) and strong (FI) interfaces taking the value of  $k_{sh}$  as 70 MPa and  $1.0 \times 10^{15}$  MPa respectively and these results are produced by the proposed model according to HBT as well as TBT. The beam is subjected to a uniformly distributed load, which is increased incrementally from zero to 100 kN/mm to trace the entire nonlinear response. This specific problem is chosen

from the study [9], where analytical models have been developed based on TBT to predict the linear response of this beam taking simply supported boundary condition and interfacial properties.

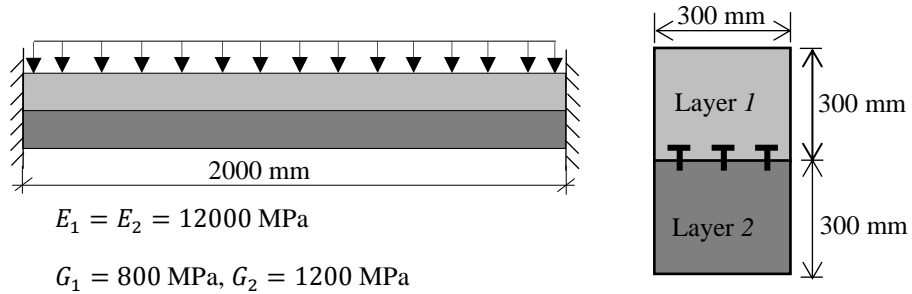


Fig. 11. Composite beam having fixed supports at its two ends

The computational time required for solving this problem was 8.1 sec (total number of iterations: 202) where 30 beam elements (total DOF: 488) and 100 load increments are used. The load deflection curves obtained at the mid-span section of the beam using different modelling options as mentioned above (GNL, GL, PI, FI, HBT and TBT) are plotted in Fig. 12, which show the relative performance of the different modelling techniques. The variation of deflection along the length of the beam obtained with the same modelling techniques is presented in Fig. 13 where all these results are corresponding to a load intensity of 50 kN/mm. Similarly, the variation of interfacial shear slip along the length of the beam having flexible interface ( $k_{sh} = 70 \text{ MPa}$ ) is plotted in Fig. 14, which shows an expected pattern of shear slip in a fixed beam problem.

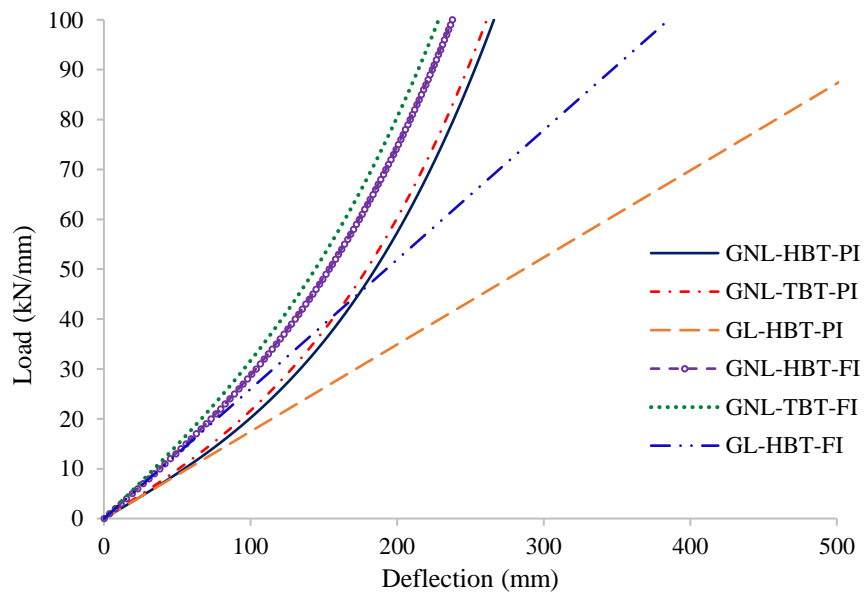


Fig. 12. Mid-span deflection of the fixed ended composite beam (Fig. 11).

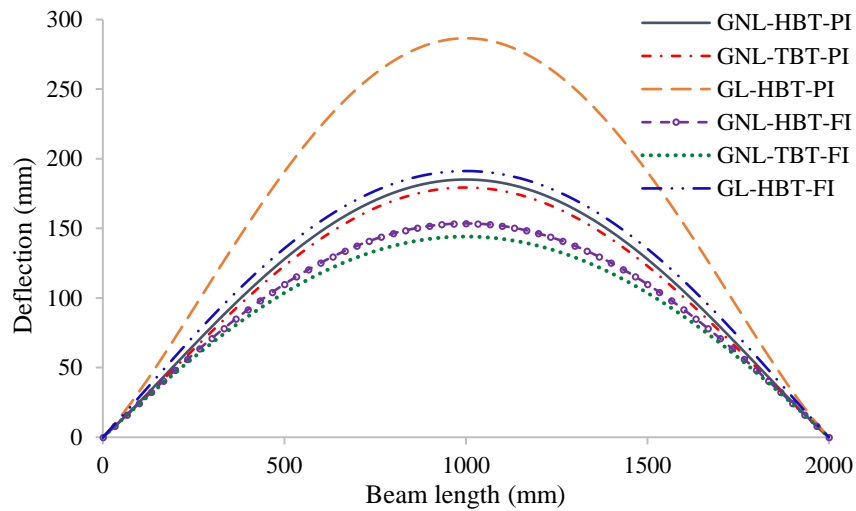


Fig. 13. Deflection of the fixed ended composite beam (Fig. 11) along its length under 50 kN/mm of loading

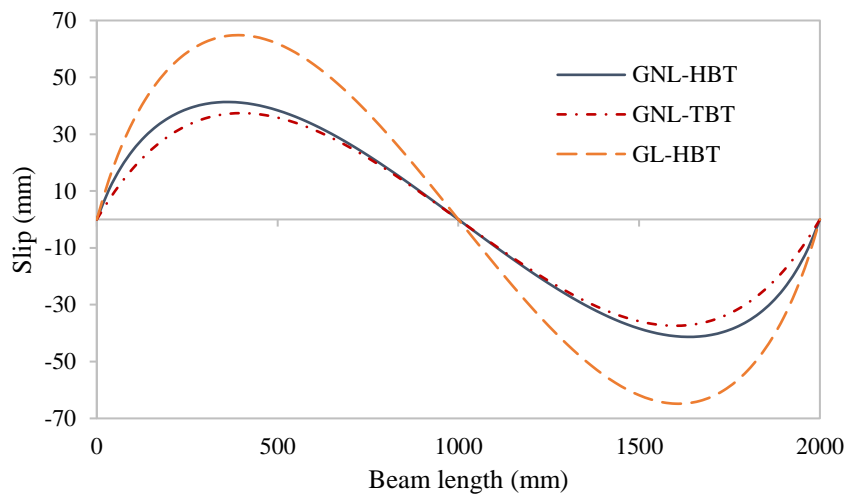


Fig. 14. Interfacial shear slip of the fixed ended composite beam (Fig. 11) along its length under 50 kN/mm of loading

For further investigation, the variation of bending stress over the beam depth obtained at one of the fixed ends using all these modelling techniques is presented in Fig. 15. It shows a significant deviation between the predictions made by HBT and TBT for the bending stress in all cases. In a similar manner, the variation of shear stress over the beam depth at a fixed end is presented in Fig. 16, which shows a huge difference between results predicted by HBT and TBT as expected. Similarly, through the depth variations of bending and shear stresses at the mid as well as quarter span section of the beam are presented in Fig. 17 and Fig. 18 respectively where a similar behaviour is observed.

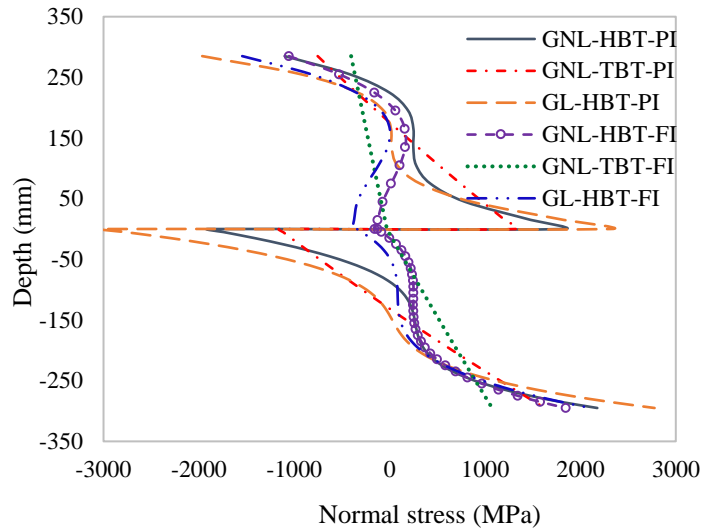


Fig. 15. Bending stress of the fixed ended composite beam (Fig. 11) at one of its end section under 50 kN/mm of loading.

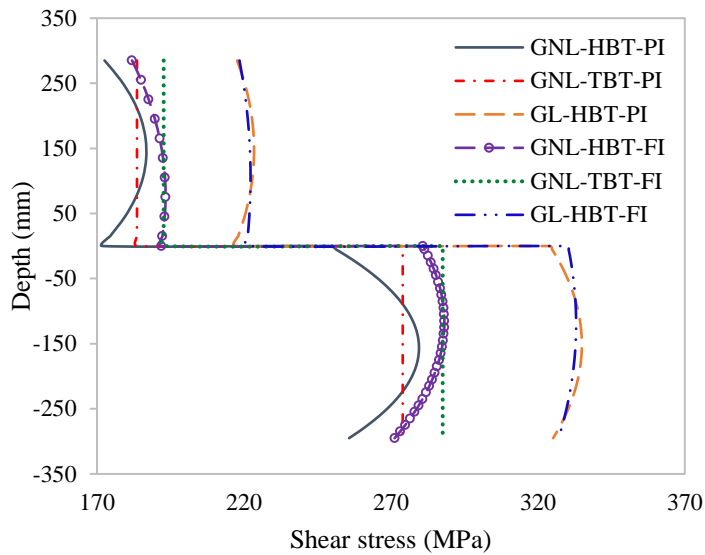


Fig. 16. Shear stress of the fixed ended composite beam (Fig. 11) at one of its end section under 50 kN/mm.

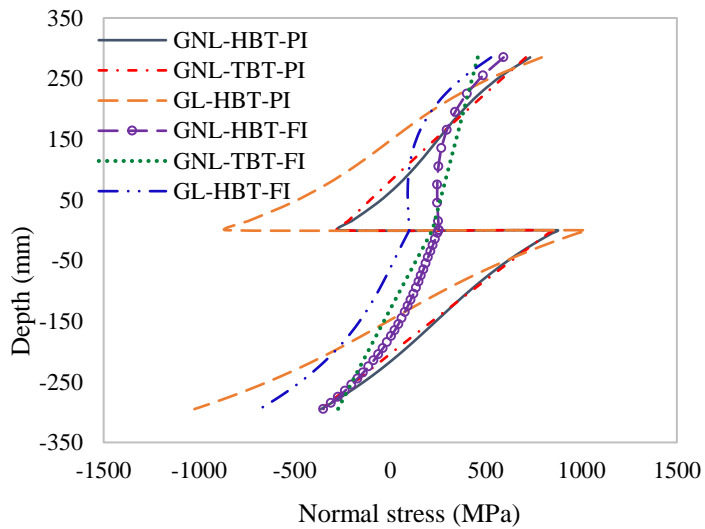


Fig. 17. Bending stress of the fixed ended composite beam (Fig. 11) at mid-span section under 50 kN/mm of loading.

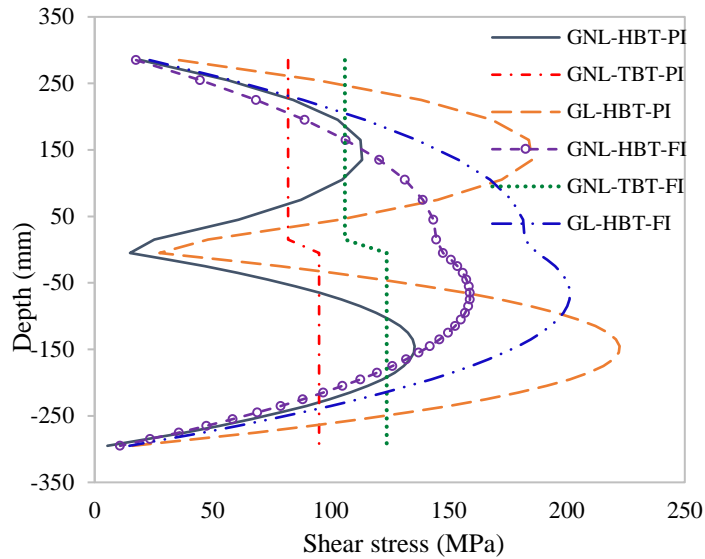


Fig. 18. Shear stress of the fixed ended composite beam (Fig. 11) at quarter-span section under 50 kN/mm of loading.

### 3.4. Steel-Concrete Composite Beam with Two Spans

A two-span continuous beam consists of a concrete slab and a steel I-girder connected by steel shear studs as shown in Fig. 19 is studied. The beam is fixed at the left end, pinned at the right end and having an intermediate roller support that divides the entire beam into two equal spans (Fig. 19). The beam is subjected to two identical point loads acting at the midpoint of these two spans as shown in Fig. 19 where each load  $P$  is varied from zero to 20,000 kN incrementally. The material properties of the concrete slab and the steel girder are taken as:  $E_c = 20,000$  MPa,  $E_s = 200,000$  MPa,  $\nu_c = 0.2$  and  $\nu_s = 0.25$ .

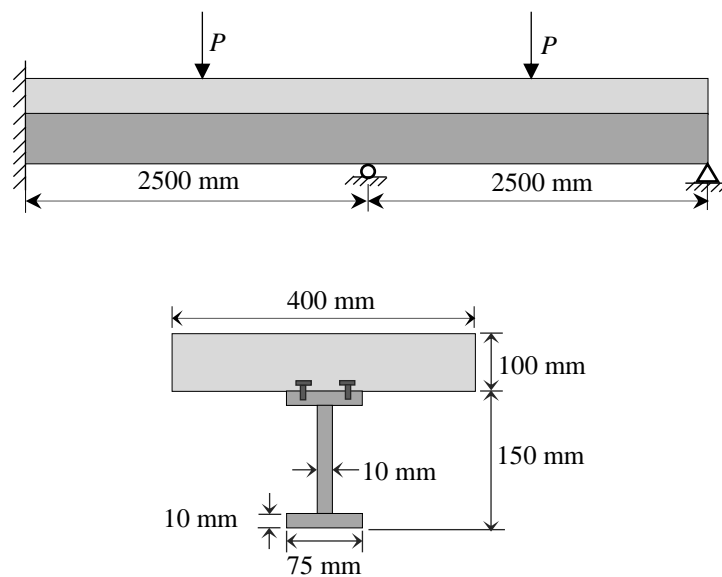


Fig. 19. Two-span steel concrete composite beam.

The beam is analysed with the proposed finite element model based on HBT and compared with TBT where the interfacial shear stiffness is taken as 10 MPa (PI) and  $1.0 \times 10^{15}$  MPa (FI). This problem also required 30 beam elements (total DOF: 488 DOF) and the analysis is carried with 100 load increments where the maximum number iteration required in a load increment was 5 for HBT as well as TBT. The total number of iteration required for these 100 load increments was 199 which required a computing time of 11 sec. The load-deflection curves obtained at the mid-point of these two spans are presented in Fig. 20 and Fig. 21. It is observed that the discrepancy between the deflections predicted by HBT and TBT is less for the flexible interface compared to the strong interface.

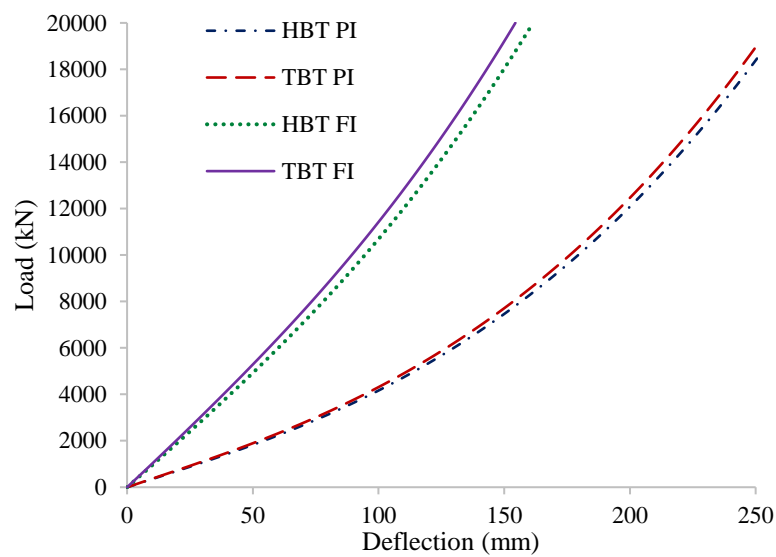


Fig. 20. Deflection under the point load on the left span of the two span composite beam (Fig. 19).

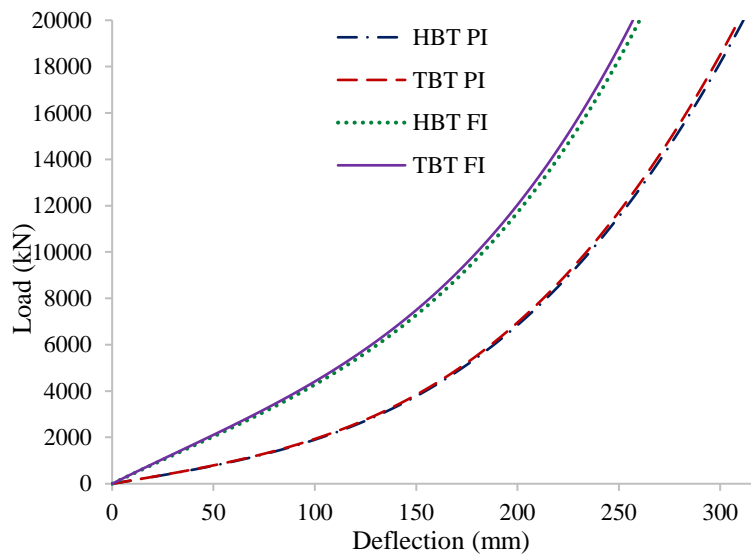


Fig. 21. Deflection under the point load on the right span of the two span composite beam (Fig. 19).

The variations of bending and shear stresses over the beam depth obtained at the mid-point of the left span corresponding to the highest load ( $P = 20,000$  kN) are plotted in Fig. 22 and Fig. 23 respectively. Similar to the deflection, the difference between the bending stress results predicted by these two beam theories (Fig. 22) is highlighted in the case of strong interface. Fig. 23 demonstrates that TBT is not able to capture the true shear stress distribution as also observed in the previous examples.

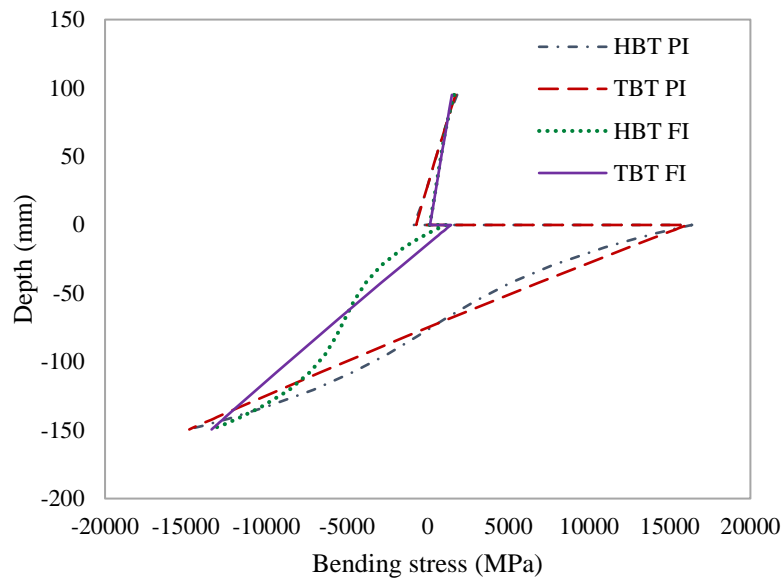


Fig. 22. Bending stress at the middle of the left span of the two span composite beam (Fig. 19) under maximum load ( $P = 20,000$  kN).

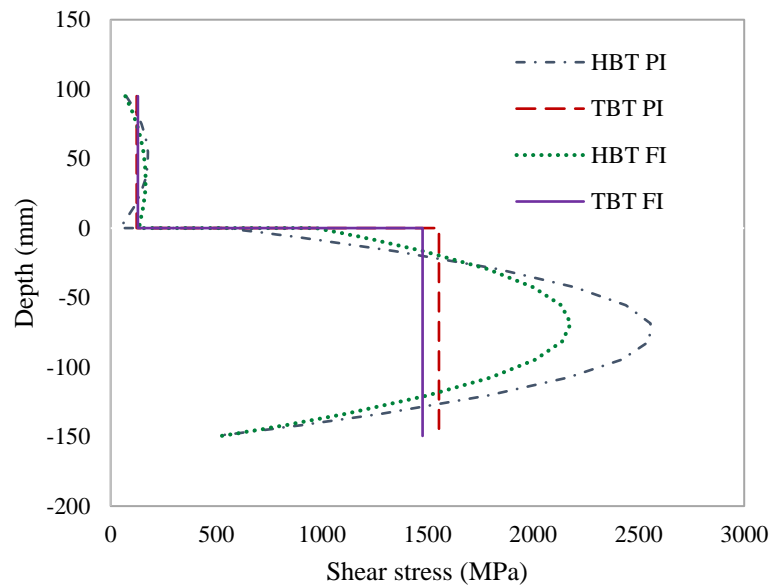


Fig. 23. Shear stress at the middle of the left span of the two span composite beam (Fig. 19) under maximum load ( $P = 20,000$  kN).

#### **4. CONCLUSIONS**

An efficient one dimensional finite element model based on a higher-order beam theory (HBT) is developed for an accurate prediction of the geometrically nonlinear response of two layered composite beams. The partial shear interaction caused by the longitudinal separation or shear slip of the two layers at their interface due to the deformability of shear connectors is considered and modelled as distributed shear springs along the entire length of the beam.

The HBT provides a true parabolic variation of the shear stress over the beam depth, and therefore does not require the use of a potentially arbitrary shear correction factor for the correct prediction of the global response such as deflection. Moreover, the model is capable of predicting the local response such as the distribution of stresses realistically.

The Green-Lagrange strain is used to develop the proposed finite element model for incorporating the effects of geometric nonlinearity. The principle of virtual work is applied to derive the nonlinear governing equations which are solved by an incremental-iterative approach following the Newton-Raphson technique.

Numerical examples of composite beams are solved by the proposed model taking into account different layer configurations, loading, support conditions, and interactions to assess the performance and range of applicability of the model. The published results are used for the validation of the proposed model, and a detailed two-dimensional finite element model is used for verifying the response of composite beams.

The numerical analysis has confirmed that the proposed model has improved capabilities compared with existing techniques in predicting the local response of composite beams. It is also observed that an improvement in the prediction of global response of these beams is achieved when the current model is applied.

#### **5. ACKNOWLEDGEMENT**

The financial support provide by the University of Adelaide in the form of an Adelaide Scholarship International (ASI) awarded to the first author for his doctoral studies is gratefully acknowledged.

## 6. REFERENCE

- [1] D. Oehlers, M.A. Bradford, *Composite Steel and Concrete Structural Members, Fundamental Behaviour*, Australia, (1995).
- [2] H. Loh, B. Uy, M. Bradford, The effects of partial shear connection in the hogging moment regions of composite beams: Part I—Experimental study, *Journal of constructional steel research*, 60 (2004) 897-919.
- [3] B. Uy, D. Nethercot, Effects of partial shear connection on the required and available rotations of semi-continuous composite beam systems, *The Structural Engineer* 83 (2005).
- [4] G. Ranzi, M. Bradford, B. Uy, A general method of analysis of composite beams with partial interaction, *Steel and Composite Structures*, 3 (2003) 169-184.
- [5] G. Ranzi, M. Bradford, B. Uy, Analytical solutions for the viscoelastic response of composite beams including partial interaction, *Advances in Structural Engineering*, 9 (2006) 11-18.
- [6] E. Tan, B. Uy, Experimental study on straight composite beams subjected to combined flexure and torsion, *Journal of Constructional Steel Research*, 65 (2009) 784-793.
- [7] S. Berczyński, T. Wróblewski, Vibration of steel–concrete composite beams using the Timoshenko beam model, *Journal of Vibration and Control*, 11 (2005) 829-848.
- [8] R. Xu, Y. Wu, Static, dynamic, and buckling analysis of partial interaction composite members using Timoshenko's beam theory, *International Journal of Mechanical Sciences*, 49 (2007) 1139-1155.
- [9] S. Schnabl, M. Saje, G. Turk, I. Planinc, Locking-free two-layer Timoshenko beam element with interlayer slip, *Finite Elements in Analysis and Design*, 43 (2007) 705-714.
- [10] A. Zona, G. Ranzi, Finite element models for nonlinear analysis of steel–concrete composite beams with partial interaction in combined bending and shear, *Finite Elements in Analysis and Design*, 47 (2011) 98-118.
- [11] G. Ranzi, A. Zona, A steel–concrete composite beam model with partial interaction including the shear deformability of the steel component, *Engineering Structures*, 29 (2007) 3026-3041.
- [12] U.A. Girhammar, A simplified analysis method for composite beams with interlayer slip, *International Journal of Mechanical Sciences*, 51 (2009) 515-530.
- [13] A. Adekola, Partial interaction between elastically connected elements of a composite beam, *International Journal of Solids and Structures*, 4 (1968) 1125-1135.
- [14] G. Ranzi, M. Bradford, B. Uy, A direct stiffness analysis of a composite beam with partial interaction, *International Journal for Numerical Methods in Engineering*, 61 (2004) 657-672.
- [15] G. Ranzi, F. Gara, G. Leoni, M.A. Bradford, Analysis of composite beams with partial shear interaction using available modelling techniques: A comparative study, *Computers & structures*, 84 (2006) 930-941.

- [16] N. Jasim, Computation of deflections for continuous composite beams with partial interaction, *Proceedings of the Institution of Civil Engineers. Structures and buildings*, 122 (1997) 347-354.
- [17] G. Ranzi, A. Dall'Asta, L. Ragni, A. Zona, A geometric nonlinear model for composite beams with partial interaction, *Engineering Structures*, 32 (2010) 1384-1396.
- [18] R.E. Erkmén, M.A. Bradford, Nonlinear elastic analysis of composite beams curved in-plan, *Engineering Structures*, 31 (2009) 1613-1624.
- [19] C. Huang, Y. Su, Dynamic characteristics of partial composite beams, *International Journal of Structural Stability and Dynamics*, 8 (2008) 665-685.
- [20] R. Brighenti, S. Bottoli, A novel finite element formulation for beams with composite cross-section, *International Journal of Mechanical Sciences*, 89 (2014) 112-122.
- [21] N.M. Newmark, C.P. Siess, I. Viest, Tests and analysis of composite beams with incomplete interaction, *Proc. Soc. Exp. Stress Anal*, 9 (1951) 75-92.
- [22] M. Hjiij, J.-M. Battini, Q.H. Nguyen, Large displacement analysis of shear deformable composite beams with interlayer slips, *International Journal of Non-Linear Mechanics*, 47 (2012) 895-904.
- [23] A. Chakrabarti, A. Sheikh, M. Griffith, D. Oehlers, Analysis of composite beams with longitudinal and transverse partial interactions using higher order beam theory, *International Journal of Mechanical Sciences*, 59 (2012) 115-125.
- [24] A. Chakrabarti, A. Sheikh, M. Griffith, D. Oehlers, Analysis of composite beams with partial shear interactions using a higher order beam theory, *Engineering Structures*, 36 (2012) 283-291.
- [25] A. Chakrabarti, A. Sheikh, M. Griffith, D. Oehlers, Dynamic response of composite beams with partial shear interaction using a higher-order beam theory, *Journal of Structural Engineering*, 139 (2012) 47-56.
- [26] J.N. Reddy, A simple higher-order theory for laminated composite plates, *Journal of applied mechanics*, 51 (1984) 745-752.
- [27] O.C. Zienkiewicz, R.L. Taylor, O.C. Zienkiewicz, R.L. Taylor, *The finite element method*, McGraw-hill London, 1977.
- [28] R.U. Vinayak, G. Prathap, B.P. Naganarayana, Beam elements based on a higher order theory—I. Formulation and analysis of performance, *Computers & Structures*, 58 (1996) 775-789.
- [29] R.D. Cook, *Concepts and applications of finite element analysis*, John Wiley & Sons, 2007.

## **Chapter 3: Material Nonlinear Model**

### **3.1 Introduction**

The manuscript contained in this chapter namely “A higher-order model for inelastic response of composite beams with interfacial slip using a dissipation based arc-length method” presents the development of a one dimensional finite element model of steel-concrete composite beam based on a higher-order beam theory (HBT) considering the effect of material nonlinearity. The purpose of the study to predict the response of these composite beams influenced by inelastic material behaviours of their constituents modelled by a plasticity model based on von Mises yield criterion with an isotropic-hardening rule and a damage mechanics model. In order to avoid any divergence in the solution of the plasticity modelling, the backward Euler stress return algorithm is incorporated in the model to update the stresses. Various types of stress-strain curve (uniaxial) are used for the different materials to have a realistic representation of their actual behaviours of the beam. A robust arc-length method is implemented for solving the nonlinear equations which helped to capture the post peak response successfully. It is also shown that the performance of the proposed model based on HBT is better than that based on existing beam theories such as EBT and TBT. Based on the accuracy and range of applicability of the proposed model, it is highly recommended for the analysis of composite beams having inelastic material behaviours.

### **3.2 List of Manuscripts**

Uddin, M. A., Sheikh, A. H., Brown, D., Bennett, T. and Uy, B. (2016). “A higher-order model for inelastic response of composite beams with interfacial slip using a dissipation based arc-length method.” *Engineering structures*, (Elsevier) (Article in Press).

### 3.3 Statement of Authorship

Title of Paper	A higher-order model for inelastic response of composite beams with interfacial slip using a dissipation based arc-length method.
Publication Status	Accepted (Article in Press).
Publication Details	Uddin, M. A., Sheikh, A. H., Brown, D., Bennett, T. and Uy, B. (2016). "A higher-order model for inelastic response of composite beams with interfacial slip using a dissipation based arc-length method." <i>Engineering structures</i> , (Elsevier) (Article in Press).

#### Principal Author

Name of Principal Author (Candidate)	Md. Alhaz Uddin		
Contribution to the Paper	Developed finite element model, performed numerical analysis and prepared manuscript.		
Overall percentage (%)	70%		
Certification:	This paper reports on original research I conducted during the period of my Higher Degree by Research candidature and is not subject to any obligations or contractual agreements with a third party that would constrain its inclusion in this thesis. I am the primary author of this paper.		
Signature		Date	

#### Co-Author Contributions

By signing the Statement of Authorship, each author certifies that:

- i. the candidate's stated contribution to the publication is accurate (as detailed above);
- ii. permission is granted for the candidate to include the publication in the thesis; and
- iii. the sum of all co-author contributions is equal to 100% less the candidate's stated contribution.

Name of Co-Author	Abdul Hamid Sheikh		
Contribution to the Paper	Supervised for development of model, helped in data interpretation, provided critical manuscript evaluation and acted as corresponding author.		
Signature		Date	22/11/2016

Name of Co-Author	David Brown		
Contribution to the Paper	Helped for incorporating the arc-length method, improvement of the stress updating, assisted in manuscript evaluation.		
Signature		Date	17/11/16

Name of Co-Author	Terry Bennett		
Contribution to the Paper	Supervised for formulating the damage model, provided for manuscript evaluation.		
Signature		Date	22/11/16.

Name of Co-Author	Brian Uy		
Contribution to the Paper	Provided for manuscript evaluation. <i>Energy manuscript reflects state of the art &amp; reviews existing experimental work.</i>		
Signature		Date	17/11/15

### **3.4 A higher order model for inelastic response of composite beams with interfacial slip using a dissipation based arc-length method**

Md. Alhaz Uddin, Abdul Hamid Sheikh, David Brown, Terry Bennett and Brian Uy

#### **ABSTRACT**

An efficient one dimensional finite element model is developed for an accurate prediction of the inelastic response of steel-concrete composite beams with partial shear interaction using a higher-order beam theory (HBT). This is achieved by taking a third order variation of the longitudinal displacement over the beam depth for the two layers separately. The deformable shear studs used for connecting the concrete slab with the steel girder are modelled as distributed shear springs along the interface between these two material layers. A plasticity model based on von Mises yield criterion and a damage model are used to simulate the inelastic behaviour of beam materials. An arc-length method based on energy dissipation is employed to capture the post peak response successfully. The capability of the proposed model is assessed through its verification and validation using existing experimental results and numerical results produced by detailed finite element modelling of these beams.

**Keywords:** Steel-concrete composite beam, Partial shear interaction, Higher-order beam theory, Inelastic material behaviour, Dissipation based arc-length method.

#### **1. INTRODUCTION**

Composite structures are widely used in various engineering activities for their superior structural performances. Steel-concrete composite beams belong to a specific type of composite structures, typically used in bridges, buildings and other civil engineering infrastructure. These structures consist of a concrete slab and a steel girder which are connected by steel shear studs to have composite action. The concrete slab is primarily utilised to carry the compressive stress whereas the steel girder carries the tensile stress to enhance the performance of the overall structural system. The shear connectors transfer shear forces at the interface between concrete and steel material layers. This leads to interfacial shear slip due to shear studs with finite stiffness which is commonly known as partial shear

interaction [1]. As the contribution of partial shear interaction on the structural behaviour is found to be significant (e.g. [2, 3]), this effect can't be ignored in the analysis of these composite beams. This is an active area of research which is best demonstrated by the large number of studies on different aspects of composite beams. However, the main aim of the present study is to develop an efficient model for accurately predicting the inelastic response of composite beams.

Newmark et al. [4] is one of the earliest researchers who developed an analytical model for composite beams where the effect of partial interaction was considered in the form of shear slip. This is a well-regarded model but only applicable to beams with simply supported boundaries and relatively simple loading due to the analytical nature of the model. In contrast, a numerical model based on finite element approximation can provide adequate generality in the analysis with sufficient accuracy. Thus a number of researchers (e.g. [5-9]) have developed finite element models for composite beams with partial interaction. However all these models [5-9] are based on elastic behaviour of beam materials. In reality, the materials of these beams are having inelastic deformations even with a low to moderate range of loading. In order to address this issue, Yasunori et al. [10] incorporated the effect of inelastic material behaviour in their finite element model of composite beams using the von Mises yield criterion. However, they [10] used a very simple material model based on an elastic perfectly-plastic idealisation for all materials including concrete which is not realistic especially for the tensile response of concrete. Similar studies have been carried out by Salari et al. [11] using a bi-linear elasto-plastic material model with a strain hardening parameter. A further development in this direction is due to Dall'Asta and Zona [12] and Erkmen and Attard [13] who have used realistic stress strain curves for the beam materials but Dall'Asta and Zona [12] have ignored the contribution of concrete in tension whereas Erkmen and Attard [13] have used the concept of tension stiffening for its modelling. A more comprehensive model is proposed by Liu et al. [14] where the tensile behaviour of concrete is simulated using a damage mechanics model which can precisely model the tensile response of plain concrete without reinforcement. Foraboschi [15] and Foraboschi et al. [16] attempted to solve the composite beam problem analytically but the structure is idealised in a different manner where the shear connector is modelled as a separate material layer with a finite thickness. Moreover, the inelastic material behaviour is consider only for this interfacial layer whereas the primary layers (concrete slab and steel girder) are treated as linear elastic materials. Anyway, all these models [4-16] are based on Euler-Bernoulli beam theory (EBT), which does not consider the effect of transverse shear deformation of the steel

and concrete layers. The effect of this shear deformation is significant in some situations such as beams with a small span-to-depth ratio, localized concentrated loads, clamped boundary conditions and some other cases.

Thus there has been a growing interest in recent years to incorporate the effect of shear deformation and the Timoshenko's beam theory (TBT) is typically used for this purpose (e.g., [17-21]). It is observed that all these investigators [17-21] have used linear elastic material behaviour to develop their models except Nguyen et al. [21], who have used a very simple constitutive model specifically for the concrete. Moreover, it should be noted that the actual variation of transverse shear stress over the beam depth is parabolic, whereas an average shear stress having a uniform distribution is taken in TBT to simplify the problem. In order to address this issue, TBT needs an arbitrary shear correction factor which helps to predict the global response such as deflection or vibration frequency well, but it is not sufficient for an accurate prediction of the local response such as the stress distributions within these structures [22-24]. Moreover, the calculation of the exact value of this shear correction factor for a composite beam with partial shear interaction is cumbersome in comparison with that of a single layer homogeneous beam.

In order to address the aforementioned issues related to shear deformation of the beam material layers, a higher-order beam theory (HBT) has recently been developed by Sheikh and co-workers [22-24] for an accurate prediction of global as well as local responses of these composite beams. The cross-sectional warping of the beam layers produced by the transverse shear stress is modelled with a higher order (3rd order) variation of longitudinal displacement of the fibres over the beam depth. This beam theory (HBT) utilized the concept of Reddy's higher order shear deformation theory [25] developed for multi-layered laminated composite plates modelled as single layered plates without interfacial slip. In these investigations [22-24], HBT has been implemented in a one dimensional finite element model which has exhibited very good performance, though these studies are restricted to linear elastic analysis of these composite beams with interfacial slip.

Considering the aforementioned aspects, an attempt is made in this study to develop an efficient numerical model based on HBT for accurately predicting the inelastic response of composite beams. The inelastic material behaviour is responsible for inducing nonlinearity in the structural response, which can be manifested in the form of nonlinear load-deflection curves. These curves can sometimes have a descending branch after attaining the peak load due to the strain-softening of concrete. It is observed that most of the investigations carried

out on the inelastic response of composite beams [10-14, 21] could not capture the descending branch of the nonlinear load-deflection curve successfully. The solution of this typical nonlinear problem is quite challenging and a load control based technique cannot trace the descending branch of the load-deflection curve. In order to overcome this problem, a displacement control based technique may be used but it will fail if the load-deflection curve has a snap-back response. In this situation, an arc-length based solution technique seems to be the only possible option.

The arc-length method was proposed by Riks [26] and subsequently enhanced by various investigators (e.g. Crisfield [27, 28]) for solving different nonlinear problems. Though these developments helped to solve complex geometric nonlinear problems successfully, but they encountered severe convergence problem in solving material nonlinear problems especially relating to concrete structures which have failure/crack localizations. In order to address this specific issue, the localized nature of damage has been utilised by May and Duan [29] to develop a new arc length method known as a damage localization approach. This method can provide a satisfactory solution of a problem [30] but it requires the position of damaged elements, which may be difficult to locate in a complex structural system. A further advancement in this direction is due to Gutiérrez [31] who proposed a dissipation based arc-length method where the energy dissipated by the entire structure due to its damage and plastic deformations is utilised as a stepping parameter for controlling the incremental iterative process. The success of this method is primarily due to the stepping parameter as it is always positive regardless of the sign of the tangential stiffness.

In this study, a computationally efficient one dimensional finite element model is developed using a higher order variation of the longitudinal displacement along the beam depth according to HBT and inelastic material behaviours of the beam constituents. The von Mises plasticity theory with an isotropic hardening rule is used for modelling the inelastic behaviour of steel girders, concrete slabs under compression, steel reinforcements, and steel shear studs. A damage mechanics model is used for modelling the inelastic behaviour of concrete under tension. A dissipation based arc-length method is employed to capture the post peak response successfully. Numerical examples of composite beams are solved by the proposed model. The results predicted by the models are validated with the published experimental results and the numerical results produced by a detailed two-dimensional finite element model of these beams using a reliable finite element software. As the number of results available in the inelastic range of composite beams is limited and no one has reported

any results for the stress distributions within these structures, a number of new results are presented for future references.

## 2. MATHEMATICAL FORMULATION

The formulation of the proposed model is based on the following major assumptions:

a) the beam has an uniform cross-section along its length, b) the beam deformation is small which excludes any effect due to change in geometry, c) there is no vertical separation between two material layers, d) the applied load passes through the vertical plane of symmetrical of the beam which excludes any torsional effect, and e) local buckling of the steel I girder is not considered.

### 2.1. Higher-order Beam Theory (HBT)

Fig. 1 shows a steel-concrete composite beam which is typically a two layered composite beam with a flexible interface. According to the HBT, the variation of longitudinal displacement of the concrete and steel layers over their depths can be expressed as

$$u_c = u_{c0} - y_c \theta_c + y_c^2 \alpha_c + y_c^3 \beta_c \quad (1)$$

$$u_s = u_{s0} - y_s \theta_s + y_s^2 \alpha_s + y_s^3 \beta_s \quad (2)$$

where  $u_{c0}$  and  $u_{s0}$  are longitudinal displacements of the concrete slab and the steel girder at their reference axes ( $y_c = 0$  and  $y_s = 0$ ) respectively,  $\theta_c$  and  $\theta_s$  are bending rotations of these layers, and  $\alpha$  and  $\beta$  are the higher order terms. As vertical separation between the layers is not commonly observed in a straight composite beam under a static load, it is not considered in this study. Thus the vertical displacement will be the same for both layers and it can be expressed as

$$w_c = w_s = w \quad (3)$$

The partial shear interaction between the concrete and steel layers is characterised by the slip at their interface. This is defined as the relative longitudinal displacement of these material layers and it can be expressed as

$$s = \bar{u}_s - \bar{u}_c \quad (4)$$

where  $\bar{u}_c$  is the longitudinal displacement at the bottom fibre of the concrete layer and  $\bar{u}_s$  is that at the top fibre of the steel layer.

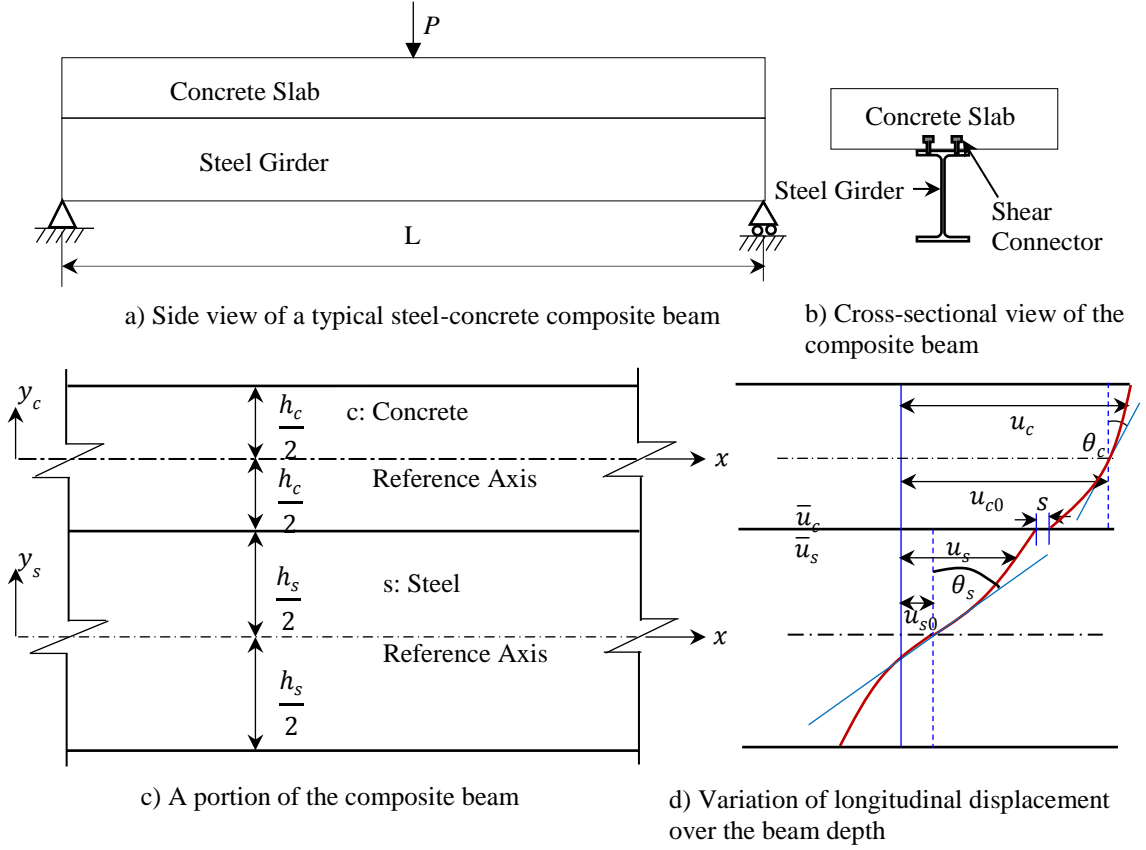


Fig. 1. Typical Steel-concrete composite beam with displacement variations over the beam depth.

The shear strain for the upper material layer of the beam ( $\gamma_c$ ) at its top surface is zero, as the shear stress ( $\tau_c = G_c \gamma_c$ ) becomes zero at this free surface. Using Eqs. (1) and (3), the shear strain at any point of the upper layer may be expressed as

$$\gamma_c = \frac{\partial u_c}{\partial y_c} + \frac{\partial w}{\partial x} = -\theta_c + 2\alpha_c y_c + 3\beta_c y_c^2 + \frac{dw}{dx} \quad (5)$$

The shear stress free condition at the top surface of the upper material layer can now be employed by substituting  $y_c = h_c/2$  (Fig. 1) in the above equation which is lead to

$$-\theta_c + \alpha_c h_c + \frac{3}{4} \beta_c h_c^2 + \frac{dw}{dx} = 0 \quad (6)$$

Similarly, the shear stress free condition at the bottom surface of the lower material layer ( $\tau_s = G_s \gamma_s = 0$  at  $y_s = -h_s/2$ ) can be employed to get the following equation

$$-\theta_s - \alpha_s h_s + \frac{3}{4} \beta_s h_s^2 + \frac{dw}{dx} = 0 \quad (7)$$

Now, substituting  $y_c = -h_c/2$  in Eq. (1), the longitudinal displacement at the bottom surface of the upper material layer  $\bar{u}_c$  can be expressed as

$$\bar{u}_c = u_{c0} + \frac{h_c}{2} \theta_c + \alpha_c \frac{h_c^2}{4} - \beta_c \frac{h_c^3}{8} \quad (8)$$

Similarly, substituting  $y_s = h_s/2$  in Eq. (2), the longitudinal displacement at the top surface of the lower material layer  $\bar{u}_s$  can be expressed as

$$\bar{u}_s = u_{s0} - \frac{h_s}{2} \theta_s + \alpha_s \frac{h_s^2}{4} + \beta_s \frac{h_s^3}{8} \quad (9)$$

These four equations (6-9) are used to eliminate the four higher order non-physical terms ( $\alpha_c, \beta_c, \alpha_s, \beta_s$ ) appeared in Eqs. (1) and (2) are these two equations are rewritten as

$$u_c = A_c u_{c0} + B_c \bar{u}_c + C_c \theta_c + D_c \phi \quad (10)$$

$$u_s = A_s u_{s0} + B_s \bar{u}_s + C_s \theta_s + D_s \phi \quad (11)$$

where  $A, B, C$  and  $D$  are functions of  $y$ , cross-sectional properties of the two layers and their material properties. The explicit expression of these parameters are as follows:

$$\begin{aligned} A_c &= 1 - \frac{12}{5h_c^2} y_c^2 + \frac{16}{5h_c^3} y_c^3, & B_c &= \frac{12}{5h_c^2} y_c^2 - \frac{16}{5h_c^3} y_c^3, & C_c &= -y_c - \frac{4}{5h_c} y_c^2 + \frac{12}{5h_c^2} y_c^3, \\ D_c &= -\frac{2}{5h_c} y_c^2 - \frac{4}{5h_c^2} y_c^3, & A_s &= 1 - \frac{12}{5h_s^2} y_s^2 - \frac{16}{5h_s^3} y_s^3, & B_s &= \frac{12}{5h_s^2} y_s^2 + \frac{16}{5h_s^3} y_s^3, \\ C_s &= -y_s + \frac{4}{5h_s} y_s^2 + \frac{12}{5h_s^2} y_s^3, & D_s &= \frac{2}{5h_s} y_s^2 - \frac{4}{5h_s^2} y_s^3. \end{aligned}$$

In the equations above,  $\phi$  ( $=dw/dx$ ) is taken as an independent field variable to have a  $C^0$  continuous formulation for the finite element implementation of this beam theory.

## 2.2. Variational Formulations and its Finite Element Implementation

The equilibrium equation can be derived using the principle of virtual work and it can be expressed as

$$\int_x \int_{A_c} \{d\varepsilon\}_c^T \{\sigma\}_c dAdx + \int_x \int_{A_s} \{d\varepsilon\}_s^T \{\sigma\}_s dAdx + \int_x d\tau_{sh} dx = \int_x dwq dx, \quad (12)$$

where  $d$  is used to show the variation of any parameter,  $\{\varepsilon\}_c$  and  $\{\varepsilon\}_s$  are strain vectors (consisting of longitudinal normal and transverse shear strains) of the concrete and steel layers respectively,  $\{\sigma\}_c$  and  $\{\sigma\}_s$  are stress vectors (consisting of longitudinal normal and transverse shear stresses) of these layers,  $\tau_{sh}$  is the distributed shear force (per unit length) at their interface,  $q$  is the distributed external load (per unit length) acting on the beam, and  $A$  is the cross-sectional area.

Using Eqs. (10) and (11), the strain vectors of the two layers may be written in terms of their cross-sectional matrices and one dimensional strain vectors (dependent on  $x$  only) as

$$\{\varepsilon\}_l = \begin{Bmatrix} \varepsilon_l \\ \gamma_l \end{Bmatrix} = \begin{Bmatrix} \frac{\partial u_l}{\partial x} \\ \frac{\partial u_l}{\partial y_l} + \frac{\partial w}{\partial x} \end{Bmatrix} = [H]_l \{\bar{\varepsilon}\}_l, \quad (13)$$

where the subscript  $l = c$  for the concrete layer and  $l = s$  for the steel layer. The cross-sectional matrices and one dimensional strain vectors are as follows.

$$[H]_l = \begin{bmatrix} A_l & B_l & C_l & D_l & 0 & 0 & 0 & 0 & 0 \\ 0 & 0 & 0 & 0 & \frac{dA_l}{dy_l} & \frac{dB_l}{dy_l} & \frac{dC_l}{dy_l} & \frac{dD_l}{dy_l} & 1 \end{bmatrix}. \quad (14)$$

$$\{\bar{\varepsilon}\}_l^T = \left( \frac{du_{l0}}{dx} \quad \frac{d\bar{u}_l}{dx} \quad \frac{d\theta_l}{dx} \quad \frac{d\phi}{dx} \quad u_{l0} \quad \bar{u}_l \quad \theta_l \quad \phi \quad \frac{dw}{dx} \right). \quad (15)$$

For the finite element implementation of the proposed beam model, a displacement based quadratic isoparametric beam element with three nodes is used for a simple formulation and does not involve any unexpected numerical inconsistencies. However, a displacement based formulation can have a locking problem, which is eliminated by using the field consistent technique [32]. The field variables of the element are  $u_{c0}$ ,  $\bar{u}_c$ ,  $\theta_c$ ,  $w$ ,  $\phi$ ,  $u_{s0}$ ,  $\bar{u}_s$  and  $\theta_s$ , which can be expressed in terms of their nodal unknowns using interpolation functions of the element [24]. This leads to express the one dimensional strain vectors (15) in terms of the nodal displacement vector  $\{\Delta\}$  as

$$\{\bar{\varepsilon}\}_l = \begin{bmatrix} [B_1]_l & [B_2]_l & [B_3]_l \end{bmatrix} \begin{Bmatrix} \{\Delta_1\} \\ \{\Delta_2\} \\ \{\Delta_3\} \end{Bmatrix} = [B]_l \{\Delta\}, \quad (16)$$

where,  $[B]_l$  is the strain-displacement matrix for the concrete/steel layer [24]. Similarly, the interfacial slip (4) can be expressed in terms of a strain-displacement matrix for the interfacial slip  $[B]_{sh}$  and nodal displacement vector [24] as

$$s = (\bar{u}_s - \bar{u}_c) = [B]_{sh} \{\Delta\}. \quad (17)$$

The virtual work due to the external load  $q$  as expressed on the right hand side of Eq. (12) can be further expressed in terms of the external load vector  $\{F_{ext}\}$  and incremental nodal displacement vector  $\{d\Delta\}$  as

$$\int dwq dx = \{d\Delta\}^T \{F_{ext}\}, \quad (18)$$

$$\text{where } \{F_{ext}\} = \int [N]^T q dx \quad (19)$$

The matrix  $[N]$  in the above equation contains shape functions of the transverse displacement,  $w$  [24].

Substituting Eqs. (13), (16), (17) and (18) into Eq. (12), the equilibrium equation can be obtained and it is expressed as

$$\int_x \int_{A_c} [B]_c^T [H]_c^T \{\sigma\}_c dA dx + \int_x \int_{A_s} [B]_s^T [H]_s^T \{\sigma\}_s dA dx + \int_x [B]_{sh}^T \tau_{sh} dx = \{F_{ext}\} \quad (20)$$

For the solution of the above equation, the stresses are to be expressed in terms of strains which can subsequently be expressed in terms of nodal displacements  $\{\Delta\}$  using Eqs. (16) and (17). However, for a material having inelastic deformations, the stress-strain relationship is nonlinear and must be expressed in its incremental form as the stresses cannot be expressed in terms of strains in their total form due to the load history dependent material behaviour. Thus the above equation cannot be solved directly and an iterative approach will be required for solving this nonlinear equation. To facilitate this, the left hand side of the equilibrium equation (20) is defined as the internal nodal force vector  $\{P_{int}\}$  (dependent on nodal displacement vector  $\{\Delta\}$ ), which leads to an expression for Eq. (20) in a compact form as

$$\{P_{int}(\{\Delta\})\} = \{F_{ext}\} \text{ or } \{\Psi\} = \{P_{int}\} - \{F_{ext}\} = \{0\} \quad (21)$$

The Newton Raphson method is used to solve the above equation iteratively where the nodal displacement vector  $\{\Delta\}^{j+1}$  at the iteration  $j+1$  can be computed from that obtained in the previous iteration  $\{\Delta\}^j$  as

$$\{\Delta\}^{j+1} = \{\Delta\}^j + \{d\Delta\}^{j+1} = \{\Delta\}^j + \left[ \left( \frac{\partial\{\Psi\}}{\partial\{\Delta\}} \right)^j \right]^{-1} \{-\Psi(\{\Delta\}^j)\} \quad (22)$$

From the above equation, the incremental nodal displacement  $\{d\Delta\}$  within an iteration can be written as

$$\frac{\partial\{\Psi\}}{\partial\{\Delta\}} \{d\Delta\} = -\{\Psi\} \quad (23)$$

Substituting Eqs. (20) and (21) into the above equation and defining its right hand side as the residual load vector  $\{dR\}$  ( $= -\{\Psi\}$ ), it can be rewritten as

$$\int_x \int_{A_c} [B]_c^T [H]_c^T \{d\sigma\}_c dA dx + \int_x \int_{A_s} [B]_s^T [H]_s^T \{d\sigma\}_s dA dx + \int_x [B]_{sh}^T d\tau_{sh} dx = \{dR\} \quad (24)$$

Now the incremental stresses in Eq. (24) can be expressed in terms of incremental strains using a suitable constitutive relationship (provided in the following section) as

$$\{d\sigma\}_l = [E^t]_l \{d\varepsilon\}_l; \quad d\tau_{sh} = k_{sh}^t ds \quad (25)$$

where  $[E^t]$  is the tangential material stiffness matrix (elasto-plastic/damage stiffness matrix) of the steel/concrete layer and  $k_{sh}^t$  is the tangential material stiffness (elasto-plastic stiffness) of the shear connectors. Substituting Eqs. (13), (16), (17) and (25) into Eq. (24), the incremental equation can be written in its final form as

$$[K_T] \{d\Delta\} = \{dR\} \quad (26)$$

where  $[K_T]$  is the tangent stiffness matrix of the structure that can be expressed as

$$[K_T] = \int_x [B]_c^T \left( \int_{A_c} [H]_c^T [E^t]_c [H]_c dA \right) [B]_c dx + \int_x [B]_s^T \left( \int_{A_s} [H]_s^T [E^t]_s [H]_s dA \right) [B]_s dx + \int_x [B]_{sh}^T K_{sh}^t [B]_{sh} dx \quad (27)$$

In order to ensure that the solution of the nonlinear equation is converged, the abovementioned iteration process will continue until the residual force vector  $\{dR\}$  is reduced to a specified tolerance as follows

$$\frac{\sqrt{\{\delta R\}^T \{\delta R\}}}{\sqrt{\{F_{ext}\}^T \{F_{ext}\}}} \times 100 \leq Tol \quad (28)$$

where  $Tol$  is the convergence tolerance which is taken as 1% in the present study.

It should be noted that the external loading with its maximum value is not to be applied at once, and it is rather be applied gradually in a number of steps in order to avoid convergence problems in the iterative solution process and also to trace the entire equilibrium path. Moreover, this is a load control technique which will not be adequate to trace the post peak inelastic response of composite beams. This problem is typically solved by using a robust arc-length method which is presented in Section 2.4.

### 2.3. Constitutive Relationship

The von Mises yield criterion with an isotropic-hardening rule [33] is used for modelling the inelastic behaviour of steel girders, reinforcement and steel shear studs. This modelling approach is also applied to the region of concrete slab subjected to compressive stress for simplicity. A damage mechanics model [34, 35] is adopted to simulate the cracking behaviour of the concrete under tensile stress.

#### 2.3.1. Constitutive Relationship for Steel and Concrete in Compression

According to the von Mises yield criterion, the stress state must be on (plastic loading) or within (elastic loading and unloading) the yield surface which may be written for the steel/concrete layer subjected to bending and shear stresses as

$$f_l = \sigma_{ef,l} - \sigma_{y,l} \leq 0 \quad (29)$$

In the above equation,  $\sigma_{y,l}$  is the uniaxial yield stress and  $\sigma_{ef,l}$  is the effective stress, which can be written in terms of bending stress  $\sigma_l$  and shear stress  $\tau_l$  as

$$\sigma_{ef,l} = \sqrt{\sigma_l^2 + 3\tau_l^2} \quad (30)$$

In order to correlate a multiaxial stress state (usually found in a real problem) with the uniaxial yield stress, the uniaxial yield stress can be expressed in terms of equivalent plastic strain  $\varepsilon_{ef,l}^p = \sqrt{(\varepsilon_l^p)^2 + (\gamma_l^p)^2} / \sqrt{3}$  as

$$\sigma_{y,l} = \sigma_{y0,l} + \int_0^{\varepsilon_{ef,l}^p} H'_l \delta \varepsilon_{ef,l}^p \quad (31)$$

where  $\sigma_{y0,l}$  is the initial value of the uniaxial yield stress for a material layer and  $H'_l$  is the strain hardening parameter of the layer.

As mentioned in the previous section, the stress-strain relationship must be expressed in its incremental form due to inelastic material behaviour. Thus the strain vector is taken in its incremental form and can be expressed in terms of its elastic and plastic components as

$$\{d\varepsilon\}_l = \{d\varepsilon^e\}_l + \{d\varepsilon^p\}_l \quad (32)$$

The elastic strain increment can simply be obtained from the incremental stress using Hooke's law as

$$\{d\varepsilon^e\}_l = \{d\varepsilon\}_l - \{d\varepsilon^p\}_l = [E^e]_l^{-1} \{d\sigma\}_l = \begin{bmatrix} E_l & 0 \\ 0 & G_l \end{bmatrix}^{-1} \{d\sigma\}_l \quad (33)$$

where  $E_l$  and  $G_l$  are the elastic modulus and shear modulus of the material layer respectively.

As an associated flow rule is used, the plastic strain increments can be determined [36] using Eq. (29) as

$$\{d\varepsilon^p\}_l = d\lambda_l \frac{\partial f_l}{\partial \{\sigma\}_l} = \frac{d\lambda_l}{\sigma_{ef,l}} \begin{Bmatrix} \sigma_l \\ 3\tau_l \end{Bmatrix} = d\lambda_l \{a\}_l \quad (34)$$

where  $d\lambda_l$  is the incremental plastic strain multiplier and the vector  $\{a\}_l$  gives the direction of plastic flow, which is normal to the yield surface. Using the consistency condition of the yield function (29) along with the above equations (29, 30, 33 and 34), the incremental plastic strain multiplier can be derived following the usual operations used in a plasticity formulation [36] and it can be expressed as

$$d\lambda_l = \frac{\{a\}_l^T [E^e]_l \{d\varepsilon\}_l}{\{a\}_l^T [E^e]_l \{a\}_l + H'_l} \quad (35)$$

For the von Mises yield criterion, the equivalent plastic strain increment will be the incremental plastic strain multiplier  $d\lambda_l$  [36]. Using Eqs. (33) to (35), the incremental stress-strain relationship can be obtained which is expressed as

$$\{d\sigma\}_l = [E^{ep}]_l \{d\varepsilon\}_l = \left( [E^e]_l - \frac{[E^e]_l \{a\}_l \{a\}_l^T [E^e]_l}{\{a\}_l^T [E^e]_l \{a\}_l + H_l} \right) \{d\varepsilon\}_l \quad (36)$$

where  $[E^{ep}]_l$  is the elasto-plastic constitutive matrix that can be used for  $[E^e]_l$  in Eq. (25).

This constitutive relationship is also applied for the modelling of reinforcement bars by eliminating the contribution of shear stress/strain.

### 2.3.2. Constitutive Relationship for Concrete in Tension

The concrete under tensile stress (major principal stress) is treated as an elastic material up to its uniaxial ultimate tensile stress ( $\sigma_{t0}$ ) where cracks are initiated. The crack initiation is detected according to Rankine's failure criterion [37] as follows.

$$f_t = \sigma_{\max} - \sigma_{t0} = 0 \quad (37)$$

where  $\sigma_{\max}$  is the maximum principle stress which can be evaluated using the following equation.

$$\sigma_{\max} = \frac{\sigma_c}{2} + \sqrt{\frac{\sigma_c^2}{4} + \tau_c^2} \quad (38)$$

The material behavior in tension is modelled with an elastic damage mechanics model taking a linear strain softening branch for simulating the post cracking response [35]. Fig. 2 shows a typical one dimensional damage model where the damage parameter  $\omega$  ranges from 0 (damage initiation) to 1 (complete damage) to characterize the extent of cracking. The damage parameter is used to quantify the loss of material stiffness due to cracking, which is illustrated with the unloading path from any point on the softening branch, in the form of its secant stiffness. The loading function for the damage can be expressed as

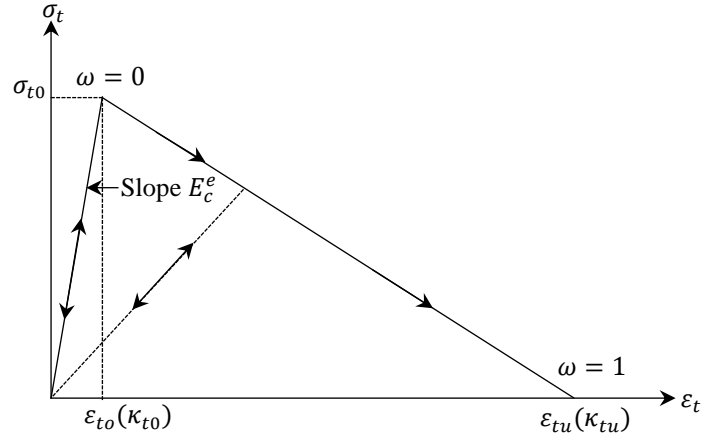


Fig. 2. Uniaxial strain softening model in tension.

$$f_{cr} = \kappa_{ef} - \max(\kappa_{old}, \kappa_{t0}) \leq 0 \quad (39)$$

where  $f_{cr} = 0$  indicates loading (i.e., damage growth) and  $f_{cr} < 0$  indicates unloading. The equivalent strain parameter  $\kappa_{ef}$  (similar to equivalent plastic strain in plasticity) in the above equation (scalar quantity) is taken as

$$\kappa_{ef} = \sqrt{\frac{1}{E} \{\boldsymbol{\varepsilon}\}_c^T [E^e]_c \{\boldsymbol{\varepsilon}\}_c} \quad (40)$$

where  $\kappa_{old}$  is its value obtained in the previous iteration of the analysis and  $\kappa_{t0}$  corresponds to that at the instance of damage initiation i.e.,  $\varepsilon_t = \varepsilon_{t0}$  (Fig. 2). In the case of unloading, the value of  $\kappa_{old}$  will be unaltered but it must be updated with the new value of  $\kappa_{ef}$  for loading in order to satisfy Eq. (39). Similarly, the damage parameter  $\omega$  will retain its old value for unloading but it is to be updated for damage growth (loading) as

$$\omega = \frac{\kappa_{tu}(\kappa_{ef} - \kappa_{t0})}{\kappa_{ef}(\kappa_{tu} - \kappa_{t0})} \quad (41)$$

where  $\kappa_{tu}$  corresponds to complete damage i.e.,  $\varepsilon_t = \varepsilon_{tu}$  (Fig. 2).

In the modelling of concrete under tensile stress, it is observed that the solution is dependent on the mesh size in a traditional strength based analysis. This is a typical problem which is eliminated in the present study using the concept of crack band theory proposed by Bazant and Oh [38]. This concept is based on fracture mechanics principles which utilize fracture toughness  $G_f$  (energy required to produce a crack of unit area) as a material property. This will be utilised to estimate the value of  $\varepsilon_{tu}$  used in Fig. 2 ( $\omega=1$ ) considering the area under

the stress strain curve as  $g_f = G_f / w_c$  where  $w_c$  is the crack band width and the energy  $G_f$  is assumed to be distributed over the crack band width [38]. This is an important concept that helps to treat the discrete nature of cracking within a continuum model. It is obvious that the exact location and size of the damage localisation over a finite length (i.e. a crack) cannot be predicted by a smeared crack model based on the usual local constitutive relationship adopted in the present study but crack band model will help to predict the overall response of the structure satisfactorily. As the element length  $l_e$  is related to the crack band in a smear crack model, the final expression of  $\varepsilon_{tu}$  can be written as

$$\varepsilon_{tu} = \frac{2G_f}{\alpha_w l_e \sigma_{t0}} \quad (42)$$

where  $\alpha_w l_e$  is defined as the characteristic length. The value of  $\alpha_w$  depends on the order of element which is 1.0 in the present case as a quadratic element is used [38].

With the damage parameter (41), the stress-strain relationship can be written as

$$\{\sigma\}_c = (1 - \omega)[E^e]_c \{\varepsilon\}_c \quad (43)$$

where  $(1 - \omega)[E^e]_c$  is the secant damage stiffness matrix (Fig. 2).

Finally, the incremental stress-strain relationship of the damaged concrete may be written as

$$\{d\sigma\}_c = [E^{cr}] \{d\varepsilon\}_c \quad (44)$$

where the tangent damage stiffness matrix  $[E^{cr}]$  can be expressed with the following equation and it can be used in Eq. (25) for  $[E^t]_l$ .

$$[E^{cr}] = (1 - \omega)[E^e]_c - \frac{K_{tu} K_{t0}}{K_{ef}^2 (K_{tu} - K_{t0})} \{\sigma\}_c^T \{\sigma\}_c \quad (45)$$

The above equation is applicable for damage growth while  $[E^{cr}]$  will be the secant damage stiffness matrix  $(1 - \omega)[E^e]_c$  for unloading.

### 2.3.3. Constitutive Relationship for Shear Connectors

The shear connectors are idealised as a distributed spring layer which transfers a distributed shear force between steel and concrete layers at their interface tangentially. The von Mises yield criterion used to model the shear connectors can be written as

$$f_{sc} = \tau_{ef} - \tau_y \quad (46)$$

where the effective shear stress (force per unit length)  $\tau_{ef}$  is the absolute value of the interfacial shear force  $\tau_{sh}$ , and  $\tau_y$  is the corresponding yield stress (force per unit length) that may be expressed in terms of the effective plastic shear slip  $s_{ef}^p$  (absolute value of the plastic shear slip  $s^p$ ) as

$$\tau_y = \tau_{y0} + \int_0^{s_{ef}^p} H'_{sc} \delta s_{ef}^p \quad (47)$$

where  $\tau_{y0}$  is the initial yield stress (force per unit length) of this interfacial shear, and  $H'_{sc}$  is the hardening parameter. In this case, the slip ( $s$ ) is taking the role of strains and it is to be expressed in terms of its elastic ( $s^e$ ) and plastic ( $s^p$ ) components. Following the usual steps of plasticity, the increments of these plastic slip components may be expressed as

$$ds^e = d\tau_{sh} / k_{sh} \quad (48)$$

$$ds^p = \frac{k_{sh}}{H'_{sc} + k_{sh}} ds \quad (49)$$

where  $k_{sh}$  is the elastic stiffness of the distributed interfacial shear springs. Finally, the incremental relationship between interfacial shear force and slip may be written as

$$d\tau_{sh} = k_{sh}^{ep} ds = \left( k_{sh} - \frac{k_{sh}^2}{H'_{sc} + k_{sh}} \right) ds \quad (50)$$

where  $k_{sh}^{ep}$  is the elasto-plastic tangent stiffness for the shear connectors that can be utilized in Eq. (25) as  $k_{sh}^t$ .

## 2.4. Arc-length Technique

The dissipation based arc-length method has initially been proposed by Gutiérrez [31] considering damage as the only energy dissipation mechanism. Subsequently, this method has been extended by Verhoosel et al. [39] to include plasticity as an additional mechanism, which is applied to the present problem. As the value of the external loading will not increase in the post peak range, the equilibrium equation (21) is expressed in terms of an unknown load factor (or multiplier)  $\mu$  as

$$\{P_{\text{int}}\} = \mu\{F\} \quad (51)$$

where  $\{F\}$  is the external load vector due to one unit of applied load. In order to avoid any convergence problems and trace the entire structural response in the pre-peak as well as post-peak ranges, the equilibrium path is divided into a number of steps by adjusting the value of  $\mu$  and the nonlinear equation is solved iteratively within each load step. As  $\mu$  is also an unknown parameter and its value is adjusted by this technique, an additional equation is required which is taken in the form of a constraint as follows

$$C(\{\Delta_0\}, \mu_0, \{\delta\Delta\}, \delta\mu, e_d) = 0 \quad (52)$$

where  $(\{\Delta_0\}, \mu_0)$  is a point on the equilibrium path (a converged solution at the end of a load step),  $\{\delta\Delta\}$  is the incremental nodal displacement vector for the next load step,  $\delta\mu$  is the corresponding incremental load factor and  $e_d$  is the prescribed dissipation energy required for estimating the step size. It should be noted that  $\{\delta\Delta\}$  is the value of  $\{\Delta\}$  within a load step whereas  $\{d\Delta\}$  used in Section 2.2 is the value of  $\{\Delta\}$  within an iteration. The incremental energy dissipation  $U_d$  of a structure due to inelastic deformations within a load step is used to define the constraint  $C$  in the above equation as

$$C = U_d - e_d \quad (53)$$

As the energy dissipation can be obtained from the work done by the external loads  $W_e$  (i.e., total energy supplied to the structural system) and the elastic energy  $U_e$  retained by the system, the incremental energy dissipation within a load step can be written as

$$U_d = \delta W_e - \delta U_e \quad (54)$$

With the external load vector as expressed in Eq. (51), the incremental work done by the external loads used in the above equation can be written as

$$\delta W_e = \mu \{F\}^T \{\delta \Delta\} \quad (55)$$

In case of a structure having plastic deformations, the strain will have an elastic component and a plastic component where the elastic strain can be used to obtain the elastic energy of a composite beam  $U_e$  and it can be expressed as

$$U_e = \frac{1}{2} \int \{\varepsilon^e\}_c^T \{\sigma\}_c dv + \frac{1}{2} \int \{\varepsilon^e\}_s^T \{\sigma\}_s dv + \frac{1}{2} \int s^e \tau_{sh} dx \quad (56)$$

Using the constitutive relationships of the different beam components, the elastic strains in the above equation can be replaced with the corresponding stresses as

$$U_e = \frac{1}{2} \int \{\sigma\}_c^T [E^e]_c^{-1} \{\sigma\}_c dv + \frac{1}{2} \int \{\sigma\}_s^T [E^e]_s^{-1} \{\sigma\}_s dv + \frac{1}{2} \int \tau_{sh} k_{sh}^{-1} \tau_{sh} dx \quad (57)$$

Now the incremental elastic energy within a load step can be obtained from the above equation and it is written as

$$\delta U_e = \int \{\delta \sigma\}_c^T [E^e]_c^{-1} \{\sigma\}_c dv + \int \{\delta \sigma\}_s^T [E^e]_s^{-1} \{\sigma\}_s dv + \int \delta \tau_{sh} k_{sh}^{-1} \tau_{sh} dx \quad (58)$$

Using the elasto-plastic constitutive relationships from Eq. (25) with reference to the starting point of the load step, the incremental stresses in the above equation can be expressed in terms of incremental strains as

$$\delta U_e = \int \{\delta \varepsilon\}_c^T [E^t]_c^T [E^e]_c^{-1} \{\sigma\}_c dv + \int \{\delta \varepsilon\}_s^T [E^t]_s^T [E^e]_s^{-1} \{\sigma\}_s dv + \int \delta \varepsilon_{sh}^t k_{sh}^{-1} \tau_{sh} dx \quad (59)$$

Using Eqs. (13), (16) and (17), the strains in the above equation can be expressed in the form of incremental nodal displacement vector and Eq. (59) can be rewritten as

$$\delta U_e = \{\delta \Delta\}^T \{\hat{F}\} \quad (60)$$

where

$$\{\hat{F}\} = \int [B]_c^T [H]_c^T [E^t]_c^T [E^e]_c^{-1} \{\sigma\}_c dv + \int [B]_s^T [H]_s^T [E^t]_s^T [E^e]_s^{-1} \{\sigma\}_s dv + \int [B]_{sh}^T k_{sh}^t k_{sh}^{-1} \tau_{sh} dx \quad (61)$$

Using the forward Euler discretisation with respect to the converged solution ( $\{\Delta_0\}, \mu_0$ ) of the previous time step, the constraint in Eq. (53) can be expressed with the help of Eqs. (54), (55) and (60) as

$$C = \{\delta \Delta\}^T (\mu_0 \{F\} - \{\hat{F}_0\}) - e_d \quad (62)$$

In case of a structure having damage [39], the above equation can similarly be derived and it can be expressed as

$$C = \frac{1}{2} \{F\}^T (\mu_0 \{\delta\Delta\} - \delta\mu \{\Delta_0\}) - e_d \quad (63)$$

Now Eq. (52) is combined with Eq. (51) to have the augmented system of equations as

$$\begin{Bmatrix} \{P_{\text{int}}\} - \mu\{F\} \\ C \end{Bmatrix} = \begin{Bmatrix} \{0\} \\ 0 \end{Bmatrix} \quad (64)$$

Now, the Newton Raphson method can be used to solve above equation iteratively as

$$\begin{Bmatrix} \{\delta\Delta\}^{j+1} \\ \delta\mu^{j+1} \end{Bmatrix} = \begin{Bmatrix} \{\delta\Delta\}^j \\ \delta\mu^j \end{Bmatrix} + \begin{Bmatrix} \{d\Delta\}^{j+1} \\ d\mu^{j+1} \end{Bmatrix} \quad (65)$$

$$\text{where } \begin{Bmatrix} \{d\Delta\}^{j+1} \\ d\mu^{j+1} \end{Bmatrix} = \left( \begin{bmatrix} \frac{\partial(\{P_{\text{int}}\} - \mu\{F\})}{\partial\{\Delta\}} & \frac{\partial(\{P_{\text{int}}\} - \mu\{F\})}{\partial\mu} \\ \frac{\partial C}{\partial\{\Delta\}} & \frac{\partial C}{\partial\mu} \end{bmatrix}^{-1} \right)^j \begin{Bmatrix} \mu\{F\} - \{P_{\text{int}}\} \\ -C \end{Bmatrix}^j \quad (66)$$

Using Eqs. (62), (63) and relevant equations in Section 2.2, the above equation can be rewritten as

$$\begin{Bmatrix} \{d\Delta\} \\ d\mu \end{Bmatrix} = \begin{bmatrix} [K_T] & -\{F\} \\ \{G\}^T & h \end{bmatrix}^{-1} \begin{Bmatrix} \{dR\} \\ -C \end{Bmatrix} \quad (67)$$

where  $\{G\} = \mu_0 \{F\} - \{\hat{F}_0\}$  and  $h = 0$  for plasticity; and  $\{G\} = \frac{1}{2} \mu_0 \{F\}$  and  $h = -\frac{1}{2} \{F\}^T \{\Delta_0\}$  for damage. The above equation in its present form is not suitable for its solution due to the incorporation of an additional row and column for including the additional unknown (load factor) which has destroyed the banded nature of the matrix system to be operated. In order to overcome this problem, the Sherman-Morrison formula [40] is used for solving the above equation as follows

$$\begin{Bmatrix} \{d\Delta\} \\ d\mu \end{Bmatrix} = \begin{Bmatrix} \{\Delta_I\} \\ -C \end{Bmatrix} - \frac{1}{\{G\}^T \{\Delta_{II}\} - h} \begin{Bmatrix} (\{G\}^T \{\Delta_I\} + C) \{\Delta_{II}\} \\ -\{G\}^T \{\Delta_I\} - C(1 + \{G\}^T \{\Delta_{II}\} - h) \end{Bmatrix} \quad (68)$$

where  $\{\Delta_I\} = [K_T]^{-1} \{dR\}$  and  $\{\Delta_{II}\} = -[K_T]^{-1} \{F\}$ .

Using Eqs. (65) and (68), the nodal displacement vectors and load factor can finally be updated as

$$\{\delta\Delta\}^{j+1} = \{\delta\Delta\}^j + \{\Delta_I\}^j - (\phi_f)^j \{\Delta_{II}\}^j \quad (69)$$

$$\delta\mu^{j+1} = \delta\mu^j + (\phi_f)^j \quad (70)$$

$$\text{where } \phi_f = \frac{\{G\}^T \{\Delta_I\} + C}{\{G\}^T \{\Delta_{II}\} - h}$$

As this arc-length method utilises the energy dissipated in a load step, the application of the method is not convenient at the initial loading steps where the structural deformations may be in the elastic range and have no energy dissipation. Thus a hybrid approach of solution strategy is adopted in the present study where the load control method is applied for some initial load steps and it is switched to the arc-length method when the energy dissipation  $U_d$  in a load step exceeds  $e_{d-\min}$ , which is the minimum value of  $e_d$  prescribed by the user. Actually, the value of  $e_d$  is updated in each load step when the arc-length method is activated in order to reduce the solution time. The value of  $e_d$  in a load step  $i+1$  can be estimated with the value of  $U_d$  in the previous load step [41] as

$$(e_d)_{i+1} = 0.5^\gamma (U_d)_i \quad (71)$$

where  $\gamma = 0.25(j - j_p)$  in which  $j$  is the iteration number and,  $j_p$  is the desired number of iterations to get convergence. In order to avoid any divergence problems, the value of  $e_d$  should be restricted within its minimum value  $e_{d-\min}$  and maximum value  $e_{d-\max}$ , which is another user specified value.

## 2.5. Stress Update

The nonlinear equilibrium equation is solved iteratively as mentioned in the above sections where the stresses are updated after every iteration as the total stress cannot be expressed in terms of total strain in the case of plastic deformations. In that situation, the incremental nodal displacements  $\{d\Delta\}_i^j$  obtained in an iteration  $j$  are used to evaluate the corresponding incremental strains  $\{d\varepsilon\}_i^j$  using Eqs. (13) and (16) in their incremental form which are subsequently utilised to compute the incremental stresses  $\{d\sigma\}_i^j$  of that iteration using the elastic constitutive relationship as

$$\{d\sigma\}_i^j = [E^e]_i \{d\varepsilon\}_i^j \quad (72)$$

The above equation is written for a material layer but it is similarly applicable to the shear studs. Now the stresses can be updated by adding the incremental stresses  $\{\dot{\sigma}\}_l^j$  with the stresses accumulated in the previous iteration  $\{\sigma\}_l^{j-1}$  as

$$\{\sigma\}_l^j = \{\sigma\}_l^{j-1} + \{\dot{\sigma}\}_l^j \quad (73)$$

The updated stresses are substituted into the yield criteria as given in Eq. (29) which will lead to  $f_l > 0$  that indicates plastic deformations of the material or  $f_l \leq 0$  for its elastic deformations. For plastic deformations ( $f_l > 0$ ), the updated stress vector  $\{\sigma\}_l^j$  estimated by Eq. (73) is unfortunately not the final stress vector and it is rather defined as the trial stress vector  $\{\sigma^t\}_l$  which is adjusted to bring it on the yield surface. This is accomplished by using the backward Euler return technique [36], a robust stress return algorithm, in the present investigation. The starting estimate of the adjusted stress vector can be obtained from the trial stress vector as

$$\{\sigma\}_l = \{\sigma^t\}_l - d\lambda_l [E^e]_l \{a\}_l \quad (74)$$

$$\text{where } d\lambda_l = \frac{f_l}{\{a\}_l^T [E^e]_l \{a\}_l + H'_l} \quad (75)$$

and  $\{a\}_l$  can be calculated using Eq. (34). Both  $\{a\}_l$  and  $d\lambda_l$  are calculated based on the trial stresses. As the above stress vector  $\{\sigma\}_l$  does not usually satisfy the yield function, an iterative approach is used where the starting or first estimate of the stress vector is defined as  $\{\sigma\}_l^1$  and the corresponding incremental plastic strain multiplier as  $d\lambda_l^1$ . The value of the stress vector and the incremental plastic strain multiplier is iteratively improved till a desired level of convergence is achieved as follows.

$$\{\sigma\}_l^{k+1} = \{\sigma\}_l^k + \{\dot{\sigma}\}_l^k \quad (76)$$

$$d\lambda_l^{k+1} = d\lambda_l^k + \dot{\lambda}_l^k \quad (77)$$

where  $k (\geq 1)$  is the iteration used for the stress return algorithm. The expressions used to determine the value of  $\{\dot{\sigma}\}_l^k$  and  $\dot{\lambda}_l^k$  are given below.

$$\{\dot{\sigma}\}_l^k = -[M]_l^k \{r\}_l^k - \dot{\lambda}_l^k [M]_l^k [E^e]_l \{a\}_l^k \quad (78)$$

$$\{r\}_l^k = \{\sigma\}_l^k - \left( \{\sigma^t\}_l - d\lambda_l^k [E^e]_l \{a\}_l^k \right) \quad (79)$$

$$[M]_l^k = \left[ [I] + d\lambda_l^k [E^e] \left[ \frac{\partial \{a\}_l}{\partial \{\sigma\}_l} \right]^k \right]^{-1} \quad (80)$$

$$\lambda_l^k = \frac{f_l^k - \{\{a\}_l^k\}^T [M]_l^k \{r\}_l^k}{\{\{a\}_l^k\}^T [M]_l^k [E^e] \{a\}_l^k + H_l^k} \quad (81)$$

The superscript  $k$  used with any parameter in the above equations indicates that that parameter is calculated at iteration  $k$ . The vector norm of the residual stress  $\{r\}_l^k$  with respect to the current stress  $\{\sigma\}_l^k$  is used to check the convergence of the above iterative process. For the present problem, the derivative of  $\{a\}_l$  used in Eq. (80) can be written as

$$\frac{\partial \{a\}_l}{\partial \{\sigma\}_l} = \frac{1}{\sigma_{ef,l}} \begin{bmatrix} 1 - \frac{\sigma_l^2}{\sigma_{ef,l}^2} & -\frac{3\sigma_l\tau_l}{\sigma_{ef,l}^2} \\ -\frac{3\sigma_l\tau_l}{\sigma_{ef,l}^2} & 3 - \frac{9\tau_l^2}{\sigma_{ef,l}^2} \end{bmatrix} \quad (82)$$

As the equilibrium path is divided into a number of load steps and the nonlinear equilibrium equation is solved within each load step iteratively, the stress return algorithm presented above is implemented in a slightly different manner so as to avoid any convergence problem. For an iteration within a load step, the incremental strains accumulated from the beginning of that load step  $\{\delta\varepsilon\}_l^j$  are used instead of  $\{d\varepsilon\}_l^j$  in Eq. (72) to get the incremental stresses  $\{\delta\sigma\}_l^j$  of that load step which are added with the converged stresses of the previous load step to evaluate the trial stresses of that iteration which is adjusted by the stress return algorithm presented above.

### 3. NUMERICAL RESULTS

#### 3.1. Two Layered Composite Beam with Rectangular Section – Numerical Verification

In this example, a composite beam consisting of two material layers having rectangular sections as shown in Fig. 3 is used for numerical verification of the proposed model. For this purpose, the beam is also analysed with a well-regarded finite element software (ABAQUS) where the numerical results produced by a detailed 2D model of the beam are utilised to compare the results predicted by the proposed model. For the upper material layer of the beam, the Hognestad model [42] as shown in Fig. 4 is used for defining its uniaxial stress-strain curves that may be expressed as

$$\sigma_c = f'_c \left[ \frac{2\varepsilon_c}{\varepsilon_{c0}} - \left( \frac{\varepsilon_c}{\varepsilon_{c0}} \right)^2 \right] \quad \varepsilon_c < \varepsilon_{c0} \quad (83)$$

$$\sigma_c = f'_c [83(\varepsilon_{c0} - \varepsilon_c) + 1] \quad \varepsilon_{c0} \leq \varepsilon_c \leq \varepsilon_{cu} \quad (84)$$

where  $f'_c$  is the peak compressive strength,  $\varepsilon_{c0}$  is the strain corresponding to  $f'_c$  and  $\varepsilon_{cu}$  is the ultimate compressive strain.

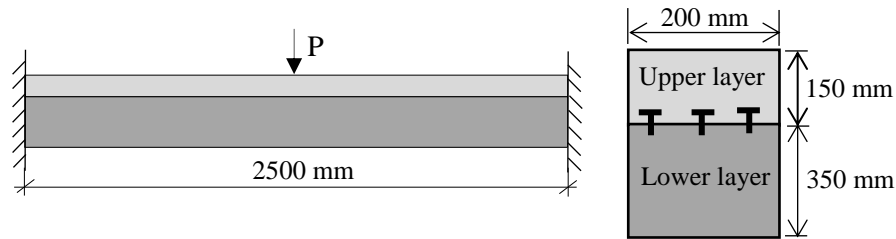


Fig. 3. Composite beam having fixed supports at its two ends

For the present problem, the values of these material parameters are taken as:  $f'_c = 25$  MPa,  $\varepsilon_{c0} = 0.002$  and  $\varepsilon_{cu} = 0.038$  along with the elastic modulus of 20,000 MPa and Poisson's ratio of 0.25 for the upper layer.

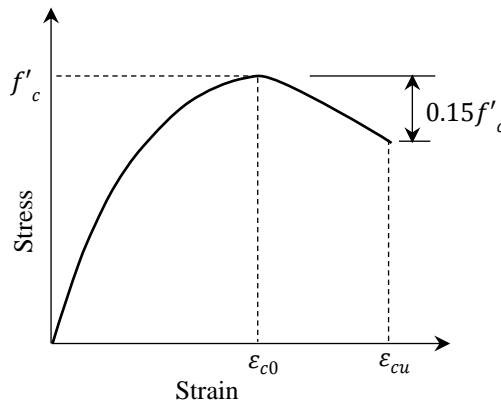


Fig. 4. Uniaxial stress-strain curve for the upper material layer (concrete)

For the lower layer of the beam, a hypothetical material is used and its uniaxial stress-strain relationship both in tension and compression is defined with a simple bi-linear model as shown in Fig. 5 where the strain softening branch is deliberately taken to produce a prominent descending branch of the load-deflection curve of the composite beam. This is actually a theoretical problem devised to show the capability of the proposed model in tracing the descending branch of the load-deflection curve successfully. The present analysis is carried out taking the ultimate stress  $f_u = 40$  MPa, elastic modulus  $E = 30,000$  MPa, Poisson's ratio  $\nu = 0.25$  and hardening parameter of the strain softening branch  $H = -3000$  MPa for the lower material layer which is assumed to follow the von Mises plasticity model

both in tension and compression. For the sake of comparison of the proposed model with the ABAQUS model, the upper layer is also treated as a hypothetical material where von Mises plasticity theory is used in compression as well as tension regions. Moreover, the uniaxial stress-strain curve of the material in both compression and tension is defined by the Hognestad model [42], which is typically used for concrete in compression for all other examples.

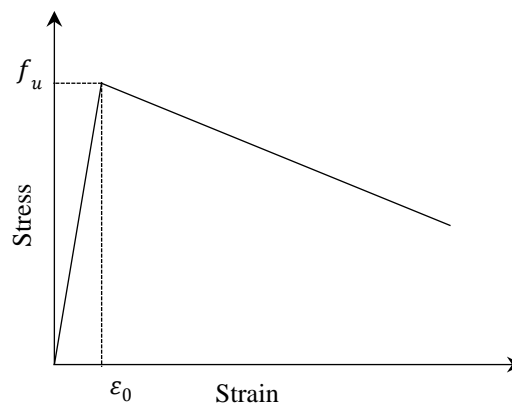


Fig. 5. Uniaxial stress-strain curve for the lower material layer

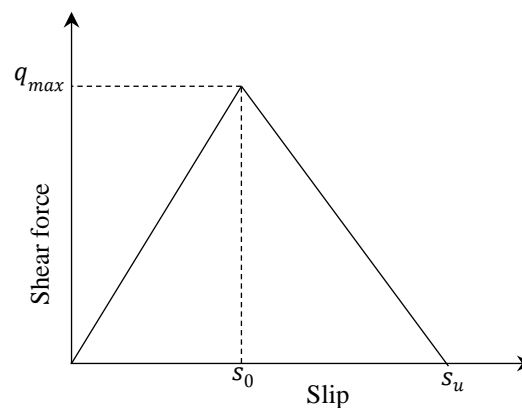


Fig. 6. Interfacial shear force (per unit length) slip relationship for shear connectors

The interface between these material layers can be modelled by ABAQUS where the contact mechanics is typically used and the interfacial slip can be simulated by using a cohesive contact model which is similar to the damage model presented in Section 2.3.2. Though a plasticity based constitutive model proposed in Section 2.3.3 is used for modelling the shear connectors in other examples, a damage mechanics based model is used in this example to have a parity with the ABAQUS as this software does not have the capability of modelling an elasto-plastic interface. The formulation for the damage mechanics model of the shear connectors is not presented but it can easily be derived utilising the concepts presented in Sections 2.3.2 and 2.3.3. Fig. 6 shows the interfacial shear force (per unit length)-slip

relationship used for this damage model where the fracture energy ( $G_f$ ) is used to estimate the maximum slip  $s_u$ . To define the damage model for the shear connectors (Fig. 6), the values of the different material parameters used are:  $k_{sh} = 100$  MPa,  $q_{max} = 150$  MPa,  $s_u = 3$  mm.

The beam is analysed with the proposed 1D finite element (FE) model using different number of elements and the results show that an acceptable level of convergence is achieved with 20 elements for this beam. The computing time needed to complete the analysis using the proposed model was 75.81 sec where an ordinary desktop computer (i5-3470T CPU @ 2.90 GHz and RAM 8.0 GB, 64 bit operating system) was used. Though the proposed element is based on HBT (3<sup>rd</sup> order theory), it can easily be amended to TBT (1<sup>st</sup> order theory) by dropping the higher order terms. For the analysis of the beam using ABAQUS, the 2D plane stress rectangular element (CPS4R) are used to model both layers by discretising these layers along their lengths and depths assuming no normal stress across the beam width where the mesh convergence study is similarly conducted. The shear connectors are modelled using the cohesive contact model place at the interface between the elements used for upper and lower layers. The same computer is used for running this 2D analysis where the computing time consumed was 730.66 sec for solving the problem. It should be noted that the solver used by ABAQUS is expected to be more efficient than a relatively simple solver used in the computer program (FORTRAN) developed for implementing the proposed model. Moreover, it needs a significant amount of time for model generation in ABAQUS.

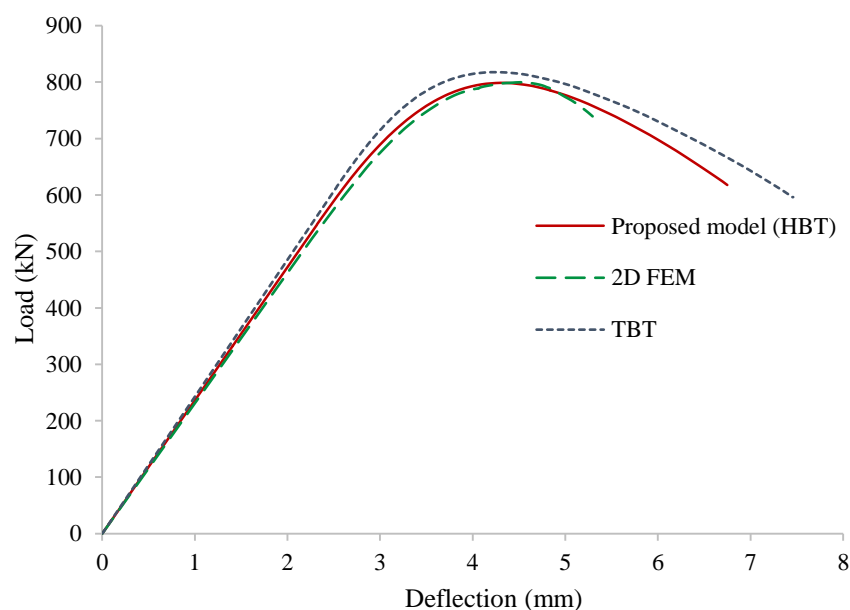


Fig. 7. Mid-span deflection of the two-layer composite beam

The variation of mid-span deflection with respect to the applied load predicted by the proposed 1D FE model based on HBT as well as TBT is presented in Fig. 7 along with the results produced by the detailed 2D FE model. The figures shows a good correlation between the results obtained from the three models where the performance of HBT is relatively better than TBT if compared with the 2D FE model. It also shows that the post-peak response of the beam is successfully traced by the proposed model and it performed better than ABAQUS in the sense that the nonlinear solution process of this software is terminated earlier than the proposed model. The variations of the vertical displacement and the interfacial slip along the beam length corresponding to 700 kN of the applied load ( $P$ ) predicted by these approaches are presented in Fig. 8 and Fig. 9, respectively.

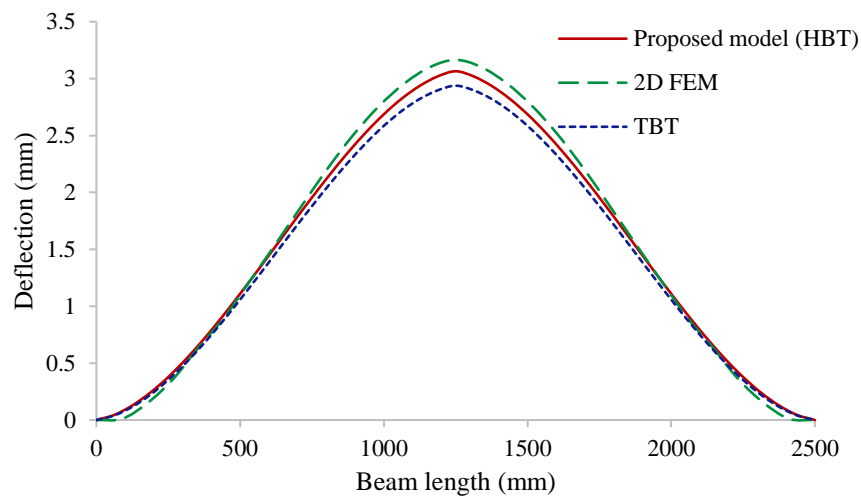


Fig. 8. Deflection along the length of the two-layered composite beam

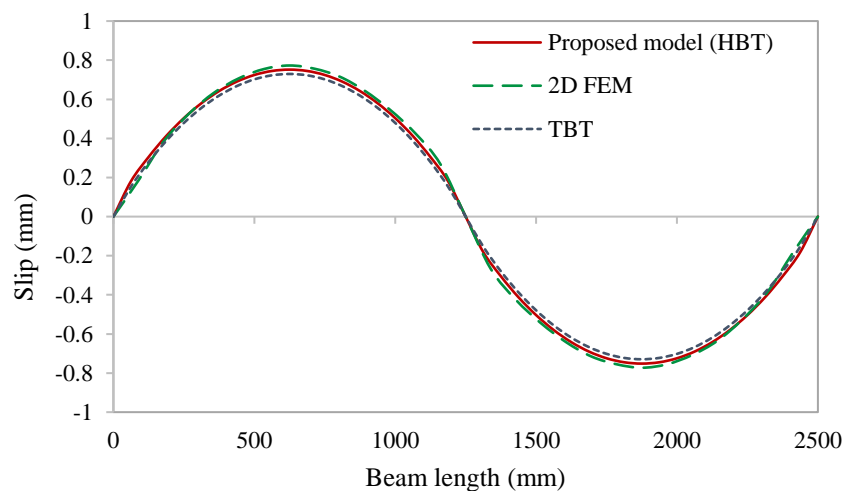


Fig. 9. Interfacial shear slip of the two-layered composite beam along its length

Finally, the variation of von Mises stress over the beam depth obtained at two sections of the beam by these three approaches for  $P = 700$  kN is plotted in Fig. 10 and Fig. 11, which

shows a very good performance of HBT. The performance of TBT is not generally good due to the assumption of average shear strain and the performance is severely affected at the quarter span (Fig. 11) where the contribution of shear stress is predominant as the bending moment/stress is less at this section.

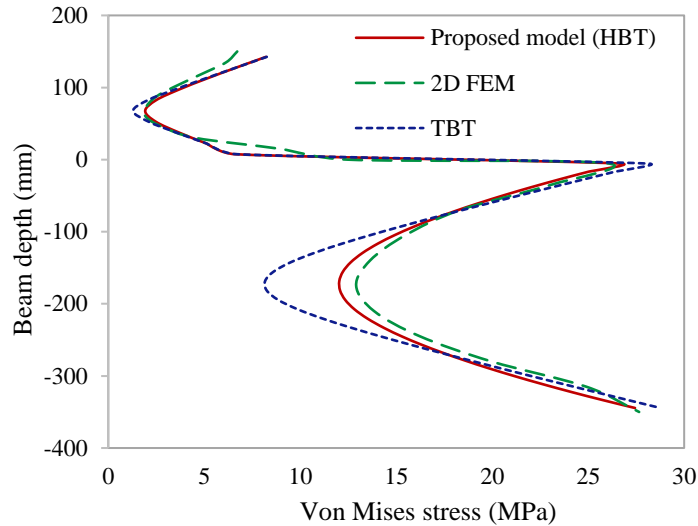


Fig. 10. Von Mises stress at a section 1m away from a support of the two-layered composite beam

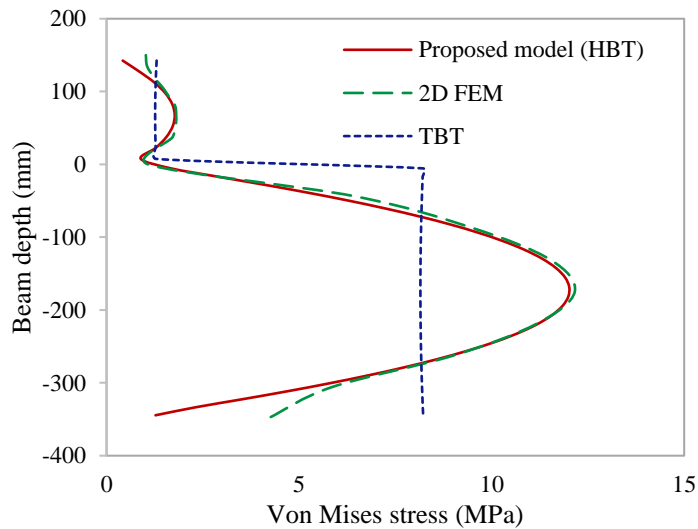


Fig. 11. Von Mises stress at the quarter span of the two-layered composite beam

### 3.2. Steel-concrete Composite Beam Subjected to Three Point Bending – Experimental Validation

A 5.5 m long steel-concrete composite beam tested by Chapman and Balakrishnan [43] is used in this example for the experimental validation of the proposed model. The beam

consisting of a concrete slab and a steel I-girder connected by steel shear studs as shown in Fig. 12 was simply supported at its two ends and subjected to a point load at the mid-span.

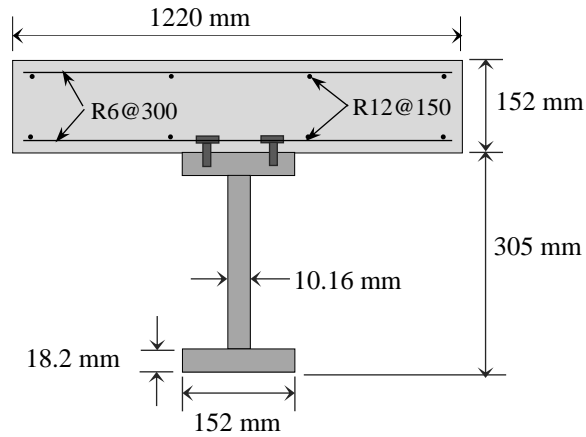


Fig. 12. Cross-section of composite beam

The Hognestad model [42] as shown in Fig. 4 is used for the uniaxial stress-strain relationship of concrete in compression while the bi-linear model as shown in Fig. 2 is used for this in tension. The steel girder is assumed to follow a bi-linear model with a strain hardening branch as shown in Fig. 13 for its uniaxial stress-strain relationship both in tension and compression. For the shear connectors idealised as a distributed shear springs layer, a bi-linear model as shown in Fig. 14 is used to define the relationship between the interfacial shear force per unit length  $q$  and the shear slip  $s$  using two values of the hardening parameter which is zero in one case. The concrete slab is reinforced with longitudinal steel bars R12@150mm in its top and bottom regions (Fig. 12). The re-bars are modelled as 1D members under uniaxial stress where an elastic-perfectly plastic material behaviour is adopted.

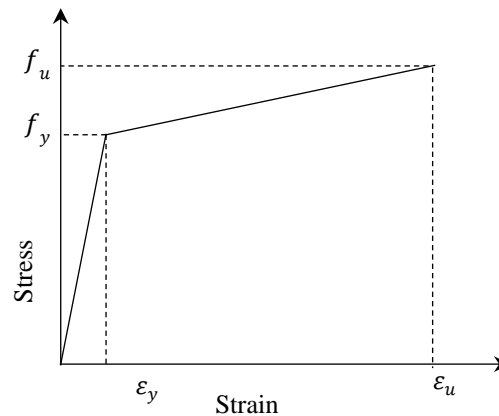


Fig. 13. Bi-axial stress-strain curve for steel girder

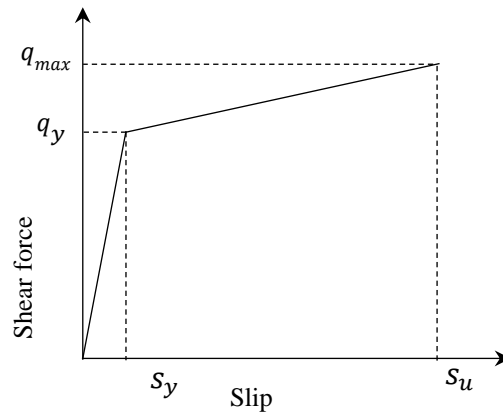


Fig. 14. Bi-axial stress-strain curve for shear connector

The material properties used for characterising the different components of the composite beam are given in Table 1 which also contains the material properties of the beam considered in the next example. The problem is solved by the proposed nonlinear model based on HBT using 20 elements, and the variation of mid-span deflection with respect to the applied load obtained with two different hardening parameters of the shear connectors are presented in Fig. 15 along with the experimental result obtained by Chapman and Balakrishnan [43]. Fig. 15 also includes numerical results reported by Liang et al. [44] who obtained this result from a detailed 3D finite element model of the beam using ABAQUS. The figure shows a very good correlation between the results obtained from different approaches where the proposed model (considering no hardening for the shear connectors) is found to perform better than ABAQUS when compared with the experimental result.

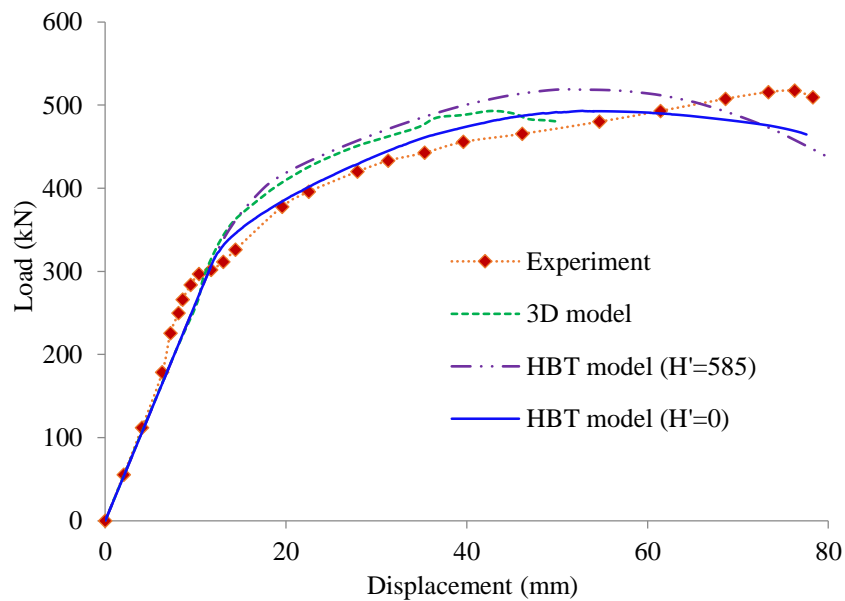


Fig. 15. Vertical displacement at mid-span of composite beam.

**Table 1.** Material properties of composite beams

Material	Property	Liang et al. [44]	Tan and Uy [45]
Concrete slab	Elastic modulus, $E_c$	32,920 MPa	20,000 MPa
	Poisson's ratio, $\nu$	0.15	0.10
	Compressive strength, $f'_c$	42.5 MPa	25 MPa
	Strain, $\epsilon_{c0}$	0.002	0.002
	Ultimate tensile stress, $f_t$	3.553 MPa	2.5 MPa
	Fracture energy, $G_f$	0.208 N/mm	0.1875 N/mm
	Ultimate tensile strain, $\epsilon_{tu}$	0.0016	0.0019
Steel girder	Elastic modulus, $E_s$	205,000 MPa	200,000 MPa
	Poisson's ratio, $\nu$	0.3	0.3
	Yield stress, $f_y$	265 MPa	300 MPa
	Ultimate stress, $f_u$	410 MPa	500 MPa
	Ultimate strain, $\epsilon_u$	0.25	0.11
Shear connector	Yield shear force, $q_y$	435 MPa	
	Ultimate shear force, $q_{max}$	565 MPa	743.86 N/mm‡ 396.49 N/mm†
	Elastic stiffness, $k_{sh}$	2491.46 MPa	717.74 MPa‡ 597.61 MPa†
	Maximum slip, $s_u$	6 mm	7 mm‡ 10 mm†
Reinforcement in concrete slab	Modulus of elasticity, $E_s$	200,000 MPa	200,000 MPa
	Poisson's ratio, $\nu$	0.3	0.25
	Yield stress, $f_y$	250 MPa	550 MPa
	Ultimate strain, $\epsilon_u$	0.25	0.11

Note: † = Single shear stud in a row

‡ = Double shear stud in a row

### 3.3. Steel-concrete Composite Beam Under Four Point Bending – Experimental Validation

A steel-concrete composite beam (Fig. 16) tested by Tan and Uy [45] under four point bending is used in this example. The concrete slab (including re-bars) and steel girder are modelled in a similar manner as followed in the previous example.

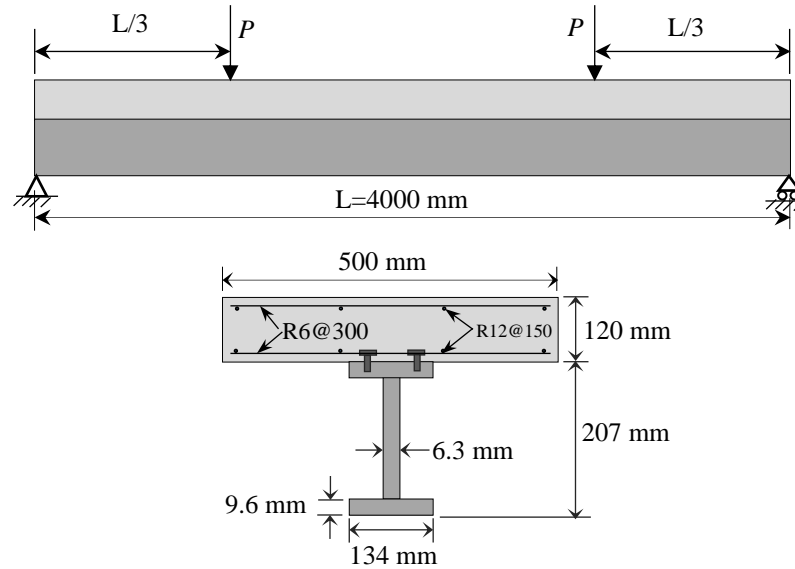


Fig. 16. Simply supported steel-concrete composite beam

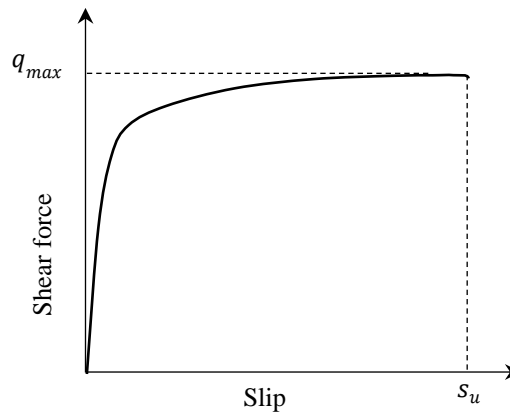


Fig. 17. Exponential model for the uniaxial stress-strain curve for shear connector

For the simulation of steel shear studs used for connecting the concrete slab with the steel girder, the exponential model of Olgaard et al. [46] as shown in Fig. 17 is used which can be given by

$$\tau_{sh} = q_{\max} \left[ 1 - e^{(-0.71s)} \right]^{2/5} \quad s \leq s_u \quad (85)$$

where  $q_{max}$  is the ultimate value of the interfacial shear force (per unit length) and  $s_u$  is the ultimate slip. This model (Fig. 17) is chosen on the basis of the trend of results obtained in the push out test [45].

For the present study, two different beam specimens tested by Tan and Uy [45] are used where the number shear studs used in a row along the beam width is one in the first case while it is two in the other case. Table 1 includes all the material properties used for defining the different constituents of the composite beam. The beam is analysed with the proposed technique and the result obtained in the form of variation of mid-span deflection with respect to mid-span moment is presented in Fig. 18 along with the experimental results reported by Tan and Uy [45]. The figure shows a good correlation between the numerical and experimental results. For this statically determinant beam, the mid-span moment can easily be determined with the value of applied loads and their locations.

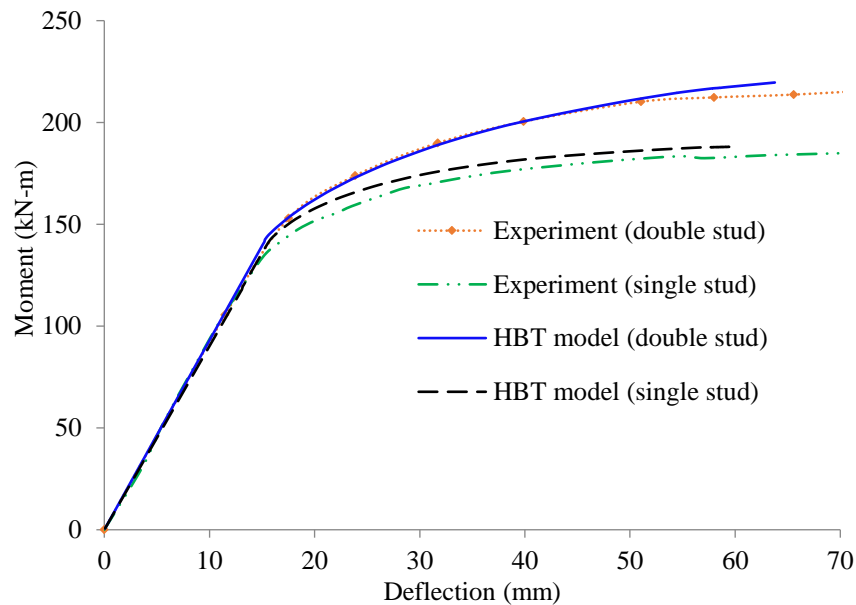


Fig. 18. Variation of mid-span deflection with respect to mid-span moment of the composite beam (Tan and Uy [45]).

### 3.4. Two Span Steel-concrete Composite Beam

The problem of a two-span continuous beam consisting of a concrete slab and a steel I-girder connected by steel shear studs (Fig. 19) is studied using the proposed model which is carefully verified and validated in the above sections. Fig. 19 shows the dimensions of different components of the beam and its boundary and loading conditions chosen for the present study. The behaviour of concrete slab and shear connectors is modelled in a similar

manner as followed in the previous example. For the steel girder, an elastic-perfectly plastic with strain hardening model [14] as shown in Fig. 20 is employed for defining its uniaxial stress-strain relationship in both tension and compression. According to Liu et al. [14], the strain hardening branch of the stress-strain curve (Fig. 20) can be expressed as

$$\sigma_s = f_y + (f_u - f_y) \left[ 1 - e^{-\frac{(\varepsilon_{sh} - \varepsilon_s)}{a}} \right] \quad \varepsilon_{sh} \leq \varepsilon_s \leq \varepsilon_u \quad (86)$$

where  $f_y$  is the yield stress,  $f_u$  is the ultimate stress,  $\varepsilon_y$  is the yield strain,  $\varepsilon_{sh}$  is the strain at the beginning of strain hardening, and  $\varepsilon_u$  is the ultimate strain. The material constant  $a$  used in Eq. (86) can be determined with the above parameters as

$$a = \frac{0.028(\varepsilon_{sh} - \varepsilon_u)}{\varepsilon_{sh} - 0.16} \quad (87)$$

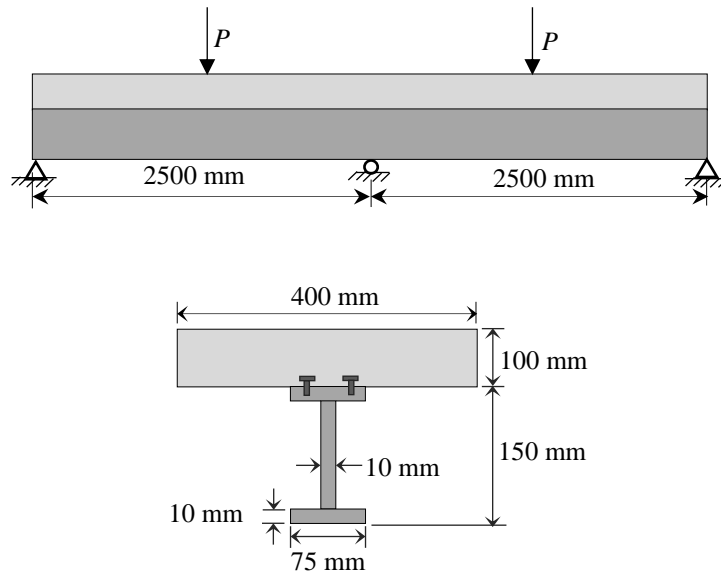


Fig. 19. Two-span steel concrete composite beam.

For the present problem, the values used for the material parameters of concrete are:  $f'_c = 25$  MPa,  $\varepsilon_{c0} = 0.002$ ,  $\varepsilon_{cu} = 0.038$ ,  $f_t = 2.5$  MPa,  $G_f = 0.1875$  N/mm,  $E_c = 20$  GPa and  $\nu_c = 0.20$ . Similarly, the material properties used for the steel girder are:  $f_y = 275$  MPa,  $f_u = 500$  MPa,  $\varepsilon_{sh} = 0.025$ ,  $\varepsilon_u = 0.11$ ,  $E_s = 200$  GPa and  $\nu_s = 0.25$ . For the shear connectors, the values of material properties are:  $q_{max} = 500$  N/mm,  $k_{sh} = 250$  MPa and  $s_u = 6$  mm.

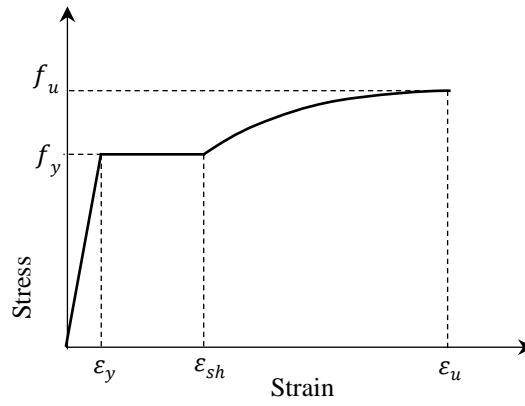


Fig. 20. Uniaxial stress-strain curve (elastic perfectly plastic with strain hardening) for the steel girder

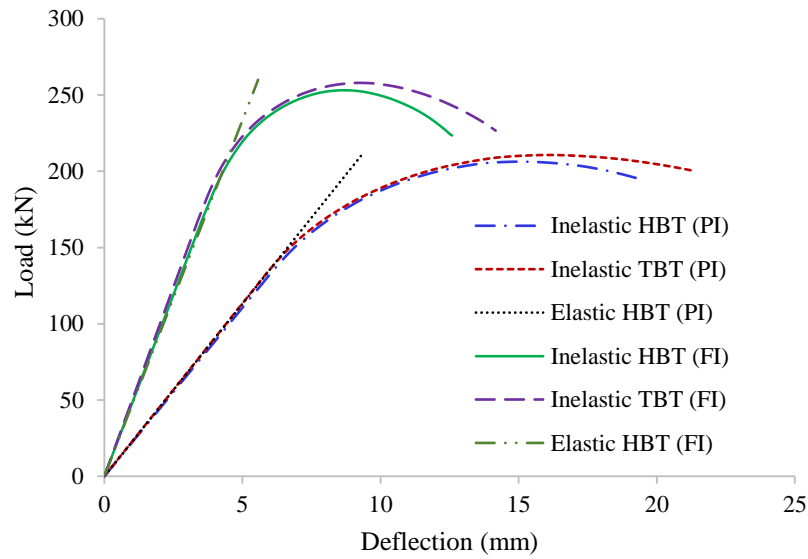


Fig. 21. Deflection under the point load on a span of the two span composite beam (Fig. 19).

The beam is analysed with the proposed nonlinear finite element model based on HBT as well as TBT. Moreover, the analysis is carried out with a very high value of  $q_{max}$  ( $1.0 \times 10^{15}$  MPa) for modelling the shear connectors in addition to its usual value as mentioned above (500 MPa), which are defined as full interaction (FI) and partial interaction (PI) conditions respectively. The load-deflection curves obtained at one of the mid-span sections for all these cases (HBT, TBT, PI and FI) are presented in Fig. 21. It is observed that the difference between the deflection values predicted by HBT and TBT is more in the case of full interaction compared to partial interaction. The variations of von Mises stress over the beam depth obtained at a section 1.0 m away from one of the end supports corresponding to the applied load  $P = 200$  kN are plotted in Fig. 22. It shows a significant deviation of results predicted by HBT and TBT where the deviation is more in the case of partial interaction. The variations of shear stress over the beam depth obtained at a quarter section from one of the end supports corresponding to the applied load  $P = 200$  kN are plotted in Fig. 23. The

figure clearly indicate that TBT is not capable of predicting the actual variation of shear stress.

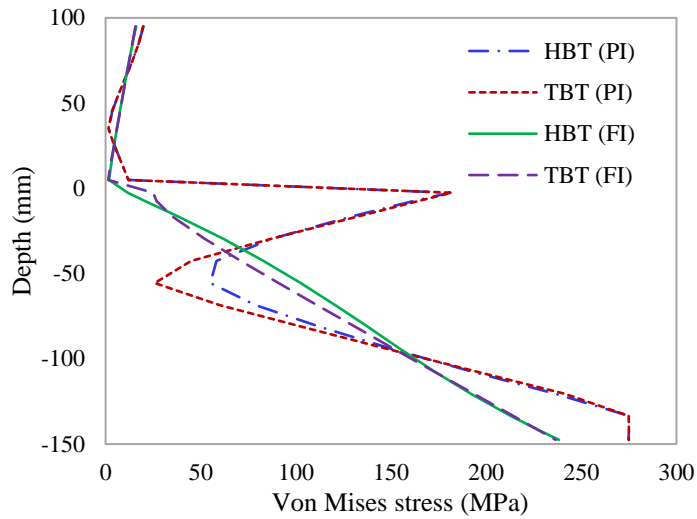


Fig. 22. Von Mises stress at a section 1m away from one of the end support of the two span composite beam under point load ( $P = 200$  kN)

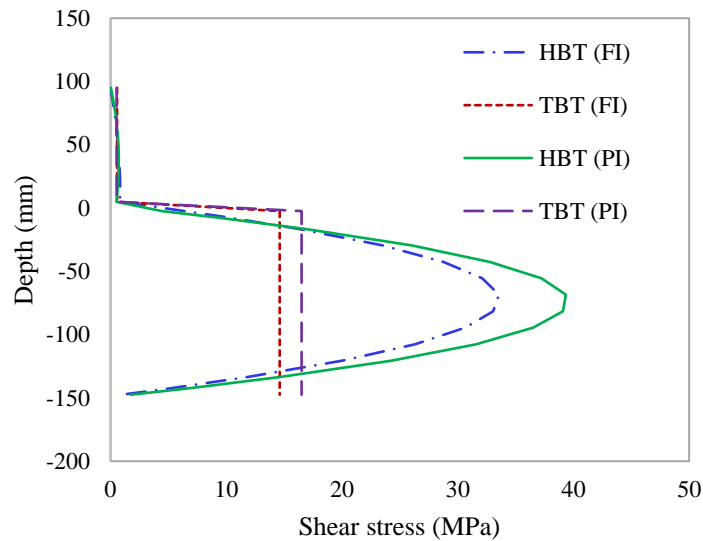


Fig. 23. Shear stress at a quarter section from one of the end support of the two span composite beam under point load ( $P = 200$  kN)

#### 4. SUMMARY AND CONCLUSIONS

An accurate and computationally efficient finite element model is developed for a reliable prediction of the inelastic response of steel-concrete composite beams. The steel shear studs used to connect the steel girder with the concrete slab are idealised as interfacial distributed springs with finite stiffness which helps to model the partial shear interaction of the composite beam. The higher order beam theory is used to develop this one dimensional finite element model with better accuracy. The von-Mises yield function with an isotropic

hardening rule and associated flow rule is used to model the behaviour of steel girders, steel reinforcements, steel shear studs and concrete slabs in compression. A damage mechanics model is used for modelling concrete slabs in tension. The mesh sensitivity associated with the damage modelling of concrete, a quasi-brittle material, in tension is eliminated using the well-known crack band theory. The inelastic material behaviour imposed a typical nonlinearity in the present problem and the solution of the governing equations becomes challenging specifically for capturing the post peak response. In order to address this issue, an energy dissipation based arc length method is employed to solve the nonlinear equations which helped to trace the descending branch of the load deflection curve successfully. Before validation of the proposed model with benchmarking experimental results, the numerical verification of the model is carried out with the help of a two-layer composite beam. For this purpose, a detailed 2D model of the composite beam is developed using a reliable commercial finite element software to produce reliable numerical results which are compared with the results produced by the proposed 1D model.

The proposed model is based on a 3<sup>rd</sup> order beam theory (HBT) but it can easily be converted to a lower order beam theory (e.g., TBT) by eliminating the higher order terms. The numerical analysis has confirmed that the model based on TBT is able to predict the global response satisfactorily with the help of a shear correction factor. However, it is observed that this factor is not sufficient even for an accurate prediction of the global response in some situation such as beams with a small span-to-depth ratio, localised concentrated loads and clamped boundary conditions. Moreover, the model based on TBT could not predict the distribution of stresses (local response) across the beam section. On the other hand, the proposed model based on HBT could realistically predict the global as well as local responses of these beams without any arbitrary factor as it takes account of the actual parabolic variation of shear strain. The major advantage of the proposed model is it can predict results very close to those produced by detailed finite element models using ABAQUS but the computational cost of the proposed model is significantly less than the ABAQUS model. Moreover, in some situations, the proposed model performed better than ABAQUS in the sense that the nonlinear solution process of this commercial software was terminated earlier than the proposed model.

The proposed model is also used to examine the effect of different levels of shear interaction between the concrete and steel layers of the composite beam. It is observed that the full shear interaction condition predicted deflection less than that for the partial interaction as expected. For both full and partial interaction conditions, the difference between the results predicted

by HBT and TBT models is found to be appreciable. Based on the accuracy and range of applicability along with the computational efficiency of the proposed model, it is highly recommended for the analysis of composite beams having inelastic material behaviours.

## 5. ACKNOWLEDGEMENT

The financial support provide by the University of Adelaide in the form of an Adelaide Scholarship International (ASI) awarded to the first author for his doctoral studies is gratefully acknowledged. The authors also acknowledge the help received from V.P. Nguyen (Department of Civil Engineering, Monash University, Australia) in implementing the arc-length method.

## 6. APPENDIX

### Nomenclature

$A_c, A_s$	cross-sectional area of concrete and steel layers of the beam
$[B]_l$	strain-displacement matrix for the $l$ -th layer ( $l=c$ for concrete, $l=s$ for steel)
$[B]_{sh}$	strain-displacement matrix for shear connectors
$\{dR\}$	residual force vector
$e_d$	prescribed dissipation energy
$E_l$	elastic modulus for the $l$ -th layer
$[E^{cr}]$	tangent damage stiffness matrix for concrete
$[E^{ep}]_l$	elasto-plastic constitutive matrix for the $l$ -th layer
$f_l$	von Mises yield function for the $l$ -th layer
$\{F_{ext}\}$	external load vector
$G_l$	shear modulus for the $l$ -th layer
$G_f$	fracture energy
$[H]_l$	cross-sectional matrix for the $l$ -th layer

$H'_l$	hardening parameter for the $l$ -th layer
$H'_{sc}$	hardening parameter for shear connectors
$k_{sh}$	elastic stiffness of distributed springs for shear connectors
$k_{sh}^{ep}$	elasto-plastic tangent stiffness for shear connectors
$[K_T]$	tangent stiffness matrix
$l_e$	element length
$N$	shape function
$\{P_{int}\}$	internal nodal force vector
$q$	distributed external load
$s$	interfacial slip between concrete and steel layers
$s^e$	elastic shear slip between concrete and steel layers
$s^p$	plastic shear slip between concrete and steel layers
$s_{ef}^p$	effective plastic shear slip between concrete and steel layers
$u_{c0}$	longitudinal displacement of the concrete layer at its centroidal or reference axis
$\bar{u}_c$	longitudinal displacement at the bottom fibre of the concrete layer
$u_{s0}$	longitudinal displacement of the steel layer at its reference axis
$\bar{u}_s$	longitudinal displacement at the top fibre of the lower layer
$w$	transverse displacement
$w_c$	crack band width
$\alpha, \beta$	higher order terms
$\{\Delta\}$	nodal displacement vector
$\{\boldsymbol{\varepsilon}\}_c, \{\boldsymbol{\varepsilon}\}_s$	strain vectors of concrete and steel layers
$\{\boldsymbol{\varepsilon}^e\}_l$	elastic strain vector for the $l$ -th layer
$\{\boldsymbol{\varepsilon}^p\}_l$	plastic strain vector for the $l$ -th layer
$\varepsilon_l^p$	plastic normal strain for the $l$ -th layer
$\varepsilon_{ef,l}^p$	equivalent plastic strain for the $l$ -th layer

$\{\bar{\varepsilon}\}_l$	one dimensional strain vector for the $l$ -th layer
$\gamma_l^p$	plastic shear strain for the $l$ -th layer
$\kappa_{ef}$	equivalent strain parameter
$d\lambda_l$	incremental plastic strain multiplier for the $l$ -th layer
$\mu$	load factor (or multiplier)
$\theta_c, \theta_s$	bending rotations of concrete and steel layers
$\{\sigma\}_c, \{\sigma\}_s$	stress vectors of concrete and steel layers
$\sigma_{ef,l}$	effective stress for the $l$ -th layer
$\sigma_{y,l}$	uniaxial yield stress for the $l$ -th layer
$\sigma_l$	bending stress for the $l$ -th layer
$\sigma_{t0}$	uniaxial ultimate tensile stress
$\sigma_{\max}$	maximum principle stress
$\tau_l$	shear stress for the $l$ -th layer
$\tau_{sh}$	distributed shear force (per unit length) at the interface between concrete and steel layers
$\omega$	damage parameter

## 7. REFERENCE

- [1] Oehlers D, Bradford MA. Composite Steel and Concrete Structural Members. Fundamental Behaviour, Australia. 1995.
- [2] Loh H, Uy B, Bradford MA. The effects of partial shear connection in the hogging moment regions of composite beams: Part I—Experimental study. Journal of constructional steel research. 2004;60:897-919.
- [3] Uy B, Nethercot D. Effects of partial shear connection on the required and available rotations of semi-continuous composite beam systems. The Structural Engineer 2005;83.
- [4] Newmark NM, Siess CP, Viest I. Tests and analysis of composite beams with incomplete interaction. Proc Soc Exp Stress Anal. 1951;9:75-92.
- [5] Ranzi G, Gara F, Leoni G, Bradford MA. Analysis of composite beams with partial shear interaction using available modelling techniques: A comparative study. Computers & structures. 2006;84:930-41.

- [6] Adekola A. Partial interaction between elastically connected elements of a composite beam. *International Journal of Solids and Structures*. 1968;4:1125-35.
- [7] Girhammar UA, Pan D. Dynamic analysis of composite members with interlayer slip. *International Journal of Solids and Structures*. 1993;30:797-823.
- [8] Jasim NA. Computation of deflections for continuous composite beams with partial interaction. *Proceedings of the Institution of Civil Engineers Structures and buildings*. 1997;122:347-54.
- [9] Nguyen Q, Hjiiaj M, Uy B. Time effects analysis of composite beams using a mixed FE formulation. *Third International Conference on Structural Engineering, Mechanics and Computation (SEMC 2007)*2007. p. 1157-63.
- [10] Yasunori A, Sumio H, Kajita T. Elastic-plastic analysis of composite beams with incomplete interaction by finite element method. *Computers & Structures*. 1981;14:453-62.
- [11] Salari MR, Spacone E, Shing PB, Frangopol DM. Nonlinear analysis of composite beams with deformable shear connectors. *Journal of Structural Engineering*. 1998;124:1148-58.
- [12] Dall'Asta A, Zona A. Non-linear analysis of composite beams by a displacement approach. *Computers & Structures*. 2002;80:2217-28.
- [13] Erkmen RE, Attard MM. Displacement-based finite element formulations for material-nonlinear analysis of composite beams and treatment of locking behaviour. *Finite Elements in Analysis and Design*. 2011;47:1293-305.
- [14] Liu X, Bradford MA, Erkmen RE. Non-linear inelastic analysis of steel–concrete composite beams curved in-plan. *Engineering Structures*. 2013;57:484-92.
- [15] Foraboschi P. Analytical solution of two-layer beam taking into account nonlinear interlayer slip. *Journal of engineering mechanics*. 2009;135:1129-46.
- [16] Focacci F, Foraboschi P, De Stefano M. Composite beam generally connected: Analytical model. *Composite Structures*. 2015;133:1237-48.
- [17] Berczyński S, Wróblewski T. Vibration of steel–concrete composite beams using the Timoshenko beam model. *Journal of Vibration and Control*. 2005;11:829-48.
- [18] Ranzi G, Zona A. A steel–concrete composite beam model with partial interaction including the shear deformability of the steel component. *Engineering Structures*. 2007;29:3026-41.
- [19] Xu R, Wu Y. Static, dynamic, and buckling analysis of partial interaction composite members using Timoshenko's beam theory. *International Journal of Mechanical Sciences*. 2007;49:1139-55.
- [20] Schnabl S, Saje M, Turk G, Planinc I. Locking-free two-layer Timoshenko beam element with interlayer slip. *Finite Elements in Analysis and Design*. 2007;43:705-14.
- [21] Nguyen Q-H, Hjiiaj M, Lai V-A. Force-based FE for large displacement inelastic analysis of two-layer Timoshenko beams with interlayer slips. *Finite Elements in Analysis and Design*. 2014;85:1-10.

- [22] Chakrabarti A, Sheikh A, Griffith M, Oehlers D. Analysis of composite beams with longitudinal and transverse partial interactions using higher order beam theory. *International Journal of Mechanical Sciences*. 2012;59:115-25.
- [23] Chakrabarti A, Sheikh A, Griffith M, Oehlers D. Analysis of composite beams with partial shear interactions using a higher order beam theory. *Engineering Structures*. 2012;36:283-91.
- [24] Chakrabarti A, Sheikh A, Griffith M, Oehlers D. Dynamic response of composite beams with partial shear interaction using a higher-order beam theory. *Journal of Structural Engineering*. 2012;139:47-56.
- [25] Reddy JN. A simple higher-order theory for laminated composite plates. *Journal of applied mechanics*. 1984;51:745-52.
- [26] Riks E. An incremental approach to the solution of snapping and buckling problems. *International Journal of Solids and Structures*. 1979;15:529-51.
- [27] Crisfield MA. A fast incremental/iterative solution procedure that handles “snap-through”. *Computers & Structures*. 1981;13:55-62.
- [28] Crisfield MA. An arc-length method including line searches and accelerations. *International journal for numerical methods in engineering*. 1983;19:1269-89.
- [29] May I, Duan Y. A local arc-length procedure for strain softening. *Computers & structures*. 1997;64:297-303.
- [30] Bennett T, Jefferson AD. Experimental Tests and Numerical Modelling of Hexagonal Concrete Specimens. *Materials and Structures*. 2007;40:491-505.
- [31] Gutiérrez MA. Energy release control for numerical simulations of failure in quasi-brittle solids. *Communications in Numerical Methods in Engineering*. 2004;20:19-29.
- [32] Vinayak RU, Prathap G, Naganarayana BP. Beam elements based on a higher order theory—I. Formulation and analysis of performance. *Computers & Structures*. 1996;58:775-89.
- [33] Chen W-F, Han D-J. *Plasticity for structural engineers*: J. Ross Publishing; 2007.
- [34] Crisfield MA. *Non-Linear Finite Element Analysis of Solids and Structures: Advanced Topics*: John Wiley & Sons, Inc.; 1997.
- [35] De Borst R, Crisfield MA, Remmers JJ, Verhoosel CV. *Nonlinear finite element analysis of solids and structures*: John Wiley & Sons; 2012.
- [36] Crisfield MA. *Non linear finite element analysis of solids and structures*, vol. 1. Wiley, New York; 1991.
- [37] Rankine WJM. *Applied Mechanics*. 1st edition ed. London 1858.
- [38] Bažant ZP, Oh BH. Crack band theory for fracture of concrete. *Matériaux et construction*. 1983;16:155-77.

- [39] Verhoosel CV, Remmers JJ, Gutiérrez MA. A dissipation-based arc-length method for robust simulation of brittle and ductile failure. *International Journal for Numerical Methods in Engineering*. 2009;77:1290-321.
- [40] Sherman J, Morrison WJ. Adjustment of an Inverse Matrix Corresponding to a Change in One Element of a Given Matrix. 1950:124-7.
- [41] Nguyen VP, Nguyen-Xuan H. High-order B-splines based finite elements for delamination analysis of laminated composites. *Composite Structures*. 2013;102:261-75.
- [42] Hognestad E, Hanson NW, McHenry D. Concrete stress distribution in ultimate strength design. *Journal Proceedings*1955. p. 455-80.
- [43] Chapman J, Balakrishnan S. Experiments on composite beams. *The Structural Engineer*. 1964;42:369-83.
- [44] Liang QQ, Uy B, Bradford MA, Ronagh HR. Strength analysis of steel–concrete composite beams in combined bending and shear. *Journal of Structural Engineering*. 2005;131:1593-600.
- [45] Tan E, Uy B. Experimental study on straight composite beams subjected to combined flexure and torsion. *Journal of Constructional Steel Research*. 2009;65:784-93.
- [46] Ollgaard JG, Slutter RG, Fisher JW. Shear strength of stud connectors in lightweight and normal-weight concrete. *AISC Engineering Journal*. 1971;8:55-64.



## **Chapter 4: Geometric and Material Nonlinear Model**

### **4.1 Introduction**

This chapter contains the manuscript entitled “Geometrically nonlinear inelastic analysis of steel-concrete composite beams with partial interaction using a higher-order beam theory”. It presents the development of a one dimensional finite element model for composite beams considering the effects of inelastic material behaviour and large deformation. The model presented in this chapter is developed by systematically combining all aspects considered to develop the two models presented in chapter 2 and chapter 3. The effect of large deformation is incorporated by using the Green-Lagrange strain vector whereas the inelastic material behaviour is modelled by the von Mises plasticity theory. A damage mechanics model is also used for modelling the inelastic behaviour of concrete under tension. It also implements the robust stress return algorithm for updating the stresses. In order to simulate a realistic response, different stress-strain relationships are used for the different materials. It is shown that a robust arc-length method used for solving the nonlinear equations helped to trace the descending branch of the load-deflection curve well. It also shown that the relative performances of the proposed model based on HBT, EBT and TBT. Based on the accuracy and range of applicability of the proposed model, it is recommended for the analysis of composite beams having large deformations as well as inelastic material behaviours.

### **4.2 List of Manuscripts**

Uddin, M. A., Sheikh, A. H., Brown, D., Bennett, T. and Uy, B. (2016). “Geometrically nonlinear inelastic analysis of steel-concrete composite beams with partial interaction using a higher-order beam theory.” *International Journal of Non-linear Mechanics*, (Elsevier), Submitted.

### 4.3 Statement of Authorship

Title of Paper	Geometrically nonlinear inelastic analysis of steel-concrete composite beams with partial interaction using a higher-order beam theory
Publication Status	Submitted (Under review)
Publication Details	Uddin, M. A., Sheikh, A. H., Brown, D., Bennett, T. and Uy, B. (2016). "Geometrically nonlinear inelastic analysis of steel-concrete composite beams with partial interaction using a higher-order beam theory." <i>International Journal of Non-linear Mechanics</i> , (Elsevier), Submitted.

### Principal Author

Name of Principal Author (Candidate)	Md. Alhaz Uddin		
Contribution to the Paper	Developed finite element model, performed numerical analysis and prepared manuscript.		
Overall percentage (%)	70%		
Certification:	This paper reports on original research I conducted during the period of my Higher Degree by Research candidature and is not subject to any obligations or contractual agreements with a third party that would constrain its inclusion in this thesis. I am the primary author of this paper.		
Signature		Date	

### Co-Author Contributions

By signing the Statement of Authorship, each author certifies that:

- i. the candidate's stated contribution to the publication is accurate (as detailed above);
- ii. permission is granted for the candidate to include the publication in the thesis; and
- iii. the sum of all co-author contributions is equal to 100% less the candidate's stated contribution.

Name of Co-Author	Abdul Hamid Sheikh		
Contribution to the Paper	Supervised for development of model, helped in data interpretation, provided critical manuscript evaluation.		
Signature		Date	22/11/2016

Name of Co-Author	David Brown		
Contribution to the Paper	Assisted in manuscript evaluation.		
Signature	/	Date	17/11/16

Name of Co-Author	Terry Bennett		
Contribution to the Paper	Provided for manuscript evaluation.		
Signature		Date	22/11/16

Name of Co-Author	Brian Uy		
Contribution to the Paper	Provided for manuscript evaluation. <i>Ending manuscript reflects state of the          art &amp; need current exper work</i>		
Signature		Date	14/11/16

#### **4.4 Geometrically nonlinear inelastic analysis of steel-concrete composite beams with partial interaction using a higher-order beam theory**

Md. Alhaz Uddin, Abdul Hamid Sheikh, David Brown, Terry Bennett and Brian Uy

##### **ABSTRACT**

A comprehensive finite element model based on a higher-order beam theory (HBT) is developed for an accurate prediction of the response of steel-concrete composite beams with partial shear interaction. The formulation of the proposed one dimensional finite element model incorporated nonlinearities due to large deformations of the beam as well as inelastic material behaviour of its constituent components. The higher-order beam model is achieved by taking a third order variation of the longitudinal displacement over the beam depth for the steel and concrete layers separately. The deformable shear studs used for connecting the concrete slab with the steel girder are modelled as distributed shear springs along the interface between these two material layers. The Green-Lagrange strain vector is used to capture the effect of geometric nonlinearity due to large deflections. The von Mises plasticity theory with an isotropic hardening rule and a damage mechanics model are incorporated within the proposed finite element model for simulating the inelastic response of the beam materials. The nonlinear governing equations are solved by an incremental-iterative technique following the Newton-Raphson method. A dissipation based arc-length method is employed to capture the post peak response of these beams successfully. The capability of the proposed model is assessed through its validation and verification using existing experimental results and numerical results produced by detailed finite element modelling of these beams.

**Keywords:** Composite beam, Partial shear interaction, Higher-order beam theory, Large deformation, Inelastic material response, Arc-length method.

##### **1. INTRODUCTION**

Steel concrete composite beams have many applications in the construction industry due to their superior performances as structural members. In these typical structural configurations, the concrete layer is primarily utilised to resist the compressive stress whereas the steel layer

resists the tensile stress to enhance the performance of the overall structural system. The composite action is commonly achieved by connecting the concrete slab with the steel girder using steel shear studs. As the stiffness of these shear connectors is finite in reality, a shear slip is always present at the interface [1] between the concrete and steel layers which results in behaviour typically referred to as partial shear interaction.

Newmark et al. [2] is one of the earliest researchers who developed an analytical model for simulating composite beams considering the effects of partial interaction. The Newmark model is one of the most popular models, but due to its analytical nature it is only applicable to composite beams having specific boundary and loading conditions. On the other hand, a numerical model using a technique such as the finite element method, possesses a better level of generality and is hence able to solve a wide range of problems. This has motivated a number of researchers (e.g. [3-7]) to develop finite element models for composite beams with partial interaction. However, these models [3-7] have been developed considering the effect of small deformation and elastic material behaviour which produces a simple linear solution to the problem. In reality, the loading can't be restricted within such a small range and these composite beams often undergo large deformations with beam materials exhibiting an inelastic response.

In order to address some of these issues, Yasunori et al. [8] incorporated the effect of inelastic material behaviour in their finite element model of composite beams using the von Mises yield criterion. However, they [8] used a very simple material model based on an elastic perfectly-plastic idealisation for all materials including concrete, which is not realistic especially for the tensile response of concrete. Similar studies have been carried out by Salari et al. [9] using a bi-linear elasto-plastic material model with a strain hardening parameter. A further development in this direction is due to Dall'Asta and Zona [10] and Erkmen and Attard [11] who have used realistic stress-strain curves for the beam materials. In their work Dall'Asta and Zona [10] have ignored the contribution of concrete in tension whereas Erkmen and Attard [11] have used the concept of tension stiffening for its modelling. However, the studies [8-11] did not consider the effects of large deformation in the modelling of composite beams. On the other hand, the effect of geometric nonlinearity due to large deformations is incorporated in the finite element models by Erkmen and Bradford [12] for the analysis of steel-concrete composite beams being curved in plane, and Battini et al. [13] and Ranzi et al. [14] for the two-layered straight composite beams. However, they [12-14] ignored the effects of inelastic material behaviour which is encountered even with a low to moderate range of loading.

A nonlinear model considering the effect of inelastic material behaviour along with the large deformation can ideally be the best model for predicting the response of these composite structures accurately. For this purpose, Hozjan et al. [15] developed a nonlinear finite element model considering the large deformation and the inelastic material behaviour of the constituents of composite beams with interfacial slip, but neglected the tensile behaviour of concrete. A comprehensive one dimensional finite element model is proposed by Liu et al. [16] where the tensile behaviour of concrete is simulated using a damage mechanics model which can precisely model the tensile response of plain concrete without reinforcement. However, all these models [3-16] are based on Euler-Bernoulli beam theory (EBT), which does not consider the effect of transverse shear deformation of the steel and concrete layers. The effect of this shear deformation is significant in some situations such as beams with a small span-to-depth ratio, localized concentrated loads, clamped boundary conditions and some other scenarios.

Thus there has been a growing interest in recent years to incorporate the effects of shear deformation and the Timoshenko's beam theory (TBT) is typically used for this purpose (e.g., [17-20]). It is observed that all these investigators [17-20] have used linear elastic material behaviour and small deflection theory to develop their models. Recently, Hijaj et al. [21] developed a model based on TBT considering the effect of large deformation. This has been extended further by Nguyen et al. [22] to incorporate the effect of inelastic material behaviour. However, they [22] have used a very simplified material model as well as treating the behaviour of concrete in tension and compression identically. Moreover, in this beam theory (TBT), the actual parabolic variation of shear stress over the beam depth is simplified by taking a constant average shear stress distribution over the beam depth. This simplification requires the use of a factor known as a shear correction factor to determine a satisfactory global response such as deflection or vibration frequency. This correction factor is not sufficient for an accurate prediction of the local response such as the stress distributions within these structures [23-25]. Furthermore, the calculation of the exact value of this shear correction factor for a composite beam with partial shear interaction is cumbersome in comparison with that of a single layer homogeneous beam.

In order to address the aforementioned issues related to shear deformation of the beam layers, a higher-order beam theory (HBT) has recently been developed by Sheikh and co-workers [23-25] for an accurate prediction of global as well as local responses of these composite beams. The cross-sectional warping of the beam layers produced by the transverse shear stress is modelled with a higher order (3<sup>rd</sup> order) variation of longitudinal displacements of

the fibres over the beam depth. This beam theory (HBT) utilized the concept of Reddy's higher order shear deformation theory [26] developed for multi-layered laminated composite plates modelled as single layered plates without interfacial slip. In these investigations [23-25], HBT has been implemented with a one dimensional finite element model which has exhibited a very good performance, though these studies are restricted to linear elastic analysis of these composite beams having small deformations.

Considering all the aforementioned aspects, an attempt is made in this study to develop an efficient numerical model based on HBT for accurately predicting the large deformation response of composite beams having inelastic material behaviour. The nonlinearity induced by the large deformation and inelastic material response is manifested in the form of nonlinear load-deflection curves. These curves can have a descending branch after attaining the peak load due to the strain-softening behaviour of concrete in its inelastic range. It is observed that most of the investigations carried out on the inelastic response of composite beams [8-11, 16, 22] could not capture the descending branch of the nonlinear load-deflection curve successfully. The solution of this typical nonlinear problem is quite challenging and a load control based technique cannot trace the descending branch of the load-deflection curve. In order to overcome this problem, a displacement control based technique may be used, however this will also fail if the load-deflection curve has a snap-back response. In this situation, an arc-length based solution technique seems to be the only possible option.

The arc-length method was initially proposed by Riks [27] and subsequently enhanced by various investigators (e.g. Crisfield [28, 29]) for solving different nonlinear problems. Though these developments helped to solve complex geometric nonlinear problems successfully, they encountered severe convergence problems in solving material nonlinear problems especially relating to concrete structures which have failure/crack localizations. In order to address this specific issue, the localized nature of damage has been utilised by May and Duan [30] to develop an arc length method known as a damage localization approach. This method can provide a satisfactory solution to a problem [31] but it requires the position of damaged elements to be known, which may be difficult to locate in a complex structural system. A further advancement in this direction is due to Gutiérrez [32] who proposed a dissipation based arc-length method where the energy dissipated by the entire structure due to its damage and plastic deformations is utilised as a stepping parameter for controlling the incremental iterative process. The success of this method is primarily due to the stepping parameter which is always positive regardless of the sign of the tangential stiffness.

For the one dimensional finite element model developed in this study, the von Mises plasticity theory with an isotropic hardening rule is used for modelling the inelastic behaviour of steel girders, concrete slabs under compression, steel reinforcements, and steel shear studs. A damage mechanics model is used for modelling the inelastic behaviour of concrete under tension. The Green-Lagrange strain vector is used to capture the effect of geometric nonlinearity in the composite beam. A dissipation based arc-length method is employed to capture the post peak response successfully. Numerical examples of composite beams are solved by the proposed model. The results predicted by the models are validated with the published experimental results and the numerical results produced by a detailed two-dimensional finite element model of these beams using a reliable finite element software. As the number of results available in the inelastic range of composite beams having large deformations is limited and no one has reported any results for the stress distributions within these structures, a number of new results are presented for future references.

## 2. MATHEMATICAL FORMULATION

### 2.1. Higher-order Beam Theory (HBT)

Fig. 1 shows a steel-concrete composite beam which is typically a two layered composite beam with a flexible interface. According to the HBT, the variation of longitudinal displacement of the concrete and steel layers over their depths can be expressed as

$$u_c = u_{c0} - y_c \theta_c + y_c^2 \alpha_c + y_c^3 \beta_c \quad (1)$$

$$u_s = u_{s0} - y_s \theta_s + y_s^2 \alpha_s + y_s^3 \beta_s \quad (2)$$

where  $u_{c0}$  and  $u_{s0}$  are the longitudinal displacements of the concrete slab and the steel girder at their reference axes ( $y_c = 0$  and  $y_s = 0$ ) respectively,  $\theta_c$  and  $\theta_s$  are bending rotations of these layers, and  $\alpha$  and  $\beta$  are the higher order terms. As vertical separation between the layers is not commonly observed in a straight composite beam under static loading, it is not considered in this study. Thus the vertical displacement will be identical for both layers and it can be expressed as

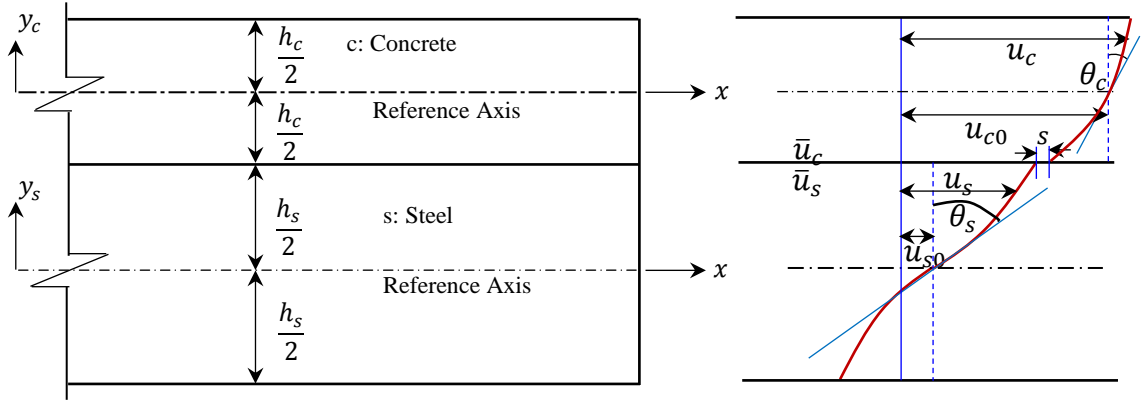


Fig. 1. Typical Steel-concrete composite beam with longitudinal displacement variations over the beam depth.

$$w_c = w_s = w \quad (3)$$

The partial shear interaction between the concrete and steel layers is characterised by the slip at their interface. This is defined as the relative longitudinal displacement of these material layers and it can be expressed as

$$s = \bar{u}_s - \bar{u}_c \quad (4)$$

where  $\bar{u}_c$  is the longitudinal displacement at the bottom fibre of the concrete layer and  $\bar{u}_s$  is the longitudinal displacement at the top fibre of the steel layer.

Utilising the shear stress free condition at the exterior surfaces ( $y_c = h_c/2$  and  $y_s = -h_s/2$ ), and taking  $\bar{u}_c$  and  $\bar{u}_s$  as independent field variables, the higher order non-physical terms appearing in Eqs. (1) and (2) can be expressed in terms of other field variables [23]. Using Eq. (3) and the above conditions, Eqs. (1) and (2) can be rewritten in terms of all physical parameters as

$$u_c = A_c u_{c0} + B_c \bar{u}_c + C_c \theta_c + D_c \phi \quad (5)$$

$$u_s = A_s u_{s0} + B_s \bar{u}_s + C_s \theta_s + D_s \phi \quad (6)$$

where  $A$ ,  $B$ ,  $C$  and  $D$  are functions of  $y$ , cross-sectional properties of the two layers and their material properties [24]. In the equations above,  $\phi$  ( $=dw/dx$ ) is taken as an independent field variable to have a  $C^0$  continuous formulation for the finite element implementation of this beam theory.

## 2.2. Variational Formulations and its Finite Element Implementation

The equilibrium equation can be derived using the principle of virtual work and it can be expressed as

$$\int_x \int_{A_c} \{d\varepsilon\}_c^T \{\sigma\}_c dAdx + \int_x \int_{A_s} \{d\varepsilon\}_s^T \{\sigma\}_s dAdx + \int_x d\tau_{sh} dx = \int_x dwq dx, \quad (7)$$

where  $d$  is used to show the variation of any parameter,  $\{\varepsilon\}_c$  and  $\{\varepsilon\}_s$  are strain vectors (consisting of normal and transverse shear strains) of the concrete and steel layers respectively,  $\{\sigma\}_c$  and  $\{\sigma\}_s$  are stress vectors (consisting of bending and shear stresses) of these layers,  $\tau_{sh}$  is the distributed shear force (per unit length) at their interface,  $q$  is the distributed external load (per unit length) acting on the beam, and  $A$  is the cross-sectional area.

The Green-Lagrange strain vector of the two layers may be written as

$$\{\varepsilon\}_k = \begin{Bmatrix} \varepsilon_k \\ \gamma_k \end{Bmatrix} = \begin{Bmatrix} \frac{\partial u}{\partial x} \\ \frac{\partial u}{\partial y} + \frac{\partial w}{\partial x} \end{Bmatrix} + \begin{Bmatrix} \frac{1}{2} \left[ \left( \frac{\partial u}{\partial x} \right)^2 + \left( \frac{\partial w}{\partial x} \right)^2 \right] \\ 0 \end{Bmatrix} = \{\varepsilon_L\}_k + \{\varepsilon_N\}_k \quad (8)$$

where  $\{\varepsilon_L\}_k$  and  $\{\varepsilon_N\}_k$  are the linear and nonlinear strain vectors in which the index  $k = c$  for the concrete layer and  $k = s$  for the steel layer. Using Eqs. (5) and (6), the linear strain vectors may be written in terms of the cross-sectional matrix  $[H_L]_k$  and the one dimensional linear strain vector  $\{\bar{\varepsilon}_L\}_k$  as

$$\{\varepsilon_L\}_k = [H_L]_k \{\bar{\varepsilon}_L\}_k, \quad (9)$$

$$\text{where, } [H_L]_k = \begin{bmatrix} A_k & B_k & C_k & D_k & 0 & 0 & 0 & 0 & 0 \\ 0 & 0 & 0 & 0 & \frac{dA_k}{dy_k} & \frac{dB_k}{dy_k} & \frac{dC_k}{dy_k} & \frac{dD_k}{dy_k} & 1 \end{bmatrix}, \quad (10)$$

$$\text{and } \{\bar{\varepsilon}_L\}_k^T = \left( \frac{du_{k0}}{dx} \quad \frac{d\bar{u}_k}{dx} \quad \frac{d\theta_k}{dx} \quad \frac{d\phi}{dx} \quad u_{k0} \quad \bar{u}_k \quad \theta_k \quad \phi \quad \frac{dw}{dx} \right). \quad (11)$$

For the finite element implementation of the proposed beam model, a displacement based quadratic isoparametric beam element with three nodes is used to have a simple formulation with no unexpected numerical inconsistencies. However, a displacement based formulation can exhibit locking phenomena, which is eliminated by using the field consistent technique [33]. The field variables of the element are  $u_{c0}$ ,  $\bar{u}_c$ ,  $\theta_c$ ,  $w$ ,  $\phi$ ,  $u_{s0}$ ,  $\bar{u}_s$  and  $\theta_s$ , which can be

expressed in terms of their nodal unknowns using the interpolation functions of the element [25]. This leads to an expression for the one dimensional linear strain vectors (11) in terms of the nodal displacement vector  $\{\Delta\}$  as

$$\{\bar{\varepsilon}_L\}_k = \begin{bmatrix} [B_L^1]_k & [B_L^2]_k & [B_L^3]_k \end{bmatrix} \begin{Bmatrix} \{\Delta_1\} \\ \{\Delta_2\} \\ \{\Delta_3\} \end{Bmatrix} = [B_L]_k \{\Delta\} \quad (12)$$

where a typical component of the linear strain-displacement matrix  $[B_L^j]_k$  corresponding to node  $j$  (1, 2 or 3) is given in [25] for the concrete/steel layer.

Now the nonlinear strain vectors may be expressed as

$$\{\varepsilon_N\}_k = \frac{1}{2} \begin{bmatrix} \frac{du}{dx} & \frac{dw}{dx} \\ 0 & 0 \end{bmatrix} \begin{Bmatrix} \frac{du}{dx} \\ \frac{dw}{dx} \end{Bmatrix} = \frac{1}{2} [A]_k \{\theta\}_k \quad (13)$$

Using Eqs. (5) and (6), the vector  $\{\theta\}_k$  may be expressed in terms of its cross-sectional matrices  $[H_N]_k$  and one dimensional strain vectors  $\{\varepsilon_{N\theta}\}_k$  (dependent on  $x$  only) as

$$\{\theta\}_k = [H_N]_k \{\varepsilon_{N\theta}\}_k, \quad (14)$$

$$\text{where, } [H_N]_k = \begin{bmatrix} A_k & B_k & C_k & D_k & 0 \\ 0 & 0 & 0 & 0 & 1 \end{bmatrix}, \quad (15)$$

$$\text{and } \{\varepsilon_{N\theta}\}_k^T = \left( \frac{du_{k0}}{dx} \quad \frac{d\bar{u}_k}{dx} \quad \frac{d\theta_k}{dx} \quad \frac{d\phi}{dx} \quad \frac{dw}{dx} \right). \quad (16)$$

The matrix  $[A]_k$  in Eq. (13) is dependent on displacements of the beam and is evaluated or updated in each iteration within the solution scheme of the nonlinear governing equations utilising  $\{\theta\}_k$ .

The one dimensional strain vector shown in Eq. (16) can be expressed in terms of the nodal displacement vector as

$$\{\varepsilon_{N\theta}\}_k = \begin{bmatrix} [G_1]_k & [G_2]_k & [G_3]_k \end{bmatrix} \begin{Bmatrix} \{\Delta_1\} \\ \{\Delta_2\} \\ \{\Delta_3\} \end{Bmatrix} = [G]_k \{\Delta\}, \quad (17)$$

$$\text{where, } [G_j]_c = \begin{bmatrix} \frac{dN_j}{dx} & 0 & 0 & 0 & 0 & 0 & 0 & 0 \\ 0 & \frac{dN_j}{dx} & 0 & 0 & 0 & 0 & 0 & 0 \\ 0 & 0 & \frac{dN_j}{dx} & 0 & 0 & 0 & 0 & 0 \\ 0 & 0 & 0 & 0 & \frac{dN_j}{dx} & 0 & 0 & 0 \\ 0 & 0 & 0 & \frac{dN_j}{dx} & 0 & 0 & 0 & 0 \end{bmatrix},$$

$$\text{and } [G_j]_s = \begin{bmatrix} 0 & 0 & 0 & 0 & 0 & \frac{dN_j}{dx} & 0 & 0 \\ 0 & 0 & 0 & 0 & 0 & 0 & \frac{dN_j}{dx} & 0 \\ 0 & 0 & 0 & 0 & 0 & 0 & 0 & \frac{dN_j}{dx} \\ 0 & 0 & 0 & 0 & \frac{dN_j}{dx} & 0 & 0 & 0 \\ 0 & 0 & 0 & \frac{dN_j}{dx} & 0 & 0 & 0 & 0 \end{bmatrix}.$$

Employing Eqs. (9), (12), (13), (14) and (17), the total strain vector as given in Eq. (8) can be expressed as

$$\{\varepsilon\}_k = \left( [H_L]_k [B_L]_k + \frac{1}{2} [A]_k [H_N]_k [G]_k \right) \{\Delta\} = \left( [\bar{B}_L]_k + \frac{1}{2} [\bar{B}_N]_k \right) \{\Delta\}. \quad (18)$$

Taking the variation of Eq. (18), the incremental strain vector can be obtained [34] and it may be expressed as

$$\{d\varepsilon\}_k = \left( [H_L]_k [B_L]_k + [A]_k [H_N]_k [G]_k \right) \{d\Delta\} = \left( [\bar{B}_L]_k + [\bar{B}_N]_k \right) \{d\Delta\} = [\bar{B}]_k \{d\Delta\}. \quad (19)$$

Similarly, the incremental form of the interfacial slip (4) can be expressed in terms of a strain-displacement matrix for the interfacial slip  $[B]_{sh}$  and nodal displacement vector [25] as

$$ds = d(\bar{u}_s - \bar{u}_c) = [B]_{sh} \{d\Delta\}. \quad (20)$$

The virtual work due to the external load  $q$  as expressed on the right hand side of Eq. (7) can be expressed further in terms of the external load vector  $\{F_{ext}\}$  and incremental nodal displacement vector  $\{d\Delta\}$  as

$$\int dwq dx = \{d\Delta\}^T \{F_{ext}\}, \quad (21)$$

$$\text{where } \{F_{ext}\} = \int [N]^T q dx \quad (22)$$

The matrix  $[N]$  in the above equation contains shape functions of the transverse displacement,  $w$  [25].

Substituting Eqs. (19), (20) and (21) into Eq. (7), the equilibrium equation can be obtained and expressed as

$$\int_x \int_{A_c} [\bar{B}]_c^T \{\sigma\}_c dA dx + \int_x \int_{A_s} [\bar{B}]_s^T \{\sigma\}_s dA dx + \int_x [B]_{sh}^T \tau_{sh} dx = \{F_{ext}\}. \quad (23)$$

The stresses in the above equation (23) can be expressed in terms of strains using appropriate constitutive relationships and these strains can subsequently be expressed in terms of nodal displacements  $\{\Delta\}$ . However, the resulting equation cannot be solved for nodal displacements directly due to the nonlinear constitutive relationships produced by inelastic material behaviours and the displacement dependent nonlinear strain displacement matrices. The nonlinear stress-strain relationship must be expressed in its incremental form as the stresses cannot be expressed in terms of strains in their total form due to the load history dependent material behaviour. To facilitate this, the left hand side of the equilibrium equation (23) is defined as the internal nodal force vector  $\{P_{int}\}$  (dependent on the nodal displacement vector  $\{\Delta\}$ ), which leads to an expression for Eq. (23) in a compact form as

$$\{P_{int}(\{\Delta\})\} = \{F_{ext}\} \text{ or } \{\Psi\} = \{P_{int}\} - \{F_{ext}\} = \{0\} \quad (24)$$

The Newton Raphson method is used to solve the above nonlinear equation iteratively where the nodal displacement vector  $\{\Delta\}^{j+1}$  at the iteration  $j+1$  can be computed from that obtained in the previous iteration  $\{\Delta\}^j$  as

$$\{\Delta\}^{j+1} = \{\Delta\}^j + \{d\Delta\}^{j+1} = \{\Delta\}^j + \left[ \left( \frac{\partial \{\Psi\}}{\partial \{\Delta\}} \right)^j \right]^{-1} \{-\Psi(\{\Delta\}^j)\} \quad (25)$$

From the above equation, the incremental nodal displacement  $\{d\Delta\}$  within an iteration can be written as

$$\frac{\partial \{\Psi\}}{\partial \{\Delta\}} \{d\Delta\} = -\{\Psi\} \quad (26)$$

Substituting Eqs. (23) and (24) into the above equation and defining its right hand side as the residual load vector  $\{dR\}$  ( $= -\{\Psi\}$ ), it can be rewritten as

$$\int_x \int_{A_c} [d\bar{B}]_c^T \{\sigma\}_c dAdx + \int_x \int_{A_c} [\bar{B}]_c^T \{d\sigma\}_c dAdx + \int_x \int_{A_s} [d\bar{B}]_s^T \{\sigma\}_s dAdx + \int_x \int_{A_s} [\bar{B}]_s^T \{d\sigma\}_s dAdx + \int_x [B]_{sh}^T d\tau_{sh} dx = \{dR\}. \quad (27)$$

The incremental strain displacement matrix of a material layer used in the above equation can be expressed with the use of Eq. (19) as

$$[d\bar{B}]_k = [d\bar{B}_N]_k = [dA]_k [H_N]_k [G]_k = [dA]_k [B_\sigma]_k. \quad (28)$$

Substituting the above equation in Eq. (27), the first and third terms in the left hand side of the equation may be expressed in terms of geometric stiffness matrices [34] and incremental nodal displacements as

$$[K_\sigma]_c \{d\Delta\} + \int_x \int_{A_c} [\bar{B}]_c^T \{d\sigma\}_c dAdx + [K_\sigma]_s \{d\Delta\} + \int_x \int_{A_s} [\bar{B}]_s^T \{d\sigma\}_s dAdx + \int_x [B]_{sh}^T d\tau_{sh} dx = \{dR\} \quad (29)$$

$$\text{where } [K_\sigma]_c = \int_x \int_{A_c} [B_\sigma]_c^T \sigma_c [B_\sigma]_c dAdx \text{ and } [K_\sigma]_s = \int_x \int_{A_s} [B_\sigma]_s^T \sigma_s [B_\sigma]_s dAdx.$$

Now the incremental stresses appearing in the above equation can be expressed in terms of incremental strains using a suitable constitutive relationship (see the Section 2.3) by using Eqs. (19) and (20) as

$$\{d\sigma\}_k = [E^t]_k \{d\varepsilon\}_k = [E^t]_k [\bar{B}]_k \{d\Delta\} \quad (30)$$

$$\text{and } d\tau_{sh} = k_{sh}^t ds = k_{sh}^t [B]_{sh} \{d\Delta\} \quad (31)$$

where  $[E^t]_k$  is the tangential material stiffness matrix (elasto-plastic/damage stiffness matrix) of the steel/concrete layer and  $k_{sh}^t$  is the tangential material stiffness (elasto-plastic stiffness) of the shear connectors.

After the substitution of Eqs. (30) and (31) into Eq. (29), the incremental equilibrium equation can finally be written as

$$[K_T] \{d\Delta\} = \{dR\} \quad (32)$$

The tangent stiffness matrix  $[K_T]$  in the above equation is the same as the term  $\frac{\partial \{\Psi\}}{\partial \{\Delta\}}$  which appeared in Eq. (26) and can be expressed as

$$[K_T] = [K_\sigma]_c + \int_x \int_{A_c} [\bar{B}]_c^T [E^t]_c [\bar{B}]_c dAdx + [K_\sigma]_s + \int_x \int_{A_s} [\bar{B}]_s^T [E^t]_s [\bar{B}]_s dAdx + \int_x [B]_{sh}^T k_{sh}^t [B]_{sh} dx \quad (33)$$

The nonlinear equation (26) is solved in an iterative process (25) using Eqs. (27), (32) and (33). In order to achieve a converged solution, the iteration process will continue until the residual force vector  $\{\delta R\}$  is reduced to a specified tolerance as follows

$$\frac{\sqrt{\{\delta R\}^T \{\delta R\}}}{\sqrt{\{F_{ext}\}^T \{F_{ext}\}}} \times 100 \leq Tol \quad (34)$$

where  $Tol$  is the convergence tolerance which is taken as 1% in the present study.

It should be noted that the entire load is divided into a number of load steps and it is applied gradually in increments where the iterative solution technique is activated within each load step. Moreover, this is a load control technique which will not be adequate for tracing the post peak response of composite beams. This problem is solved by using a robust arc-length method which is presented in Section 2.4.

### 2.3. Constitutive Relationship

The von Mises yield criterion with an isotropic-hardening rule [35] is used for modelling the inelastic behaviour of steel girders, reinforcement and steel shear studs. This modelling approach is also applied to the region of concrete slab subjected to compressive stress for simplicity. A damage mechanics model [36, 37] is adopted to simulate the cracking behaviour of the concrete under tensile stress.

#### 2.3.1. Constitutive Relationship for Steel and Concrete in Compression

According to the von Mises yield criterion, the stress state must be on (plastic loading) or within (elastic loading and unloading) the yield surface which may be written for the steel/concrete layer subjected to bending and shear stresses as

$$f_k = \sigma_{ef,k} - \sigma_{y,k} \leq 0 \quad (35)$$

In the above equation,  $\sigma_{y,k}$  is the uniaxial yield stress and  $\sigma_{ef,k}$  is the effective stress, which can be written in terms of bending stress  $\sigma_k$  and shear stress  $\tau_k$  as

$$\sigma_{ef,k} = \sqrt{\sigma_k^2 + 3\tau_k^2} \quad (36)$$

In order to correlate a multiaxial stress state (usually encountered in a real problem) with the uniaxial yield stress, the uniaxial yield stress can be expressed in terms of equivalent plastic strain  $\varepsilon_{ef,k}^p = \sqrt{(\varepsilon_k^p)^2 + (\gamma_k^p)^2} / 3$  as

$$\sigma_{y,k} = \sigma_{y0,k} + \int_0^{\varepsilon_{ef,k}^p} H'_k \delta \varepsilon_{ef,k}^p \quad (37)$$

where  $\sigma_{y0,k}$  is the initial value of the uniaxial yield stress for a material layer and  $H'_k$  is the strain hardening parameter of the layer.

As mentioned in the previous section, the stress-strain relationship must be expressed in its incremental form due to inelastic material behaviour. Thus the strain vector is taken in its incremental form and can be expressed in terms of its elastic and plastic components as

$$\{d\varepsilon\}_k = \{d\varepsilon^e\}_k + \{d\varepsilon^p\}_k \quad (38)$$

The elastic strain increment can simply be obtained from the incremental stress using Hooke's law as

$$\{d\varepsilon^e\}_k = \{d\varepsilon\}_k - \{d\varepsilon^p\}_k = [E^e]_k^{-1} \{d\sigma\}_k = \begin{bmatrix} E_k & 0 \\ 0 & G_k \end{bmatrix}^{-1} \{d\sigma\}_k \quad (39)$$

where  $E_k$  and  $G_k$  are the elastic modulus and shear modulus of the material layer respectively.

As an associated flow rule is used, the plastic strain increments can be determined [38] using Eq. (35) as

$$\{d\varepsilon^p\}_k = d\lambda_k \frac{\partial f_k}{\partial \{\sigma\}_k} = \frac{d\lambda_k}{\sigma_{ef,k}} \begin{Bmatrix} \sigma_k \\ 3\tau_k \end{Bmatrix} = d\lambda_k \{a\}_k \quad (40)$$

where  $d\lambda_k$  is the incremental plastic strain multiplier and the vector  $\{a\}_k$  gives the direction of plastic flow, which is normal to the yield surface. Using the consistency condition of the yield function (35) along with the above equations (36, 39 and 40), the incremental plastic strain multiplier can be derived following the usual operations used in a plasticity formulation [38] and it can be expressed as

$$d\lambda_k = \frac{\{a\}_k^T [E^e]_k \{d\varepsilon\}_k}{\{a\}_k^T [E^e]_k \{a\}_k + H'_k} \quad (41)$$

For the von Mises yield criterion, the equivalent plastic strain increment will be the incremental plastic strain multiplier  $d\lambda_k$  [38]. Using Eqs. (39) to (41), the incremental stress-strain relationship can be obtained which is expressed as

$$\{d\sigma\}_k = [E^{ep}]_k \{d\varepsilon\}_k = \left( [E^e]_k - \frac{[E^e]_k \{a\}_k \{a\}_k^T [E^e]_k^T}{\{a\}_k^T [E^e]_k \{a\}_k + H'_k} \right) \{d\varepsilon\}_k \quad (42)$$

where  $[E^{ep}]_k$  is the elasto-plastic constitutive matrix that can be used for  $[E^t]_k$  in Eq. (30).

This constitutive relationship is also applied for the modelling of reinforcement bars by eliminating the contribution of shear stress/strain.

### 2.3.2. Constitutive Relationship for Concrete in Tension

The concrete under tensile stress (major principal stress) is treated as an elastic material up to its uniaxial ultimate tensile stress ( $\sigma_{t0}$ ) where cracks are initiated. The crack initiation can be detected once the following equation is satisfied.

$$f_t = \sigma_{\max} - \sigma_{t0} = 0 \quad (43)$$

where  $\sigma_{\max}$  is the maximum principle stress which can be evaluated using the following equation.

$$\sigma_{\max} = \frac{\sigma_c}{2} + \sqrt{\frac{\sigma_c^2}{4} + \tau_c^2} \quad (44)$$

The material behavior in tension is modelled with a damage mechanics approach taking a linear strain softening branch for simulating the post cracking response [37]. Fig. 2 shows a typical one dimensional damage model where the damage parameter  $\omega$  ranges from 0 (damage initiation) to 1 (complete damage) to characterize the extent of cracking. The damage parameter is used to quantify the loss of material stiffness due to cracking, which is illustrated with the unloading path from any point on the softening branch, in the form of its secant stiffness. The loading function for the damage can be expressed as

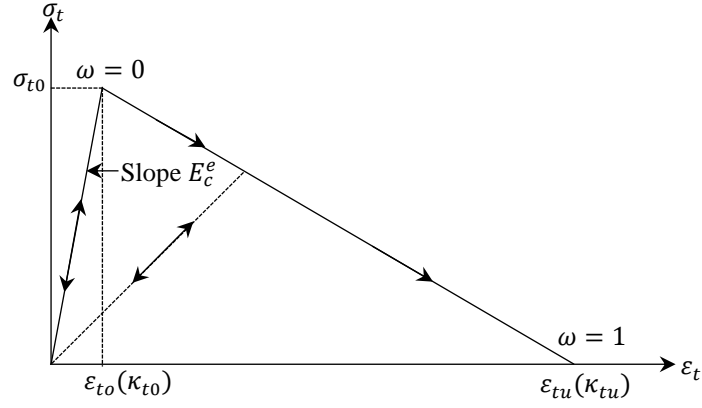


Fig. 2. Uniaxial strain softening model in tension.

$$f_{cr} = \kappa_{ef} - \max(\kappa_{old}, \kappa_{t0}) \leq 0 \quad (45)$$

where  $f_{cr} = 0$  indicates loading (i.e., damage growth) and  $f_{cr} < 0$  indicates unloading. The equivalent strain parameter  $\kappa_{ef}$  (similar to equivalent plastic strain in plasticity) in the above equation (scalar quantity) is taken as

$$\kappa_{ef} = \sqrt{\frac{1}{E} \{\boldsymbol{\varepsilon}\}_c^T [E^e]_c \{\boldsymbol{\varepsilon}\}_c} \quad (46)$$

where  $\kappa_{old}$  is its value obtained in the previous iteration of the analysis and  $\kappa_{t0}$  corresponds to that at the instance of damage initiation i.e.,  $\varepsilon_t = \varepsilon_{t0}$  (Fig. 2). In the case of unloading, the value of  $\kappa_{old}$  will be unaltered but it must be updated with the new value of  $\kappa_{ef}$  for loading in order to satisfy Eq. (45). Similarly, the damage parameter  $\omega$  will retain its old value for unloading but it is to be updated for damage growth (loading) as

$$\omega = \frac{\kappa_{tu}(\kappa_{ef} - \kappa_{t0})}{\kappa_{ef}(\kappa_{tu} - \kappa_{t0})} \quad (47)$$

where  $\kappa_{tu}$  corresponds to complete damage i.e.,  $\varepsilon_t = \varepsilon_{tu}$  (Fig. 2).

In the modelling of concrete under tensile stress, it is observed that the solution is dependent on the mesh size in a traditional strength based analysis. This is a typical problem which is eliminated in the present study using the concept of crack band theory proposed by Bazant and Oh [39]. This concept is based on fracture mechanics principles which utilize fracture toughness  $G_f$  (energy required to produce a crack of unit area) as a material property. This will be utilised to estimate the value of  $\varepsilon_{tu}$  used in Fig. 2 ( $\omega=1$ ) considering the area under the stress strain curve as  $g_f = G_f / w_c$  where  $w_c$  is the crack band width where the energy  $G_f$

is assumed to be distributed over the crack band width [39]. This is an important concept that helps to treat the discrete nature of crack within a continuum model. As the element length  $l_e$  is related to the crack band in a smear crack model, the final expression of  $\varepsilon_{tu}$  can be written as

$$\varepsilon_{tu} = \frac{2G_f}{\alpha_w l_e \sigma_{t0}} \quad (48)$$

where  $\alpha_w l_e$  is defined as the characteristic length. The value of  $\alpha_w$  depends on the order of element which is 1.0 in the present case as a quadratic element is used [39].

With the damage parameter (47), the stress-strain relationship can be written as

$$\{\sigma\}_c = (1 - \omega)[E^e]_c \{\varepsilon\}_c \quad (49)$$

where  $(1 - \omega)[E^e]_c$  is the secant damage stiffness matrix (Fig. 2).

Finally, the incremental stress-strain relationship of the damaged concrete may be written as

$$\{d\sigma\}_c = [E^{cr}] \{d\varepsilon\}_c \quad (50)$$

where the tangent damage stiffness matrix  $[E^{cr}]$  can be expressed with the following equation and it can be used in Eq. (30) for  $[E^t]_k$ .

$$[E^{cr}] = (1 - \omega)[E^e]_c - \frac{\kappa_{tu}\kappa_{t0}}{\kappa_{ef}^2(\kappa_{tu} - \kappa_{t0})} \{\sigma\}_c^T \{\sigma\}_c \quad (51)$$

The above equation is applicable for damage growth while  $[E^{cr}]$  will be the secant damage stiffness matrix  $(1 - \omega)[E^e]_c$  for unloading.

### 2.3.3. Constitutive Relationship for Shear Connectors

The shear connectors are idealised as a distributed spring layer which transfers a distributed shear force between steel and concrete layers at their interface tangentially. The von Mises yield criterion used to model the shear connectors can be written as

$$f_{sc} = \tau_{ef} - \tau_y \quad (52)$$

where the effective shear stress (force per unit length)  $\tau_{ef}$  is the absolute value of the interfacial shear force  $\tau_{sh}$ , and  $\tau_y$  is the corresponding yield stress (force per unit length)

that may be expressed in terms of the effective plastic shear slip  $s_{ef}^p$  (absolute value of the plastic shear slip  $s^p$ ) as

$$\tau_y = \tau_{y0} + \int_0^{s_{ef}^p} H'_{sc} \delta s_{ef}^p \quad (53)$$

where  $\tau_{y0}$  is the initial yield stress (force per unit length) of this interfacial shear, and  $H'_{sc}$  is the hardening parameter. In this case, the slip ( $s$ ) is taking the role of strains and it is to be expressed in terms of its elastic ( $s^e$ ) and plastic ( $s^p$ ) components. Following the usual steps of plasticity, the increments of these plastic slip components may be expressed as

$$ds^e = d\tau_{sh} / k_{sh} \quad (54)$$

$$ds^p = \frac{k_{sh}}{H'_{sc} + k_{sh}} ds \quad (55)$$

where  $k_{sh}$  is the elastic stiffness of the distributed interfacial shear springs. Finally, the incremental relationship between interfacial shear force and slip may be written as

$$d\tau_{sh} = k_{sh}^{ep} ds = \left( k_{sh} - \frac{k_{sh}^2}{H'_{sc} + k_{sh}} \right) ds \quad (56)$$

where  $k_{sh}^{ep}$  is the elasto-plastic tangent stiffness for the shear connectors that can be utilized in Eq. (31) as  $k_{sh}^t$ .

## 2.4. Arc-length Technique

The dissipation based arc-length method has initially been proposed by Gutiérrez [32] considering damage as the only energy dissipation mechanism. Subsequently, this method has been extended by Verhoosel et al. [40] to include plasticity as an additional mechanism, which is applied to the present problem. As the value of the external loading will not increase in the post peak range, the equilibrium equation (24) is expressed in terms of an unknown load factor (or multiplier)  $\mu$  as

$$\{P_{int}\} = \mu \{F\} \quad (57)$$

where  $\{F\}$  is the external load vector due to one unit of applied load. In order to avoid any convergence problems and trace the entire structural response in the pre-peak as well as post-

peak ranges, the equilibrium path is divided into a number of steps by adjusting the value of  $\mu$  and the nonlinear equation is solved iteratively within each load step. As  $\mu$  is also an unknown parameter and its value is adjusted by this technique, an additional equation is required which is taken in the form of a constraint as follows

$$C(\{\Delta_0\}, \mu_0, \{\delta\Delta\}, \delta\mu, e_d) = 0 \quad (58)$$

where  $(\{\Delta_0\}, \mu_0)$  is a point on the equilibrium path (a converged solution at the end of a load step),  $\{\delta\Delta\}$  is the incremental nodal displacement vector for the next load step,  $\delta\mu$  is the corresponding incremental load factor and  $e_d$  is the prescribed dissipation energy required for estimating the step size. It should be noted that  $\{\delta\Delta\}$  is the value of  $\{\Delta\}$  within a load step whereas  $\{d\Delta\}$  used in Section 2.2 is the value of  $\{\Delta\}$  within an iteration. The incremental energy dissipation  $U_d$  of a structure due to inelastic deformations within a load step is used to define the constraint  $C$  in the above equation as

$$C = U_d - e_d \quad (59)$$

As the energy dissipation can be obtained from the work done by the external loads  $W_e$  (i.e., total energy supplied to the structural system) and the elastic energy  $U_e$  retained by the system, the incremental energy dissipation within a load step can be written as

$$U_d = \delta W_e - \delta U_e \quad (60)$$

With the external load vector as expressed in Eq. (57), the incremental work done by the external loads used in the above equation can be written as

$$\delta W_e = \mu \{F\}^T \{\delta\Delta\} \quad (61)$$

In the case of a structure having plastic deformations, the strain will have an elastic component and a plastic component. The elastic strain can be used to obtain the elastic energy of a composite beam  $U_e$  and it can be expressed as

$$U_e = \frac{1}{2} \int \{\epsilon^e\}_c^T \{\sigma\}_c dv + \frac{1}{2} \int \{\epsilon^e\}_s^T \{\sigma\}_s dv + \frac{1}{2} \int s^e \tau_{sh} dx \quad (62)$$

Using the constitutive relationships of the different beam components, the elastic strains in the above equation can be replaced with the corresponding stresses as

$$U_e = \frac{1}{2} \int \{\sigma\}_c^T [E^e]_c^{-1} \{\sigma\}_c dv + \frac{1}{2} \int \{\sigma\}_s^T [E^e]_s^{-1} \{\sigma\}_s dv + \frac{1}{2} \int \tau_{sh} k_{sh}^{-1} \tau_{sh} dx \quad (63)$$

Now the incremental elastic energy within a load step can be obtained from the above equation and written as

$$\delta U_e = \int \{\delta \sigma\}_c^T [E^e]_c^{-1} \{\sigma\}_c dv + \int \{\delta \sigma\}_s^T [E^e]_s^{-1} \{\sigma\}_s dv + \int \delta \tau_{sh} k_{sh}^{-1} \tau_{sh} dx \quad (64)$$

Using the elasto-plastic constitutive relationships from Eqs. (30) and (31) with reference to the starting point of the load step, the incremental stresses in the above equation can be expressed in terms of incremental strains as

$$\delta U_e = \int \{\delta \varepsilon\}_c^T [E^t]_c^T [E^e]_c^{-1} \{\sigma\}_c dv + \int \{\delta \varepsilon\}_s^T [E^t]_s^T [E^e]_s^{-1} \{\sigma\}_s dv + \int \delta k_{sh}^t k_{sh}^{-1} \tau_{sh} dx \quad (65)$$

Using Eqs. (19) and (20), the strains in the above equation can be expressed in the form the incremental nodal displacement vector and Eq. (65) can be rewritten as

$$\delta U_e = \{\delta \Delta\}^T \{\hat{F}\} \quad (66)$$

where

$$\{\hat{F}\} = \int [\bar{B}]_c^T [E^t]_c^T [E^e]_c^{-1} \{\sigma\}_c dv + \int [\bar{B}]_s^T [E^t]_s^T [E^e]_s^{-1} \{\sigma\}_s dv + \int [B]_{sh}^T k_{sh}^t k_{sh}^{-1} \tau_{sh} dx \quad (67)$$

Using the forward Euler discretisation with respect to the converged solution  $(\{\Delta_0\}, \mu_0)$  of the previous time step, the constraint in Eq. (59) can be expressed with the help of Eqs. (60), (61) and (66) as

$$C = \{\delta \Delta\}^T (\mu_0 \{F\} - \{\hat{F}_0\}) - e_d \quad (68)$$

In the case of a structure having damage [40], the above equation can similarly be derived and expressed as

$$C = \frac{1}{2} \{F\}^T (\mu_0 \{\delta \Delta\} - \delta \mu \{\Delta_0\}) - e_d \quad (69)$$

Now Eq. (58) is combined with Eq. (57) to determine the augmented system of equations as

$$\begin{Bmatrix} \{P_{int}\} - \mu \{F\} \\ C \end{Bmatrix} = \begin{Bmatrix} \{0\} \\ 0 \end{Bmatrix} \quad (70)$$

The Newton Raphson method can be used to solve above equation iteratively as

$$\begin{Bmatrix} \{\delta \Delta\}^{j+1} \\ \delta \mu^{j+1} \end{Bmatrix} = \begin{Bmatrix} \{\delta \Delta\}^j \\ \delta \mu^j \end{Bmatrix} + \begin{Bmatrix} \{d\Delta\}^{j+1} \\ d\mu^{j+1} \end{Bmatrix} \quad (71)$$

$$\text{where } \begin{Bmatrix} \{d\Delta\}^{j+1} \\ d\mu^{j+1} \end{Bmatrix} = \left( \begin{bmatrix} \frac{\partial(\{P_{\text{int}}\} - \mu\{F\})}{\partial\{\Delta\}} & \frac{\partial(\{P_{\text{int}}\} - \mu\{F\})}{\partial\mu} \\ \frac{\partial C}{\partial\{\Delta\}} & \frac{\partial C}{\partial\mu} \end{bmatrix}^{-1} \right)^j \begin{Bmatrix} \mu\{F\} - \{P_{\text{int}}\} \\ -C \end{Bmatrix}^j \quad (72)$$

Using Eqs. (68), (69) and relevant equations in Section 2.2, the above equation can be rewritten as

$$\begin{Bmatrix} \{d\Delta\} \\ d\mu \end{Bmatrix} = \begin{bmatrix} [K_T] & -\{F\} \\ \{G\}^T & h \end{bmatrix}^{-1} \begin{Bmatrix} \{dR\} \\ -C \end{Bmatrix} \quad (73)$$

where  $\{G\} = \mu_0\{F\} - \{\hat{F}_0\}$  and  $h = 0$  for plasticity; and  $\{G\} = \frac{1}{2}\mu_0\{F\}$  and  $h = -\frac{1}{2}\{F\}^T\{\Delta_0\}$  for damage. The above equation in its present form is not suitable for its solution due to the incorporation of an additional row and column for including the additional unknown (load factor) which has destroyed the banded nature of the matrix system to be operated. In order to overcome this problem, the Sherman-Morrison formula [41] is used for solving the above equation as follows

$$\begin{Bmatrix} \{d\Delta\} \\ d\mu \end{Bmatrix} = \begin{Bmatrix} \{\Delta_I\} \\ -C \end{Bmatrix} - \frac{1}{\{G\}^T\{\Delta_{II}\} - h} \begin{Bmatrix} (\{G\}^T\{\Delta_I\} + C)\{\Delta_{II}\} \\ -\{G\}^T\{\Delta_I\} - C(1 + \{G\}^T\{\Delta_{II}\} - h) \end{Bmatrix} \quad (74)$$

where  $\{\Delta_I\} = [K_T]^{-1}\{dR\}$  and  $\{\Delta_{II}\} = -[K_T]^{-1}\{F\}$ .

Using Eqs. (71) and (74), the nodal displacement vectors and load factor can finally be updated as

$$\{\delta\Delta\}^{j+1} = \{\delta\Delta\}^j + \{\Delta_I\}^j - (\phi_f)^j \{\Delta_{II}\}^j \quad (75)$$

$$\delta\mu^{j+1} = \delta\mu^j + (\phi_f)^j \quad (76)$$

$$\text{where } \phi_f = \frac{\{G\}^T\{\Delta_I\} + C}{\{G\}^T\{\Delta_{II}\} - h}$$

As this arc-length method utilises the energy dissipated in a load step, the application of the method is not convenient at the initial loading steps where the structural deformations may be in the elastic range and have no energy dissipation. Thus a hybrid approach of solution strategy is adopted in the present study where the load control method is applied for some initial load steps and it is switched to the arc-length method when the energy dissipation  $U_d$  in a load step exceeds  $e_{d-\text{min}}$ , which is the minimum value of  $e_d$  prescribed by the user. Actually, the value of  $e_d$  is updated in each load step when the arc-length method is activated

in order to reduce the solution time. The value of  $e_d$  in a load step  $i+1$  can be estimated with the value of  $U_d$  in the previous load step [42] as

$$(e_d)_{i+1} = 0.5^\gamma (U_d)_i \quad (77)$$

where  $\gamma = 0.25(j - j_p)$  in which  $j$  is the iteration number and,  $j_p$  is the desired number of iterations to get convergence. In order to avoid any divergence problems, the value of  $e_d$  should be restricted within its minimum value  $e_{d-\min}$  and maximum value  $e_{d-\max}$ , which is another user specified value.

## 2.5. Stress Update

The nonlinear equilibrium equation is solved iteratively as mentioned in the above sections where the stresses are updated after every iteration as the total stress cannot be expressed in terms of total strain in the case of plastic deformations. In that situation, the incremental nodal displacements  $\{d\Delta\}^j$  obtained in an iteration  $j$  are used to evaluate the corresponding incremental strains  $\{d\varepsilon\}_k^j$  using Eq. (19) which are subsequently utilised to compute the incremental stresses  $\{d\sigma\}_k^j$  of that iteration using the elastic constitutive relationship as

$$\{d\sigma\}_k^j = [E^e]_k \{d\varepsilon\}_k^j \quad (78)$$

The above equation is written for a material layer but it is similarly applicable to the shear studs. Now the stresses can be updated by adding the incremental stresses  $\{d\sigma\}_k^j$  with the stresses accumulated in the previous iteration  $\{\sigma\}_k^{j-1}$  as

$$\{\sigma\}_k^j = \{\sigma\}_k^{j-1} + \{d\sigma\}_k^j \quad (79)$$

The updated stresses are substituted in the yield criteria as given in Eq. (35) which will lead to  $f_k > 0$  that indicates plastic deformations of the material or  $f_k \leq 0$  for its elastic deformations. For plastic deformations ( $f_k > 0$ ), the updated stress vector  $\{\sigma\}_k^j$  estimated by Eq. (79) are unfortunately not the final stress vector and it is rather defined as the trial stress vector  $\{\sigma^t\}_k$  which is adjusted to bring it on the yield surface. This is accomplished by using the backward Euler return technique [38], a robust stress return algorithm, in the present investigation. The starting estimate of the adjusted stress vector can be obtained from the trial stress vector as

$$\{\sigma\}_k = \{\sigma^t\}_k - d\lambda_k [E^e]_k \{a\}_k \quad (80)$$

$$\text{where } d\lambda_k = \frac{f_k}{\{a\}_k^T [E^e]_k \{a\}_k + H'_k} \quad (81)$$

and  $\{a\}_k$  can be calculated using Eq. (40). Both  $\{a\}_k$  and  $d\lambda_k$  are calculated based on the trial stresses. As the above stress vector  $\{\sigma\}_k$  does not usually satisfy the yield function, an iterative approach is used where the starting or first estimate of the stress vector is defined as  $\{\sigma\}_k^1$  and the corresponding incremental plastic strain multiplier as  $d\lambda_k^1$ . The value of the stress vector and the incremental plastic strain multiplier is iteratively improved till a desired level of convergence is achieved as follows.

$$\{\sigma\}_k^{n+1} = \{\sigma\}_k^n + \{\dot{\sigma}\}_k^n \quad (82)$$

$$d\lambda_k^{n+1} = d\lambda_k^n + \dot{\lambda}_k^n \quad (83)$$

where  $n (\geq 1)$  is the iteration used for the stress return algorithm. The expressions used to determine the value of  $\{\dot{\sigma}\}_k^n$  and  $\dot{\lambda}_k^n$  are given below.

$$\{\dot{\sigma}\}_k^n = -[M]_k^n \{r\}_k^n - \dot{\lambda}_k^n [M]_k^n [E^e]_k \{a\}_k^n \quad (84)$$

$$\{r\}_k^n = \{\sigma\}_k^n - \left( \{\sigma^t\}_k - d\lambda_k^n [E^e]_k \{a\}_k^n \right) \quad (85)$$

$$[M]_k^n = \left[ [I] + d\lambda_k^n [E^e]_k \left[ \frac{\partial \{a\}_k}{\partial \{\sigma\}_k} \right]^n \right]^{-1} \quad (86)$$

$$\dot{\lambda}_k^n = \frac{f_k^n - \{a\}_k^n^T [M]_k^n \{r\}_k^n}{\{a\}_k^n^T [M]_k^n [E^e]_k \{a\}_k^n + H'_k} \quad (87)$$

The superscript  $n$  used with any parameter in the above equations indicates that that parameter is calculated at iteration  $n$ . The vector norm of the residual stress  $\{r\}_k^n$  with respect to the current stress  $\{\sigma\}_k^n$  is used to check the convergence of the above iterative process. For the present problem, the derivative of  $\{a\}_k$  used in Eq. (86) can be written as

$$\frac{\partial \{a\}_k}{\partial \{\sigma\}_k} = \frac{1}{\sigma_{ef,k}} \begin{bmatrix} 1 - \frac{\sigma_k^2}{\sigma_{ef,k}^2} & -\frac{3\sigma_k \tau_k}{\sigma_{ef,k}^2} \\ -\frac{3\sigma_k \tau_k}{\sigma_{ef,k}^2} & 3 - \frac{9\tau_k^2}{\sigma_{ef,k}^2} \end{bmatrix} \quad (88)$$

As the equilibrium path is divided into a number of load steps and the nonlinear equilibrium equation is solved within each load step iteratively, the stress return algorithm presented above is implemented in a slightly different manner so as to avoid any convergence problem. For an iteration within a load step, the incremental strains accumulated from the beginning of that load step  $\{\delta\varepsilon\}_k^j$  are used instead of  $\{d\varepsilon\}_k^j$  in Eq. (78) to get the incremental stresses  $\{\delta\sigma\}_k^j$  of that load step which are added with the converged stresses of the previous load step to evaluate the trial stresses of that iteration which is adjusted by the stress return algorithm presented above.

### 3. NUMERICAL RESULTS

#### 3.1. Two Layered Composite Beam having a Rectangular Section – Numerical Verification

An 8.0 m long composite beam consisting of two layers having rectangular sections of equal width (200 mm) and equal depth (300 mm) is used in this section for the numerical verification of the proposed model. The beam is simply supported at its two ends and subjected to a point load  $P$  at its mid span. For the upper material layer of the beam, the Hognestad model [43] as shown in Fig. 3 is used for defining its uniaxial stress-strain curves that may be expressed as

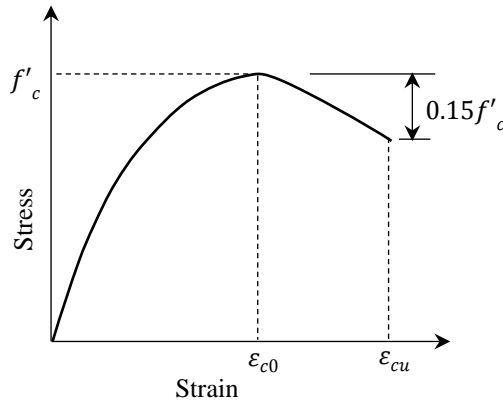


Fig. 3. Uniaxial stress-strain curve for the upper material layer (concrete)

$$\sigma_c = f'_c \left[ \frac{2\varepsilon_c}{\varepsilon_{c0}} - \left( \frac{\varepsilon_c}{\varepsilon_{c0}} \right)^2 \right] \quad \varepsilon_c < \varepsilon_{c0} \quad (89)$$

$$\sigma_c = f'_c [83(\varepsilon_{c0} - \varepsilon_c) + 1] \quad \varepsilon_{c0} \leq \varepsilon_c \leq \varepsilon_{cu} \quad (90)$$

where  $f'_c$  is the maximum compressive strength,  $\varepsilon_{c0}$  is the strain corresponding to  $f'_c$  and  $\varepsilon_{cu}$  is the ultimate compressive strain. For the present problem, the values of these material parameters are taken as:  $f'_c = 30$  MPa,  $\varepsilon_{c0} = 0.002$  and  $\varepsilon_{cu} = 0.038$  along with the elastic modulus of 25 GPa and Poisson's ratio of 0.25 for the upper layer. For the lower layer of the beam, a hypothetical material is used and its uniaxial stress-strain relationship both in tension and compression is defined with an elastic-perfectly plastic model. The present analysis is carried out taking the ultimate stress  $f_u = 50$  MPa, elastic modulus  $E = 40$  GPa and Poisson's ratio  $\nu = 0.25$  for the lower material layer. The relationship between the interfacial shear force (per unit length) and the shear slip of the shear connectors is idealised as distributed interfacial springs and defined by the exponential model of Olgaard et al. [44] as shown in Fig. 4. This relationship is given by

$$\tau_{sh} = q_{max} \left[ 1 - e^{(-0.71s)} \right]^{2/5} \quad s \leq s_u \quad (91)$$

where  $q_{max}$  is the ultimate value of the interfacial shear force (per unit length) and  $s_u$  is the ultimate slip. For the present analysis, the values of these parameters are taken as:  $k_{sh} = 10$  MPa,  $q_{max} = 460$  MPa,  $s_u = 6$  mm.

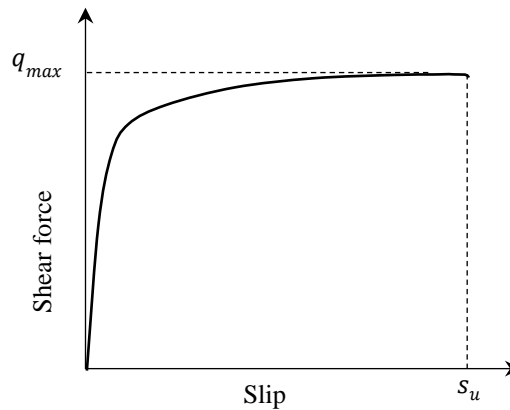


Fig. 4. Exponential model for the uniaxial stress-strain curve for shear connector

Though the effects of geometric nonlinearity (GN) due to large deformations as well as material nonlinearity (MN) due to inelastic material behaviour are incorporated in the proposed 1D finite element (FE) model, provision is kept to deactivate GN or MN in the computer program developed for implementing the model. This function is utilised to have three different options (1: with GN only, 2: with MN only, and 3: with both i.e. GN+MN) of the proposed model and they are used to analyse the beam to show the contribution of the individual nonlinearities and their combination. The beam is analysed with this 1D finite element model using different number of elements and the results show that the maximum

number of elements required to get convergence is 30 which is used in all cases. Though the proposed model is based on HBT (3<sup>rd</sup> order theory), it can easily be amended to TBT (1<sup>st</sup> order theory) by dropping the higher order terms.

For the numerical verification of the proposed model, this beam is also analysed with a well-regarded finite element software (ABAQUS) where the 2D plane stress rectangular element (CPS4R) is used to model both layers by discretising these layers along their lengths and depths assuming no normal stress across the beam width. The shear connectors are modelled using the cohesive contact modelling tool of ABAQUS which is placed at the interface between the elements used for the upper and the lower layers. Both these nonlinearities are activated in this approach of analysis where the mesh refinement is similarly conducted to get a converged solution. For the sake of comparison of the proposed model with the ABAQUS model, the upper layer is treated as a hypothetical material in this example only where the von Mises plasticity theory is used in compression as well as tension regions. Moreover, the Hognestad model [43] is used to define the uniaxial stress-strain curve of the material in both compression and tension. This is typically used for concrete in compression only in other examples.

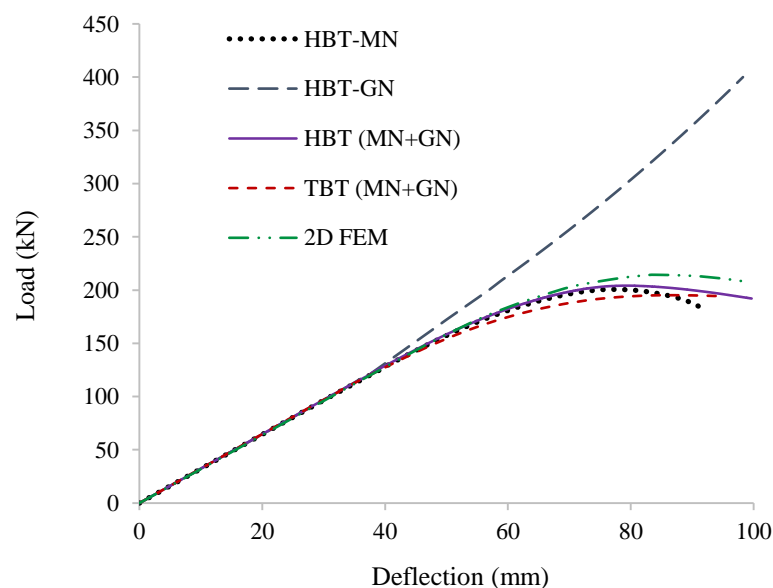


Fig. 5. Mid-span deflection of the two-layer composite beam

The variation of mid-span deflection of the beam with respect to the applied load predicted by the three options (GN, MN and GN+MN) of the proposed 1D finite element (FE) model based on HBT is presented in Fig. 5. The figure shows that the GN contributed towards stiffening the beam whereas the MN softened the beam. Moreover, the MN has the dominant contribution which is responsible for producing a softening response when both these

nonlinearities (GN+MN) are activated. Fig. 5 also includes the results obtained from 1D FE model (GN+MN) based on TBT to show the performance of HBT over TBT. The results obtained by the detailed 2D FE model are also included in Fig. 5 which shows a good agreement with the results predicted by the proposed 1D model (GN+MN) based on HBT. The figure also shows that the post-peak response of the beam is successfully traced by the proposed model.

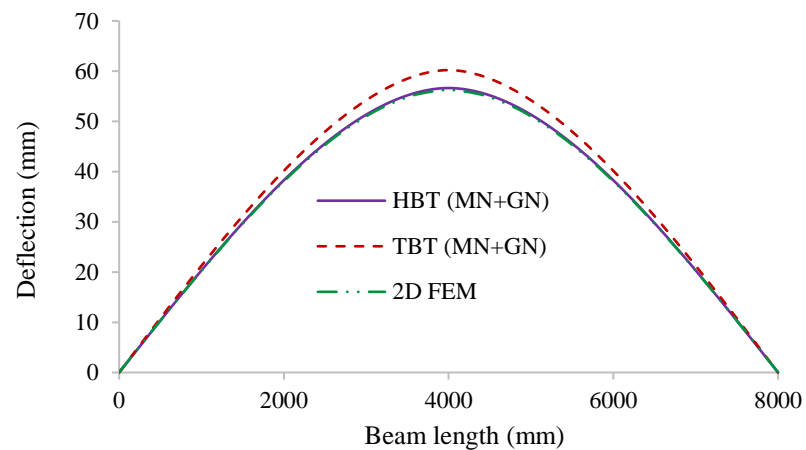


Fig. 6. Deflection along the length of the two-layered composite beam

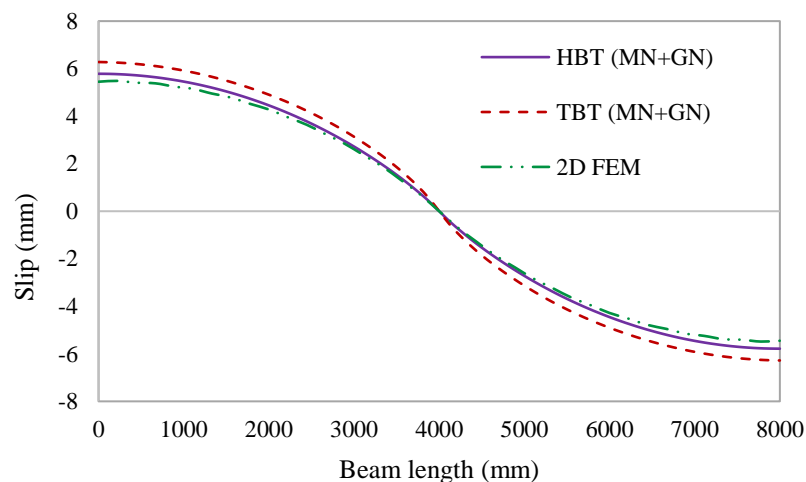


Fig. 7. Interfacial shear slip of two-layered composite beam along its length

The variations of the vertical displacement and the interfacial slip along the beam length corresponding to the applied load  $P = 175$  kN predicted by the proposed 1D FE model (GN+MN) based on HBT as well as TBT and the detailed 2D FE model are presented in Fig. 6 and Fig. 7, respectively. Similarly, the variation of von Mises stress over the beam depth obtained at quarter span of the beam predicted by these models for  $P = 175$  kN is plotted in Fig. 8.

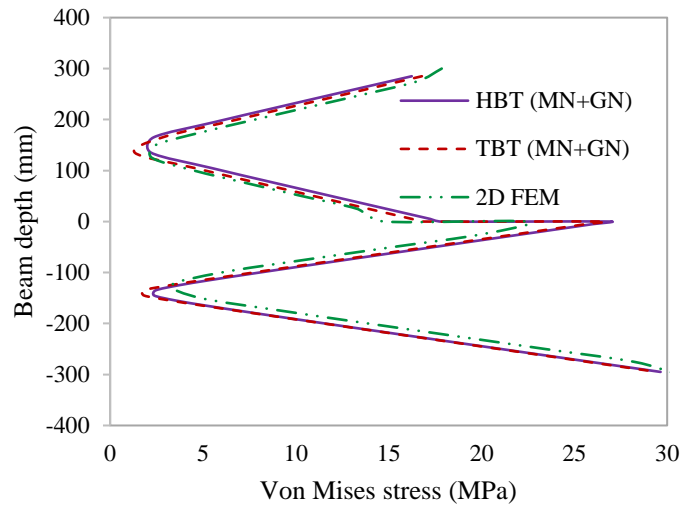


Fig. 8. Von Mises stress at the quarter span of two-layered composite beam

For further investigations, the variation of bending and shear stress over the beam depth obtained at a section 1.0 m away from one of the end supports corresponding to  $P = 175$  kN are plotted in Fig. 9 and Fig. 10 respectively. The results shown in Figs. 6 to 10 show a very good performance of the HBT model in all cases. The performance of TBT is affected due to the assumption of average shear strain and this is severe in Fig. 10.

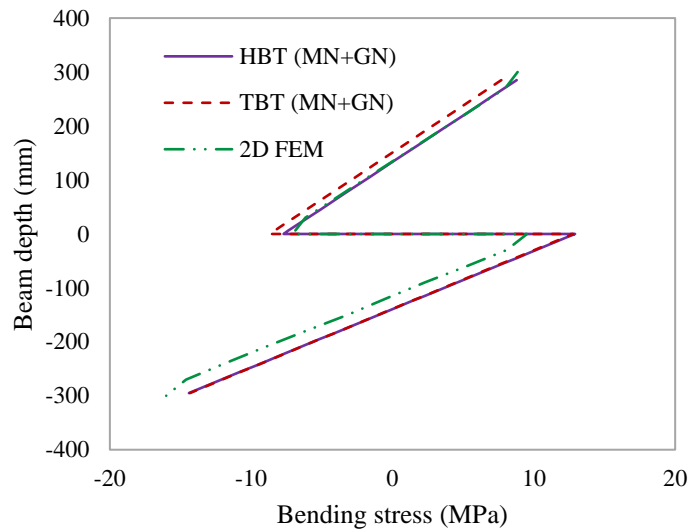


Fig. 9. Bending stress at a section 1 m away from a support of the two-layered composite beam

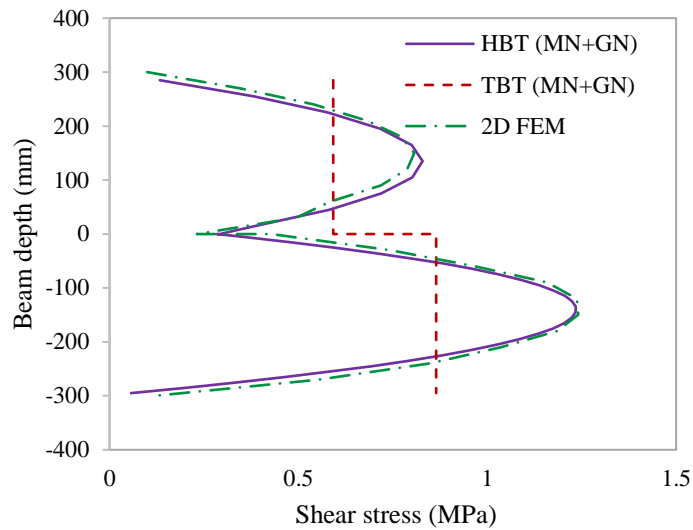


Fig. 10. Shear stress at a section 1 m away from a support of the two-layered composite beam

### 3.2. Steel-concrete Composite Beam subjected to Three Point Bending – Experimental Validation

A 5.5 m long simply supported steel-concrete composite beam tested by Chapman and Balakrishnan [45] is used in this section for the experimental validation of the proposed 1D FE model (GN+MN) based on HBT. The beam consisting of a concrete slab and a steel I-girder connected by steel shear studs as shown in Fig. 11 was tested under three point bending.

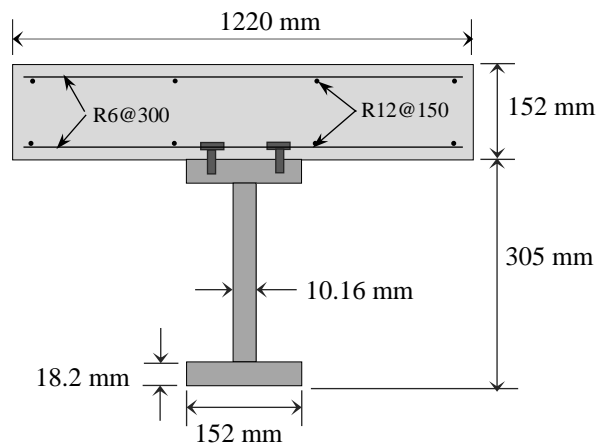


Fig. 11. Cross-section of composite beam

The Hognestad model [43] as shown in Fig. 3 is used for the uniaxial stress-strain relationship of concrete in compression while the bi-linear model as shown in Fig. 2 is used for the concrete in tension. The steel girder is assumed to follow a bi-linear model with a

strain hardening branch as shown in Fig. 12 for its uniaxial stress-strain relationship both in tension as well as compression. For the shear connectors idealised as a distributed shear springs, a bi-linear model as shown in Fig. 13 is used to define the relationship between the interfacial shear force per unit length  $q$  and the shear slip  $s$  where the value of the hardening parameter is taken as 585 MPa in one case and zero in other case. The concrete slab is reinforced with 4 longitudinal steel bars R12 in its top and bottom regions (Fig. 11). The re-bars are modelled as 1D members under uniaxial stress where an elastic-perfectly plastic material behaviour is adopted.

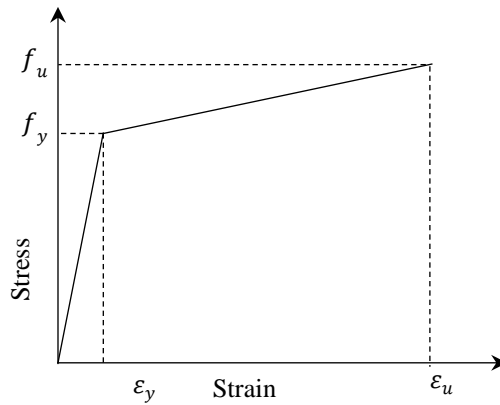


Fig. 12. Bi-axial stress-strain curve for steel girder

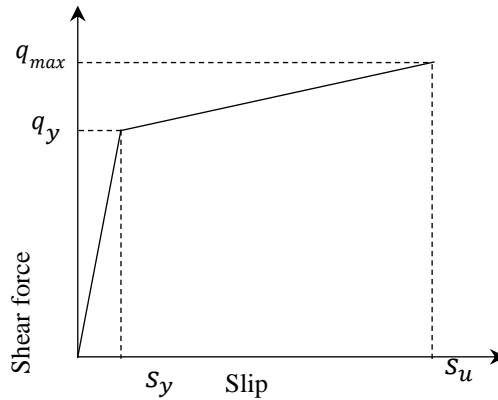


Fig. 13. Bi-axial stress-strain curve for shear connector

The material properties used for characterising the different components of the composite beam are given in Table 1 which also contains the material properties of the beam considered in the next example (Section 3.3). The problem is solved by the proposed 1D nonlinear FE model using 20 elements (based on a convergence study), and the variation of mid-span deflection with respect to the applied load obtained with the two hardening values of the shear connectors are presented in Fig. 14 along with the experimental result reported by Chapman and Balakrishnan [45]. Fig. 14 also includes the numerical results reported by

Liang et al. [46] who obtained these results from a detailed 3D nonlinear finite element model of the beam using ABAQUS. The figure shows a very good correlation between the results obtained from different approaches where the proposed model (considering no hardening for the shear connectors) is found to perform better than ABAQUS when compared with the experimental results.

Table 1. Material properties of composite beams

Material	Property	Liang et al. [46]	Tan and Uy [47]
Concrete slab	Elastic modulus, $E_c$	32,920 MPa	20,000 MPa
	Poisson's ratio, $\nu$	0.15	0.10
	Compressive strength, $f'_c$	42.5 MPa	25 MPa
	Strain, $\epsilon_{c0}$	0.002	0.002
	Ultimate tensile stress, $f_t$	3.553 MPa	2.5 MPa
	Fracture energy, $G_f$	0.208 N/mm	0.1875 N/mm
	Ultimate tensile strain, $\epsilon_{tu}$	0.0016	0.0019
Steel girder	Elastic modulus, $E_s$	205,000 MPa	200,000 MPa
	Poisson's ratio, $\nu$	0.3	0.3
	Yield stress, $f_y$	265 MPa	300 MPa
	Ultimate stress, $f_u$	410 MPa	500 MPa
	Ultimate strain, $\epsilon_u$	0.25	0.11
Shear connector	Yield shear force, $q_y$	435 MPa	
	Ultimate shear force, $q_{max}$	565 MPa	743.86 N/mm‡ 396.49 N/mm†
	Elastic stiffness, $k_{sh}$	2491.46 MPa	517.74 MPa‡ 397.61 MPa†
	Maximum slip, $s_u$	6 mm	7 mm‡ 10 mm†
Reinforcement in concrete slab	Modulus of elasticity, $E_s$	200,000 MPa	200,000 MPa
	Poisson's ratio, $\nu$	0.3	0.25
	Yield stress, $f_y$	250 MPa	550 MPa
	Ultimate strain, $\epsilon_u$	0.25	0.11

Note: † = Single shear stud in a row  
‡ = Double shear stud in a row

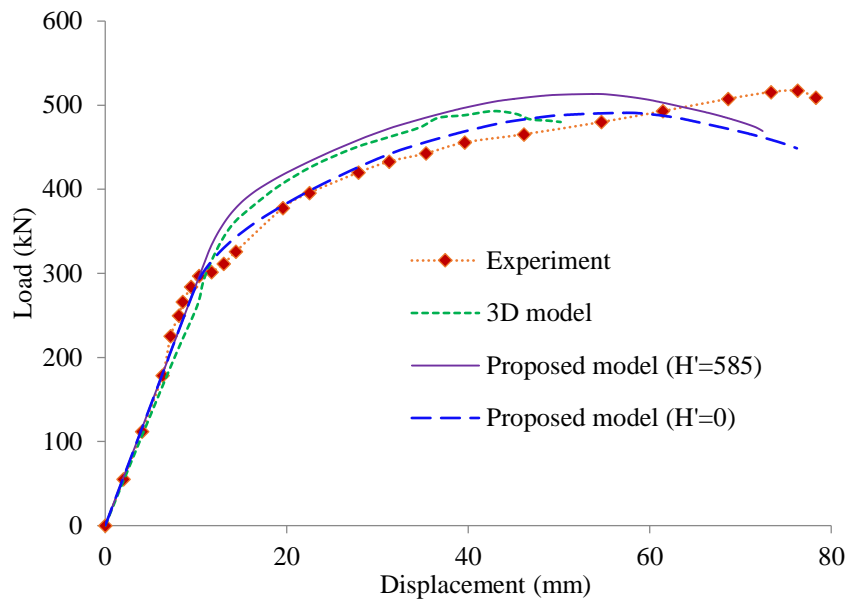


Fig. 14. Vertical displacement at mid-span of composite beam.

### 3.3. *Steel-concrete composite beam under four point bending – experimental validation*

A 4 m long steel-concrete composite beam tested by Tan and Uy [47] under four point bending is used in this example. The beam is simply supported at the two ends and subjected to two identical point loads acting symmetrically with a clearance of 4/3 m between them. The composite beam consists of a 500 mm wide and 120 mm thick concrete slab used for the upper layer, and a steel I girder (universal beam section 200UB29.8) for the lower layer. The concrete slab is reinforced with 4 longitudinal steel bars R12 in its top and bottom regions. The concrete slab (including re-bars) and the steel girder are modelled in a similar manner as followed in the previous example. For the modelling of shear connectors, the exponential model of Olgaard et al. [44] is used for this problem which is chosen on the basis of the trend of results obtained in the push out test [47].

For the present study, two different beam specimens tested by Tan and Uy [47] are used where the number of shear studs in a row at each shear stud location along the beam is one in the first case and two in the other case. Table 1 includes all the material properties used for defining the different constituents of the composite beam. The beam is analysed with the proposed model (GN+MN) and the result obtained in the form of variation of mid-span deflection with respect to the applied load is presented in Fig. 15 along with the experimental results reported by Tan and Uy [47]. The figure shows a good correlation between the numerical and experimental results.

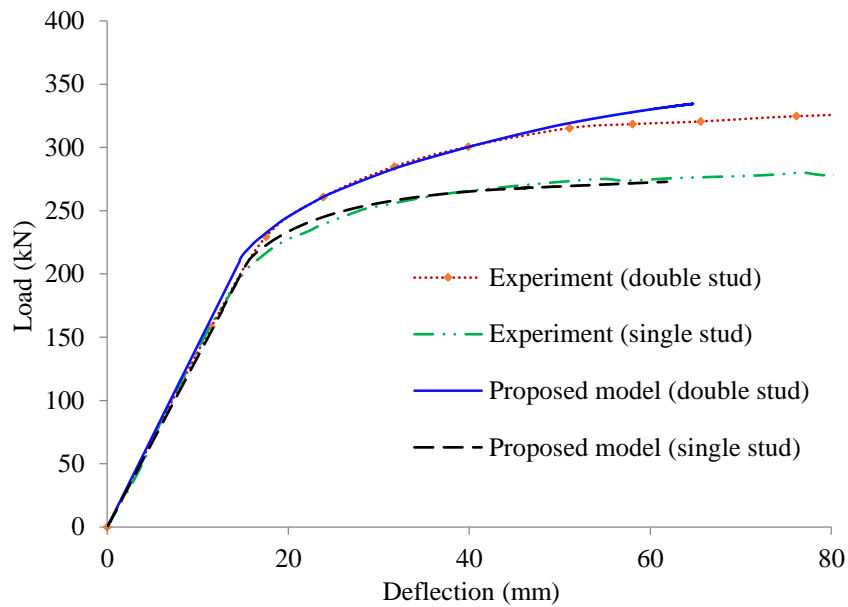


Fig. 15. Variation of mid-span deflection with respect to mid-span moment of the composite beam (Tan and Uy [47]).

### 3.4. Steel-concrete composite beam with a T-section

The problem of a 6.0 m long steel-concrete composite beam having a T-section as shown in Fig. 16 is used in this section to study the effect of interfacial shear stiffness and higher order terms used for defining the beam theory (HBT) on the response of the composite beam. The beam is simply supported at its two ends and subjected to a point load at its mid-span. The behaviour of the concrete slab and shear connectors is modelled in a similar manner as that followed in the previous example.

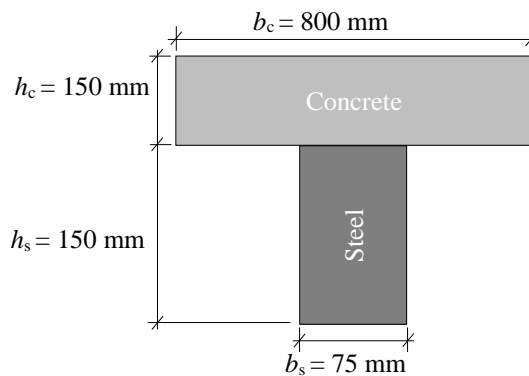


Figure 16. Cross-section of the 6 m long simply supported composite beam

For the steel girder, an elastic-perfectly plastic with strain hardening model [16] as shown in Fig. 17 is employed for defining its uniaxial stress-strain relationship in both tension and

compression. According to Liu et al. [16], the strain hardening branch of the stress-strain curve (Fig. 17) can be expressed as

$$\sigma_s = f_y + (f_u - f_y) \left[ 1 - e^{-\frac{(\varepsilon_{sh} - \varepsilon_s)}{a}} \right] \quad \varepsilon_{sh} \leq \varepsilon_s \leq \varepsilon_u \quad (92)$$

where  $f_y$  is the yield stress,  $f_u$  is the ultimate stress,  $\varepsilon_y$  is the yield strain,  $\varepsilon_{sh}$  is the strain at the beginning of strain hardening, and  $\varepsilon_u$  is the ultimate strain. The material constant  $a$  used in Eq. (92) can be determined with the above parameters as

$$a = \frac{0.028(\varepsilon_{sh} - \varepsilon_u)}{\varepsilon_{sh} - 0.16} \quad (93)$$

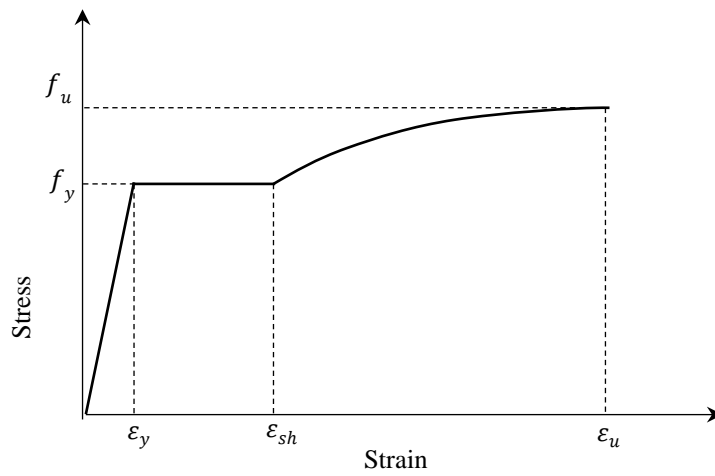


Fig. 17. Uniaxial stress-strain curve (elastic perfectly plastic with strain hardening) for the steel girder

For the present problem, the values used for the material parameters of concrete are:  $f'_c = 30$  MPa,  $\varepsilon_{c0} = 0.002$ ,  $\varepsilon_{cu} = 0.038$ ,  $f_t = 3.0$  MPa,  $G_f = 0.197$  N/mm,  $E_c = 26$  GPa and  $\nu_c = 0.15$ . Similarly, the material properties used for the steel girder are:  $f_y = 275$  MPa,  $f_u = 400$  MPa,  $\varepsilon_{sh} = 0.025$ ,  $\varepsilon_u = 0.11$ ,  $E_s = 200$  GPa and  $\nu_s = 0.25$ . For the shear connectors, the material properties are:  $q_{max} = 500$  N/mm,  $k_{sh} = 150$  MPa and  $s_u = 6$  mm.

Though the proposed model is based on a 3<sup>rd</sup> order theory (HBT), it can easily be converted to a 1<sup>st</sup> order theory (TBT) by dropping the higher order terms ( $\alpha$  and  $\beta$ ) used in Eqs. (1) and (2). In this example, the beam is analysed by the proposed model (GN+MN) based on HBT as well as TBT to show the performance of these beam theories in the nonlinear range. Moreover, the analysis is carried out using a very high value of shear connector stiffness in terms of  $q_{max} = 1.0 \times 10^{15}$  MPa (Eq. (91)) as well as a moderate value ( $q_{max} = 500$  MPa) of this

stiffness parameter, which are referred as full interaction (FI) and partial interaction (PI) conditions, respectively, in this example. The variation of mid-span deflection with respect to the applied load predicted by the different variants (HBT, TBT, PI and FI) of the proposed model is presented in Fig. 18. It shows that the higher order terms ( $\alpha$  and  $\beta$ ) used in HBT has some effect and the effect of the shear connector stiffness is substantial.

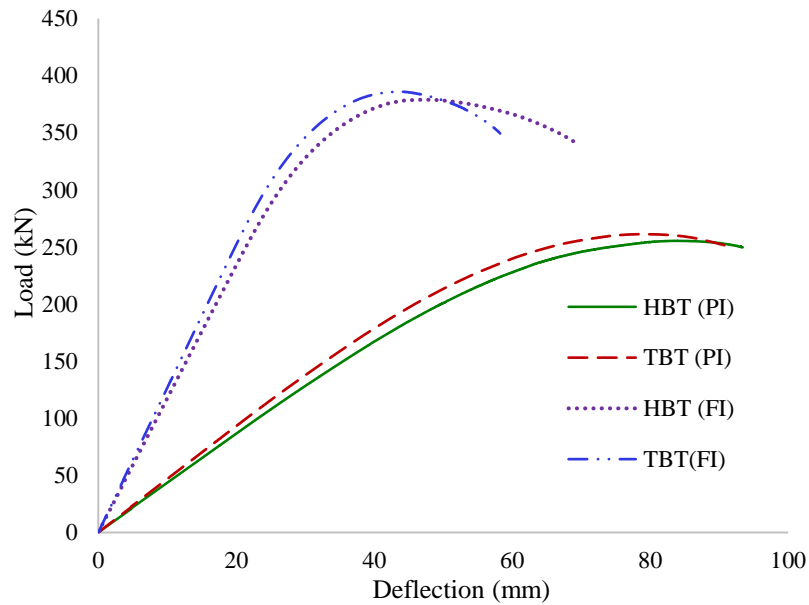


Fig. 18. Mid-span deflection of the steel-concrete composite beam with T-section

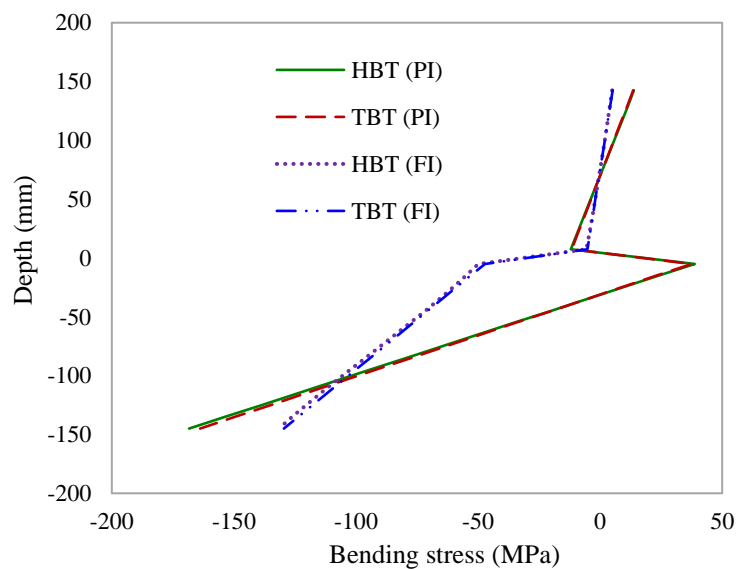


Fig. 19. Bending stress at quarter span of composite beam with T-section under point load ( $P = 250$  kN)

The variations of bending and shear stresses over the beam depth obtained at quarter span of the beam corresponding to the applied load  $P = 250$  kN are plotted in Fig. 19 and Fig. 20 respectively. It is observed that the bending stresses (Fig. 19) obtained by these four considerations followed a similar pattern as observed for the mid-span displacement.

However, the effect of both shear connector stiffness and higher order terms ( $\alpha$  and  $\beta$ ) is significant for the shear stress (Fig. 20).

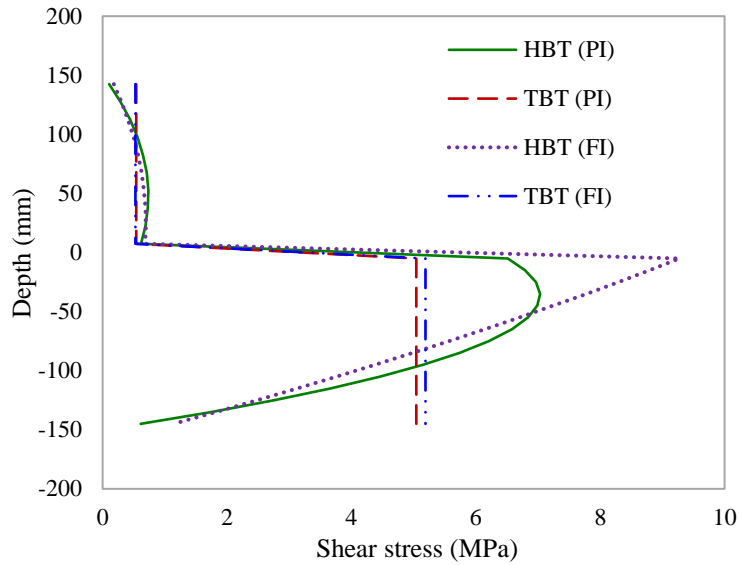


Fig. 20. Shear stress at quarter span of composite beam with T-section under point load ( $P = 250$  kN)

#### 4. CONCLUSIONS

An accurate and computationally efficient finite element model is developed for the reliable prediction of the large deformation inelastic response of steel-concrete composite beams. The steel shear studs used to connect the steel girder with the concrete slab are idealised as interfacial distributed springs with finite stiffness which enables the incorporation of partial shear interaction exhibited in composite beams. A higher order (3<sup>rd</sup> order) beam theory is used to model the cross-sectional warping which helped to accurately simulate the shear deformation of the beam without using the arbitrary shear correction factor used in Timoshenko's beam theory.

The von-Mises yield function with an isotropic hardening rule and associated flow rule is used to model the behaviour of steel girders, steel reinforcements, steel shear studs and concrete slabs in compression. A damage mechanics model is used for modelling concrete slabs in tension. The mesh sensitivity associated with the damage modelling of concrete, a quasi-brittle material, in tension is eliminated using the well-known crack band theory.

The Green-Lagrange strain is used to develop the model for incorporating the effects of geometric nonlinearity produced by the large deformation of the beam. This large deformation along with the inelastic material behaviour imposed nonlinearity in the present

problem and the solution of this nonlinear equations becomes challenging specifically for capturing the post peak response. In order to address this issue, an energy dissipation based arc length method is employed to solve the nonlinear equations which helped to trace the descending branch of the load deflection curve successfully.

The proposed one dimensional finite element model is validated with experimental results and verified with the numerical results obtained from a detailed 2D nonlinear finite element model of a composite beam developed using a reliable commercial finite element software. The numerical verifications as well as experimental validations show a very good performance of the proposed finite element model in all cases. Based on the accuracy and range of applicability of the proposed model, it is highly recommended for the analysis of composite beams having large deformation and/or inelastic material behaviours.

## **5. ACKNOWLEDGEMENTS**

The financial support provide by the University of Adelaide in the form of an Adelaide Scholarship International (ASI) awarded to the first author for his doctoral studies is gratefully acknowledged. The authors also acknowledge the help received from V.P. Nguyen (Department of Civil Engineering, Monash University, Australia) in implementing the arc-length method.

## **6. REFERENCES**

- [1] D. Oehlers, M.A. Bradford, Composite Steel and Concrete Structural Members, Fundamental Behaviour, Australia, (1995).
- [2] N.M. Newmark, C.P. Siess, I. Viest, Tests and analysis of composite beams with incomplete interaction, Proc. Soc. Exp. Stress Anal, 9 (1951) 75-92.
- [3] G. Ranzi, F. Gara, G. Leoni, M.A. Bradford, Analysis of composite beams with partial shear interaction using available modelling techniques: A comparative study, Computers & structures, 84 (2006) 930-941.
- [4] A. Adekola, Partial interaction between elastically connected elements of a composite beam, International Journal of Solids and Structures, 4 (1968) 1125-1135.
- [5] U.A. Girhammar, D. Pan, Dynamic analysis of composite members with interlayer slip, International Journal of Solids and Structures, 30 (1993) 797-823.

- [6] N. Jasim, Computation of deflections for continuous composite beams with partial interaction, *Proceedings of the Institution of Civil Engineers. Structures and buildings*, 122 (1997) 347-354.
- [7] Q. Nguyen, M. Hjiij, B. Uy, Time effects analysis of composite beams using a mixed FE formulation, in: *Third International Conference on Structural Engineering, Mechanics and Computation (SEMC 2007)*, 2007, pp. 1157-1163.
- [8] A. Yasunori, H. Sumio, T. Kajita, Elastic-plastic analysis of composite beams with incomplete interaction by finite element method, *Computers & Structures*, 14 (1981) 453-462.
- [9] M.R. Salari, E. Spacone, P.B. Shing, D.M. Frangopol, Nonlinear analysis of composite beams with deformable shear connectors, *Journal of Structural Engineering*, 124 (1998) 1148-1158.
- [10] A. Dall'Asta, A. Zona, Non-linear analysis of composite beams by a displacement approach, *Computers & Structures*, 80 (2002) 2217-2228.
- [11] R.E. Erkmen, M.M. Attard, Displacement-based finite element formulations for material-nonlinear analysis of composite beams and treatment of locking behaviour, *Finite Elements in Analysis and Design*, 47 (2011) 1293-1305.
- [12] R.E. Erkmen, M.A. Bradford, Nonlinear elastic analysis of composite beams curved in-plan, *Engineering Structures*, 31 (2009) 1613-1624.
- [13] J.-M. Battini, Q.-H. Nguyen, M. Hjiij, Non-linear finite element analysis of composite beams with interlayer slips, *Computers & Structures*, 87 (2009) 904-912.
- [14] G. Ranzi, A. Dall'Asta, L. Ragni, A. Zona, A geometric nonlinear model for composite beams with partial interaction, *Engineering Structures*, 32 (2010) 1384-1396.
- [15] T. Hozjan, M. Saje, S. Srpčič, I. Planinc, Geometrically and materially non-linear analysis of planar composite structures with an interlayer slip, *Computers & Structures*, 114-115 (2013) 1-17.
- [16] X. Liu, M.A. Bradford, R.E. Erkmen, Non-linear inelastic analysis of steel-concrete composite beams curved in-plan, *Engineering Structures*, 57 (2013) 484-492.
- [17] S. Berczyński, T. Wróblewski, Vibration of steel-concrete composite beams using the Timoshenko beam model, *Journal of Vibration and Control*, 11 (2005) 829-848.
- [18] G. Ranzi, A. Zona, A steel-concrete composite beam model with partial interaction including the shear deformability of the steel component, *Engineering Structures*, 29 (2007) 3026-3041.
- [19] R. Xu, Y. Wu, Static, dynamic, and buckling analysis of partial interaction composite members using Timoshenko's beam theory, *International Journal of Mechanical Sciences*, 49 (2007) 1139-1155.
- [20] S. Schnabl, M. Saje, G. Turk, I. Planinc, Locking-free two-layer Timoshenko beam element with interlayer slip, *Finite Elements in Analysis and Design*, 43 (2007) 705-714.

- [21] M. Hjiaj, J.-M. Battini, Q.H. Nguyen, Large displacement analysis of shear deformable composite beams with interlayer slips, *International Journal of Non-Linear Mechanics*, 47 (2012) 895-904.
- [22] Q.-H. Nguyen, M. Hjiaj, V.-A. Lai, Force-based FE for large displacement inelastic analysis of two-layer Timoshenko beams with interlayer slips, *Finite Elements in Analysis and Design*, 85 (2014) 1-10.
- [23] A. Chakrabarti, A. Sheikh, M. Griffith, D. Oehlers, Analysis of composite beams with longitudinal and transverse partial interactions using higher order beam theory, *International Journal of Mechanical Sciences*, 59 (2012) 115-125.
- [24] A. Chakrabarti, A. Sheikh, M. Griffith, D. Oehlers, Analysis of composite beams with partial shear interactions using a higher order beam theory, *Engineering Structures*, 36 (2012) 283-291.
- [25] A. Chakrabarti, A. Sheikh, M. Griffith, D. Oehlers, Dynamic response of composite beams with partial shear interaction using a higher-order beam theory, *Journal of Structural Engineering*, 139 (2012) 47-56.
- [26] J.N. Reddy, A simple higher-order theory for laminated composite plates, *Journal of applied mechanics*, 51 (1984) 745-752.
- [27] E. Riks, An incremental approach to the solution of snapping and buckling problems, *International Journal of Solids and Structures*, 15 (1979) 529-551.
- [28] M.A. Crisfield, A fast incremental/iterative solution procedure that handles “snap-through”, *Computers & Structures*, 13 (1981) 55-62.
- [29] M.A. Crisfield, An arc-length method including line searches and accelerations, *International journal for numerical methods in engineering*, 19 (1983) 1269-1289.
- [30] I. May, Y. Duan, A local arc-length procedure for strain softening, *Computers & structures*, 64 (1997) 297-303.
- [31] T. Bennett, A.D. Jefferson, Experimental Tests and Numerical Modelling of Hexagonal Concrete Specimens, *Materials and Structures*, 40 (2007) 491-505.
- [32] M.A. Gutiérrez, Energy release control for numerical simulations of failure in quasi-brittle solids, *Communications in Numerical Methods in Engineering*, 20 (2004) 19-29.
- [33] R.U. Vinayak, G. Prathap, B.P. Naganarayana, Beam elements based on a higher order theory—I. Formulation and analysis of performance, *Computers & Structures*, 58 (1996) 775-789.
- [34] O.C. Zienkiewicz, R.L. Taylor, O.C. Zienkiewicz, R.L. Taylor, *The finite element method*, McGraw-hill London, 1977.
- [35] W.-F. Chen, D.-J. Han, *Plasticity for structural engineers*, J. Ross Publishing, 2007.
- [36] M.A. Crisfield, *Non-Linear Finite Element Analysis of Solids and Structures: Advanced Topics*, John Wiley & Sons, Inc., 1997.

- [37] R. De Borst, M.A. Crisfield, J.J. Remmers, C.V. Verhoosel, *Nonlinear finite element analysis of solids and structures*, John Wiley & Sons, 2012.
- [38] M.A. Crisfield, *Non linear finite element analysis of solids and structures*, vol. 1, in, Wiley, New York, 1991.
- [39] Z.P. Bažant, B.H. Oh, Crack band theory for fracture of concrete, *Matériaux et construction*, 16 (1983) 155-177.
- [40] C.V. Verhoosel, J.J. Remmers, M.A. Gutiérrez, A dissipation-based arc-length method for robust simulation of brittle and ductile failure, *International Journal for Numerical Methods in Engineering*, 77 (2009) 1290-1321.
- [41] J. Sherman, W.J. Morrison, Adjustment of an Inverse Matrix Corresponding to a Change in One Element of a Given Matrix, (1950) 124-127.
- [42] V.P. Nguyen, H. Nguyen-Xuan, High-order B-splines based finite elements for delamination analysis of laminated composites, *Composite Structures*, 102 (2013) 261-275.
- [43] E. Hognestad, N.W. Hanson, D. McHenry, Concrete stress distribution in ultimate strength design, in: *Journal Proceedings*, 1955, pp. 455-480.
- [44] J.G. Ollgaard, R.G. Slutter, J.W. Fisher, Shear strength of stud connectors in lightweight and normal-weight concrete, *AISC Engineering Journal*, 8 (1971) 55-64.
- [45] J. Chapman, S. Balakrishnan, Experiments on composite beams, *The Structural Engineer*, 42 (1964) 369-383.
- [46] Q.Q. Liang, B. Uy, M.A. Bradford, H.R. Ronagh, Strength analysis of steel–concrete composite beams in combined bending and shear, *Journal of Structural Engineering*, 131 (2005) 1593-1600.
- [47] E. Tan, B. Uy, Experimental study on straight composite beams subjected to combined flexure and torsion, *Journal of Constructional Steel Research*, 65 (2009) 784-793.

## Chapter 5: Summary, Conclusions and Recommendations for Future Study

### 5.1 Summary and Conclusions

The higher-order beam theory (HBT) is used to develop nonlinear finite element models for steel-concrete composite beams with partial interactions. The deformable shear studs used for connecting the steel girder with the concrete slab are modelled as interfacial distributed springs with a finite stiffness which helps to model the partial shear interaction.

The proposed one-dimensional nonlinear models are developed by considering the effect of both geometric and material nonlinearities for a reliable prediction of the nonlinear response of composite beams. The effects of geometric nonlinearity due to large deformations are incorporated in the present formulation by using Green-Lagrange strain vector. In addition, the material nonlinearity due to inelastic material behaviours is incorporated by using the von-Mises yield function with an isotropic hardening rule for the steel girders, steel reinforcements, steel shear studs and concrete slabs in compression. Moreover, a damage mechanics model is adopted to simulate the cracking behaviour of the concrete under tensile stress. Furthermore, the mesh sensitivity associated with the damage modelling of concrete is eliminated using the well-known crack band theory.

An energy dissipation based robust arc-length method is employed to solve the nonlinear equations which helped to trace the descending branch of the load deflection curve successfully. The backward Euler stress return algorithm is incorporated in the present models for updating the stresses. In order to have a realistic material behaviour, different types of stress-strain curves are used for different materials in both compression and tension.

The performance and range of applicability of the present models are shown by solving numerical examples of composite beams having different loading, supporting conditions, shear interactions and some other features. The results obtained by the proposed models are validated with experimental results. The model is also verified with numerical results obtained from a detailed 2D nonlinear finite element model of composite beams developed using a reliable commercial finite element software. Through these validation and verification, the major findings from the present research are outlined below:

- The proposed model based on HBT can realistically predict the global as well as local responses of these beams without any arbitrary shear correction factor as it takes account of the actual parabolic variation of shear strain.

- The proposed model is developed based on a 3<sup>rd</sup> order beam theory (HBT) but it can easily be converted into a lower order beam theory (e.g., EBT, TBT) by eliminating the higher order terms. The numerical analysis has confirmed that the model based on EBT always underestimates the global response (e.g., deflection) of the beam as the structures become stiff for ignoring the effect of transverse shear deformation.
- The model based on TBT is usually adequate for predicting the global response satisfactorily with the help of a shear correction factor which adjusts the shear stiffness appeared in the formulation due to incorporating the transverse shear deformation. However, this factor is not sufficient even for an accurate prediction of the global response in some situation such as beams with a small span-to-depth ratio, localised concentrated loads and clamped boundary conditions. Moreover, the model based on TBT is not adequate for predicting the distribution of stresses (local response) across the beam section.
- The major advantage of the proposed model is it can predict results very close to those produced by detailed finite element models using ABAQUS but the computational cost of the proposed model is significantly less than the ABAQUS model. Moreover, in some situations, the proposed model performed better than ABAQUS in the sense that the nonlinear solution process of this commercial software is terminated earlier than the proposed model.
- The proposed model is also used to examine the effect of different levels of shear interaction between the two layers of the composite beam. It is observed that the full shear interaction condition predicted deflection less than that for the partial interaction as expected. For both full and partial interaction conditions, the difference between the results predicted by HBT and TBT models is appreciable.
- The nonlinear response of these structures in the form of load-deflection curves predicted by the proposed model could successfully traced the descending branch after attaining the peak load.
- It also observed from the load-deflection response of the composite beams that the effect of geometric nonlinearity due to large deformation contributes towards stiffening of the composite beams, whereas material nonlinearity due to inelastic material behaviour leads to softening of these beams. In all cases considered in

this investigation, the material nonlinearity is found to have the dominant contribution which is demonstrated by an overall softening response of the beams when both geometric and material nonlinearities are considered in combination. In that situation, the predicted response of these beams are found to be more close to the experimental data.

Based on the accuracy and range of applicability along with the computational efficiency of the proposed model, it is highly recommended for the analysis of composite beams having large deformation and/or inelastic material behaviours.

## **5.2 Recommendations for Future Study**

Though a comprehensive numerical model is developed in this study for accurately predicting the nonlinear response of steel-concrete composite beams, a number of possible scopes exist for the extension of the model to capture many other features. Some of the obvious scopes of these future investigations are listed below:

- The current model is restricted to the prediction of static response of composite beams having large deformations and inelastic material behaviours. Therefore, the model can be extended so as to capture the nonlinear dynamic response of these structures which are commonly encountered in a structure subjected to earthquake loading, blast loading, and other form of impact loading.
- This model can be extended to buckling and post buckling analysis of the steel-concrete composite beams which will find their applications in long slender bridges and other structures.
- A current model is developed using a relatively simple constitutive model for simulating the inelastic response of the concrete slab. Thus, a very good opportunity exists for the enhancement of the inelastic material model for concrete.
- Some complex behaviors of reinforced concrete, such as aggregate interlocking, bond slip, tension stiffening and other effects, which are ignored in the current research can be incorporated in future studies.
- The current models can be extended to incorporate the long term effects such as creep, shrinkage and temperature, specifically for the concrete slab, to predict accurate response under sustained loading.